MINIMIZING HYDROPONIC NUTRIENT POLLUTION THROUGH PH-BASED CONTROL ALGORITHMS

by

Ignatius Leopoldus van Rooyen
29236178

Under the supervision of
Prof. Willie Nicol and Prof. Hendrik Brink

Submitted in partial fulfilment of the requirements for the degree
Doctor of Philosophy

In the Faculty of Engineering, Built Environment, and IT
Department of Chemical Engineering, University of Pretoria

July 2022

Minimizing hydroponic nutrient pollution through pH-based control algorithms

Author/Student: Ignatius van Rooyen, https://orcid.org/0000-0003-0405-0753

Supervisor: Willie Nicol, https://orcid.org/0000-0003-1130-319X

Co-supervisor: Hendrik Brink, https://orcid.org/0000-0002-4699-6152

University: University of Pretoria, https://www.up.ac.za

Department: Chemical Engineering

Degree: Doctor of Philosophy in Chemical Engineering

Keywords: Nitrate, phosphate, ammonium, concentration, nitrification, agriculture, proton, hydroxide

SYNOPSIS

It is well established that mankind's current economic practices are unsustainable. Consequences such as food shortages and climate change are predicted in the coming decades and efforts to help avert these impending crises remain warranted. This is particularly true for agriculture. Not only must food production increase to support the rapidly growing human population but the environmental impacts caused by agricultural pollution continue to grow in severity. Around 50 % of the fertilizer applied to crop fields is washed away into surrounding habitats resulting in eutrophication, biodiversity loss and stratospheric ozone depletion, to name but a few (Kanter *et al*., 2020).

As specified in the Title, the scope of this work surrounds nutrient pollution from hydroponic systems. Soilless agriculture is growing exponentially worldwide and will likely play a key role in the future of sustainable food production. Unlike conventional agriculture, the nutrient solution is physically contained, and thus nutrient discharge can be monitored and controlled. Despite this advantage, hydroponic systems are known to produce large amounts of nutrient laden wastewater. This wastewater results from frequent solution replacements (or high

throughputs for continuous systems) to maintain high nutrient concentrations and to prevent the build-up of inert and toxic species, which accumulates rapidly due to transpiration.

The nutrients of concern are nitrogen and phosphorous. These nutrients are typically limiting in natural ecosystems and thus causes the aforementioned environmental impacts when discharged. The aim of this work is therefore to minimize the nitrogen and phosphorous discharge rates from hydroponic systems. This can be accomplished by controlling their concentrations at low levels in solution. This strategy is not new and nutrient concentration control is often employed in hydroponic systems. The electrical conductivity method is the most common but is ill-suited for operation at low concentrations. Ion-selective-electrodes have also been used but these are expensive and generally not economically viable.

The novelty of this work lies in the use of pH as the sole measured variable to control the nitrogen and phosphorous concentrations at low levels in hydroponic systems. Nitrogen is supplied to hydroponic systems either as nitrate or ammonium, and phosphorous is supplied as phosphate. Separate control methodologies were designed for each of these three nutrients. The control systems were able to reduce nitrogen and phosphorous pollution from the system by around an order of magnitude as compared with traditional hydroponic methods. Advantages and drawbacks are also discussed and compared with existing methods.

RESEARCH OUTPUTS Journal Articles

First Author:

1. Optimal hydroponic growth of *Brassica oleracea* at low nitrogen concentrations using a novel pH-based control strategy. *Science of The Total Environment*, Elsevier. https://doi.org/10.1016/j.scitotenv.2021.145875
2. Inferential control of the phosphate concentration in hydroponic systems via measurement of the nutrient solution's pH-buffering capacity. *Scientia Horticulturae*, Elsevier. https://doi.org/10.1016/j.scienta.2021.110820
3. Nitrogen management in nitrification-hydroponic systems by utilizing their pH characteristics. *Environmental Technology and Innovation*, Elsevier. https://doi.org/10.1016/j.eti.2022.102360
4. pH-based control strategies for the nitrification of high-ammonium wastewaters. *Fermentation*, MDPI. https://doi.org/10.3390/fermentation7040319

Contributing Author:

1. Diazotrophic behaviour in a non-sterile bioreactor: The effect of O_2-availability. *Processes*. MDPI. https://doi.org/10.3390/pr9112039
2. Optimal growth conditions for *Azolla pinnata* R. Brown: Impacts of light intensity, nitrogen addition, pH control, and humidity. *Plants*, MDPI. https://doi.org/10.3390/plants11081048
3. Online control of *Lemna minor* L. phytoremediation: Using pH to minimize the nitrogen outlet concentration. *Plants*, MDPI. https://doi.org/10.3390/plants11111456

DECLARATION

I, Ignatius Leopoldus van Rooyen, declare that the thesis, which I hereby submit for the degree Doctor of Philosophy at the University of Pretoria, is my own work and has not previously been submitted by me for a degree at this or any other tertiary institution. The fifth chapter of this dissertation (titled “Nitrate”) is based on work done for my previous degree (Master of Engineering). This work is presented again because it forms part of the complete story.

ETHICS STATEMENT

The author, whose name appears on the title page of this dissertation declares that ethics did not pertain the work done after he observed the ethical standards required in terms of the University of Pretoria’s Code of Ethics for Researchers and the Policy guidelines for responsible research.

Signature: 

Student name: Ignatius Leopoldus van Rooyen

Month Year: July 2022

ACKNOWLEDGEMENTS

To my fellowship, who is best left Anonymous, and without whom this work would have been an impossible feat. To my parents, Ig van Rooyen and Elbe Naude, who supported me with all they had and never stopped believing in me. To my supervisors, Willie Nicol and Hendrik Brink, for their continued input, involvement and encouragement. To my colleagues and friends, Nico de Jong and Reuben Swart, who made me feel a-part-of and were always willing to help. To Ryan Merckel, who helped spark my passion for research initially. Thank you for some of the best years of my life.

This project was partly supported by the National Research Foundation of South Africa
Reference: MND200615532008

NOMENCLATURE

β	pH-buffering capacity of the solution.	mmol H^+ pH^{-1} L^{-1}
δ	Hydroxide-to-ammonium ratio in the digestate feed. Specifically, the mols of hydroxide required to raise the pH of the digestate (containing 1 mol of ammonium) from the operating pH of the hydroponic system to the current pH of the digestate.	mol mol^{-1}
η_1	Effective proton uptake by plant the (total of all acidic and basic effects) per nitrate absorbed	mol mol^{-1}
η_2	Effective proton exudation by the plant (total of all acidic and basic effects) per ammonium absorbed	mol mol^{-1}
η_3	Effective proton exudation by the nitrifying bacteria (total of all acidic and basic effects) per ammonium oxidized	mol mol^{-1}
υ_{max}	Michaelis-Menten maximum reaction rate	*specific to chapter*
σ	Standard deviation	
D_{H^+}	Proton dosing rate required for pH control	*specific to chapter*
$D_{NH_4^+}$	Ammonium dosing rate	*specific to chapter*
$D_{NO_3^-}$	Nitrate dosing rate	*specific to chapter*
D_{OH^-}	Hydroxide dosing rate required for pH control	*specific to chapter*
ΔpH	Change in pH due to acid dosing	pH
∇pH	Rate of change of pH as caused by the plant, $\partial \text{pH}/\partial t$	pH h^{-1}
FFM	Final fresh mass of plant	g
IFM	Initial fresh mass of plant	g
LMF	Leaf mass fraction (dry mass basis)	g g^{-1}
n	Number of sample points.	

N	Nitrogen	
P	Phosphorous	
Pi	Inorganic phosphate: $H_3PO_4/H_2PO_4^-/ HPO_4^{2-}/PO_4^{3-}$	
RDR	Relative dosing rate $\left(\ln\left[D_{NO_3^-,t}\right] - \ln\left[D_{NO_3^-,t+\Delta t}\right]\right)/\Delta t$	day^{-1}
RGR	Relative growth rate of plant $(\ln[FFM] - \ln[IFM])/\Delta t$	day^{-1}
$r_{NH_4^+}^B$	Ammonium oxidation rate by the bacteria	mol day^{-1}
$r_{NH_4^+}^P$	Ammonium uptake rate by the plant	mol day^{-1}
$r_{NO_3^-}^P$	Nitrate uptake rate by the plant	mol day^{-1}
r_N^P	Total nitrogen uptake rate by the plant	mol day^{-1}
$F_{NH_4^+}^P$	Fraction of the dosed ammonium which is absorbed by the plant $(r_{NH_4^+}^P/D_{NH_4^+})$	mol mol^{-1}
t	time	day
TPC	Total plant phosphorous content (fresh mass basis)	mg-P g^{-1}

TABLE OF CONTENTS

LIST OF FIGURES

LIST OF TABLES

CHAPTER 1 General introduction

Plants require seventeen elements to grow (Mahler, 2004). Besides carbon, hydrogen, and oxygen, which form the carbohydrate backbone of the plant, the remaining fourteen elements are absorbed from the soil via the plant roots. These nutrients return to the soil when the plants (or organism higher up on the food chain) die and decompose. This natural cycling of nutrients does not occur in conventional agriculture since the plants are removed from the region. Nutrients in crop fields inevitably deplete and additional nutrients (fertilizer) must be supplied to maintain high crop production. Manure and wood ash were some of the first fertilizers used by man, but their supply could not keep up with the rapidly growing human population. Industrial fertilizers were first developed early in the 19th century which allowed increases in crop production (Russel & Williams, 1977). These synthetic fertilizers became progressively cheaper and higher in quality. By the 20th century, industrial agriculture boomed (known as the "green revolution") and the human population expanded exponentially (Erisman *et al*., 2008). High fertilizer application rates were standard protocol to ensure consistently high crop yields. These practices however were associated with low nutrient use efficiencies. Since crop fields do not have physical/chemical boundaries, much of the nutrients applied (around 50 %) was lost to the surroundings (Zhang *et al*., 2015).

Nitrogen (N) and phosphorous (P) are two plant nutrients which are typically limiting in natural ecosystems (Guignard *et al*., 2017). The delicate balance between the ecosystem's inhabitants therefore pivots on the natural cycling of N and P. The artificial addition of N and P severs this interconnectedness and hence poses a great environmental hazard. Much damage has been caused over the past decades ranging from eutrophication and air pollution to biodiversity loss, climate change and stratospheric ozone depletion (Galloway *et al*., 2008). Although efforts

have been made to reduce agricultural nutrient pollution, the task remains difficult given the lack of an isolated system.

Soilless agriculture, such as hydroponics and aquaponics, have the advantage pollution control since a physical barrier exists between the fertilizer (nutrient solution) and the environment (Christie, 2014). With full nutrient containment, complete nutrient utilization is theoretically possible. Other than their pollution control potential, hydroponic systems claim several advantages over conventional agriculture such as reduced water consumption and independence on fertile land (Bradley & Marulanda, 2000). Drawbacks include higher capital and operational costs (Jensen, 1999). Regardless, the hydroponic industry is growing exponentially worldwide and will likely play a key role in the future of sustainable food production (Grand View Research, 2020). Despite their pollution control potential, hydroponic systems are known to produce large amounts of nutrient laden wastewater (Boneta *et al*., 2019). Some soilless systems make use of artificial soil-like mediums (such as sand, rockwool and peat moss). These systems function much like conventional (soil-based) greenhouses where the wastewater results from leaching. In true hydroponics, no artificial soil is used, and plant roots are submerged directly into the nutrient solution (Christie, 2014). This nutrient solution is free-flowing and must therefore be fully contained (no leaching occurs). The wastewater in these systems results from discharging the nutrient solution. Frequent replacement (discharging) of the nutrient solution is required to maintain high nutrient concentrations since plants consume nutrients relatively quickly. Also, plants transpire a lot of water (requiring water addition to control the solution volume), which results in rapid accumulation of inert and toxic species (Silberbush & Ben-Asher, 2001). Many hydroponic systems are small (backyard), and their wastewater is likely discharged directly to the environment. These systems, in which no effort is made to recycle the liquid medium, are known as “open hydroponic systems”. Large scale hydroponic farms are more strictly bound to legal limits of N and P discharge. These farms often make use of nutrient concentration control strategies (adding additional nutrient to prevent depletion), which allows for extended use of the solution until inert and/or toxic species build-up dictates replacement. These systems which recycle the nutrient solution are known as “closed hydroponic systems” (Kumar & Cho, 2014). The nutrient discharge rates from closed hydroponic systems are thus proportional to the nutrient concentrations at the time of replacement. This wastewater is often treated downstream of the hydroponic unit using reverse osmosis or constructed wetlands, for example (Prystay & Lo, 2001; Rufí-Salís *et al*., 2020).

The nutrient pollution rate (or the rate at which nutrients must be removed from the wastewater) can be described by Equation 1, which is simply a mol balance over the hydroponic outlet:

$$R_i = C_i Q \tag{1}$$

Where, R_i is the discharge rate of nutrient i (in units of mol per time) from the hydroponic unit, C_i is the concentration of nutrient i in the solution (in units of mol per volume), and Q is the volumetric discharge rate from the hydroponic unit (in units of volume nutrient solution per time), which can be interpreted as the frequency of solution replacements.

Although this wastewater is often treated (via reverse osmosis, for example), the space and energy requirements of these treatment technologies incurs their own environmental costs. To minimize environmental impact, the objective would be to minimize R_i. Q can be reduced through more extensive recycling of the nutrient solution and C_i can be reduced via concentration control strategies. By controlling nutrient concentrations, Q is effectively reduced since the same nutrient solution can be used continuously until inert build-up dictates replacement. R_i is then dependent on the nutrient concentrations at the time of replacement. Therefore, to minimize R_i, concentration control of N and P at low levels is key.

Nutrient concentrations in the discharge solution (C_i) for N and P have been reported in the range of 15 to 21 mM and 1 to 3 mM, respectively (Gagnon *et al.*, 2010). These levels are around 2 orders of magnitude higher than the concentrations at which half of the maximum nutrient uptake rates would be observed (Michalis-Menten constant K_M) (Akhtar *et al.*, 2007; Kuzyakov & Xu, 2013; Le Deunff *et al.*, 2019; Lefebvre *et al.*, 1990; Wang & Shen, 2012). Therefore, N and P concentrations could theoretically be controlled at much lower levels (and hence achieve proportionally lower pollution rates) without affecting plant growth.

The most common method of nutrient concentration control is through using the electrical conductivity (EC) of the solution (Christie, 2014). The EC is near-proportional to the total amount of nutrients in solution and thus controlling the EC at a setpoint (by dosing additional nutrients) controls the total nutrient concentration. This strategy is relatively cheap and robust. However, the EC does not supply information about individual nutrients. Consequently, the build-up of salinity and inert species in the medium renders the EC signal less reliable. Also, the nutrients

being dosed to maintain the nutrient concentrations must be added in near-exact proportions to which the plants consume them, else some nutrients will deplete whilst others accumulate. As such, nutrient concentrations must be controlled at relatively high levels to ensure that individual nutrients do not deplete without warning. Therefore, although Q is minimised, C_i (for N and P) remains relatively high. Other strategies have made use of ion-selective-electrodes (ISE), which are able to measure individual nutrient concentrations (Cho *et al*., 2018). For example, a nitrate ISE can directly measure the nitrate concentration in solution and hence additional nitrate can be dosed when the nitrate concentration drops below a setpoint value. Therefore, the nitrogen pollution rate can be minimized my minimizing the nitrate concentration in solution. However, ISEs are generally much more expensive and exhibit practical limitations such as signal drift, reduced accuracy over time, and interference from other ions in solution (Kim *et al*., 2013).

The novelty of the current work lies in the use of pH measurement (instead of using EC or ISEs) as the sole controller-input to maintain N and P concentrations at low levels. Given the drawbacks of the EC and ISE methods (discussed in more detail in Chapter 2), a pH-based control system provides hydroponic operators with an alternative. pH measurement and control is standard protocol in most hydroponic systems and therefore these control systems are affordable and can be easily implemented. Control schemes were designed for phosphate (plant phosphorous source), nitrate and ammonium (plant nitrogen sources), individually. Phosphate concentration control is considered in chapter 4 exclusively, directly after the Theory and literature and Experimental chapters (chapters 2 and 3). The remaining three chapters deal with nitrogen. Nitrate is the most common nitrogen source supplied to plants and is considered in chapter 5 exclusively. The following chapter (chapter 6) concerns ammonium. Ammonium is important from an environmental perspective since most organic fertilizers contain large fractions of ammonium (Chan-Pacheco *et al*., 2021). Wastewater from the anaerobic-digestion process is used as the model ammonium-rich wastewater (termed digestate) in chapter 6 (Koszel & Lorencowicz, 2015). Nitrification of ammonium is commonly carried out since ammonium is toxic to plants when supplied as the sole nitrogen source (Hachiya & Sakakibara, 2017). Also, nitrifying bacteria inevitably establish in hydroponic systems when ammonium is present and thus their effects cannot be ignored. When nitrification occurs within the hydroponic unit, the process is referred to as *internal* nitrification. This is the process considered in chapter 6. *External* nitrification is when ammonium is nitrified in a unit upstream to the hydroponic system. This method has many merits and therefore the following chapter (chapter 7) is

devoted to the external nitrification of ammonium as a pre-treatment step. The last chapter (chapter 8) is a general discussion and conclusion on the results from the previous chapters, specifically, the integration of the control schemes developed. The outline of the chapters discussed above is presented graphically in Fig. 0 below.

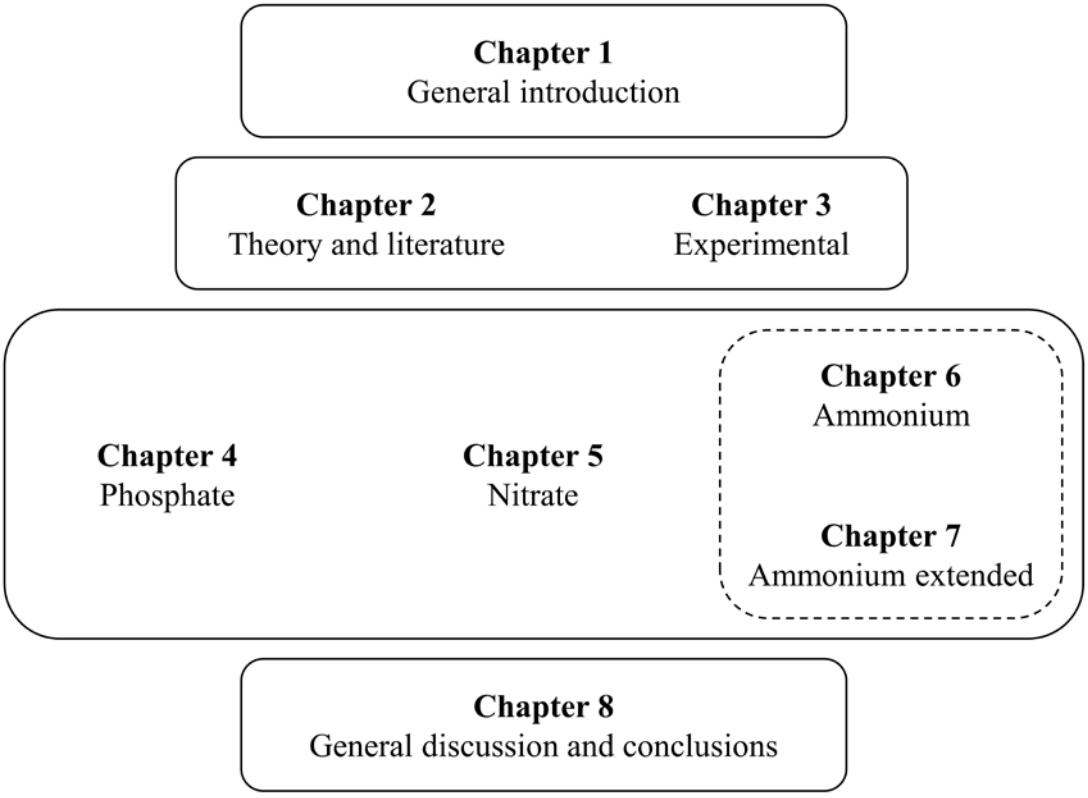

Fig. 0: Graphical outline of chapters.

CHAPTER 2 Theory and literature

2.1 Plant nutrition

The carbohydrate backbone of a plant is built during photosynthesis from carbon dioxide and water. Other elements are also required to build specialized molecules such as proteins (which contains nitrogen) and DNA (which required phosphorous). These elements are absorbed from the soil through the plant roots. Table 1 summarises these essential elements and the chemical forms in which they can be absorbed. The compounds of the first six elements (N, P, K, Ca, Mg and S) are known as macronutrients, since they are absorbed in much higher quantities as compared with the remaining compounds, known as micronutrients.

The first published hydroponic nutrient solution was formulated by Hoagland and Arnon (1938), which contained all the nutrients listed in Table 1 (in rough proportions to which plants absorb them). Nickel was not explicitly added as it was not yet known to be an essential plant nutrient (Brown, 1987). Its necessity was unnoticed due to its very low requirements and was likely present as a trace contaminant in the other nutrient salts used. Hoagland's solution contains N, P, K, Ca, Mg and S (macronutrients) in molar parts of 15 : 1 : 6 : 5 : 2 : 2. Other nutrient solution formulations followed (Hewitt, 1966; Cooper, 1979; Steiner 1984), but these varied only slightly in terms of the total nutrient concentration and the ratios between nutrients. Hoagland's solution is generally suitable for optimal plant growth and is still widely used. The macronutrient proportions of Hoagland's solution are shown in Fig. 1 (left-hand-side chart). Note that the ionic charges of each nutrient (see Table 1) are also shown in Fig. 1 (right-hand-side chart). This will be further discussed in later sections, but the importance lies in the choice of nitrogen source. Since nitrogen makes up around half of the total nutrients absorbed and can be supplied as either a cation or anion, the choice of nitrogen source dictates the overall charge

absorbed. As electrical neutrality must be maintained in the solution, the plant must exude the net charge absorbed (De Wit *et al*., 1962). For example, if ammonium is supplied as the sole nitrogen source, the net charge absorbed is positive and the plant must exude additional cations (typically H^+) to maintain electrical neutrality. For this reason, nitrate is often supplied as the primary nitrogen source since a lower net charge is absorbed.

Table 1: Essential elements required by plants together with the molecular form in which they can be absorbed (Mahler, 2004).

Essential element	**Absorbable forms**
N	NO_3^-, NH_4^+
P	$H_2PO_4^-$, HPO_4^{2-}, PO_4^{3-}
K	K^+
Ca	Ca^{2+}
Mg	Mg^{2+}
S	SO_4^{2-}
B	H_3BO_3, $H_2BO_3^-$, BO_3^{2-}
Cl	Cl^-
Cu	Cu^{2+}
Fe	Fe^{2+}
Mn	Mn^{2+}
Mo	MoO_4^{2-}
Zn	Zn^{2+}
Ni	Ni^{2+}

2.2 Nitrogen

Proteins differ from carbohydrates by the presence of a nitrogenous functional group (amine). Most organisms higher up on the food chain consist primarily of proteins (besides water), most of which (specifically, the amino acids building blocks) were originally produced by plants. The absorption of nitrogen by plants to produce proteins (including other specialized molecules such as DNA and RNA) is therefore key to life of earth. Unlike the other nutrients listed in

Table 1, nitrogen originates from the atmosphere (N_2). Plants cannot use this abundant source of nitrogen directly and instead rely on microbial processes that convert the N_2 into NH_4^+ (Burris, 2001). These bacteria are called nitrogen fixing bacteria and they have various relationships with plants. The bacteria depend on the organic carbon produced by the plants and in turn fixates N_2 for the plants (Miles *et al*., 1992). A direct symbiotic relationship exists between nitrogen fixing bacteria and legumes, where the bacteria establish within the plant root (Wang *et al*., 2018). The plant feeds the bacteria with carbonaceous molecules and the bacteria releases NH_4^+ for the plant to use. Other plant species have less direct relationships with plants, such as associative nitrogen fixation. In these relationships, the bacteria are found on the roots or in the root vicinity (rhizosphere) and consume the organic carbon exudated from the roots (Miles *et al*., 1992).

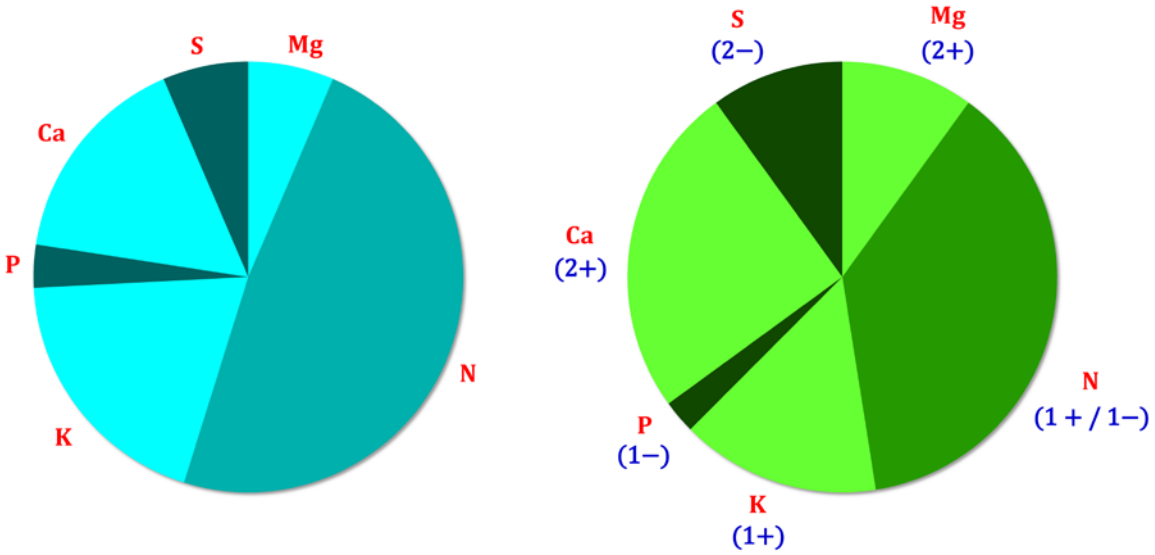

Fig. 1: Left-hand-side pie chart: Molar fractions of the macronutrients in Hoagland's solution, which are roughly in proportion to the rates at which plants absorb them. Actual molar concentrations are 15, 1, 6, 5, 2, 2 mM for N, P, K, Ca, S and Mg, respectively. Right-hand-side pie chart: Valency/charge fractions (absolute, regardless of $+/-$) of the macronutrient. For example, Hoagland's solution contains 5 mM Ca, which equates to 16 mol % of the total macronutrients as shown in the left-hand-side pie chart. Ca has a charge of 2+ and therefore constitutes 10 mM valence electrons, which is 25 % of the total valences as shown in the right-hand-side pie chart. Note that P is given the charge of -1 since $H_2PO_4^-$ is predominantly absorbed (see Table 1).

Most nitrogen fixing bacteria are not dependent on plants and can exist in the soil if organic carbon is present. When these bacteria die and decompose, organic nitrogen (bacterial proteins) accumulate in the soil. Other types of bacteria, known as mineralizing bacteria, can consume the organic nitrogen (from dead bacteria/ plant/animal material) and release NH_4^+ into the soil (Lin, 2010). Some plant species are dependent on this free ammonium source and have no direct relationship with nitrogen fixing bacteria (Miles *et al*., 1992). A different group of bacteria, known as nitrifying bacteria, derive their energy from the oxidation of ammonium. These bacteria are responsible for the input of NO_3^-, which is the second nitrogen source available to plants (Quinlan, 1984). Finally, another group of bacteria exist which uses the oxidised ammonia to make N_2, thus completing the nitrogen cycle (Eldor, 2015).

Nitrogen fixation is energy intensive, however, and thus the influx of plant-available nitrogen to the biosphere is tightly regulated by these bacteria. As such, fixed nitrogen is often the limiting nutrient for plant growth in natural ecosystems (Burris, 2001; Miles *et al*., 1992). This changed early in the 20th century with the advent of the Haber-Bosch process which converts atmospheric nitrogen into ammonia catalytically at high temperatures and pressures (Burris, 2001). The input of synthetic nitrogen has greatly disturbed the delicate balance between ecosystem inhabitants and has resulted in far reaching environmental consequences. The nitrogen cycle as described above, including the artificial addition of synthetic nitrogen is depicted in Fig. 2.

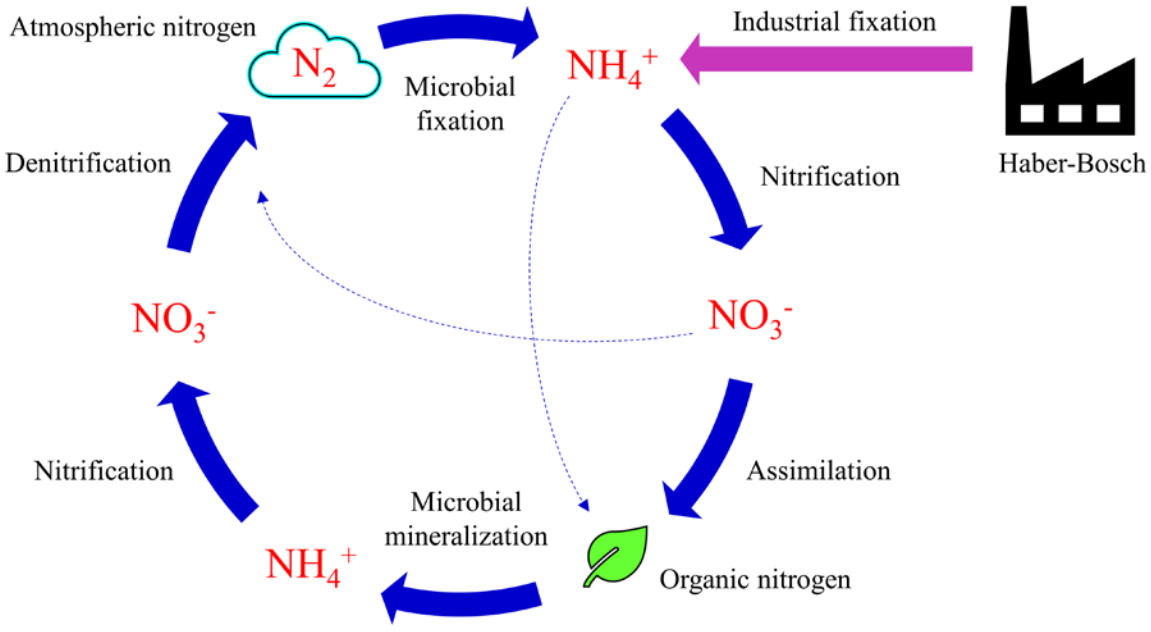

Fig. 2: Illustration of the natural nitrogen cycle including the input of synthetic nitrogen.

2.3 Phosphorous

Phosphorous (P) forms part of several fundamental biological molecules such as DNA and ATP, which are essential to all life on earth. P enters natural ecosystems via the slow process of rock weathering, where a fraction is recycled within local food chains and the remainder exits into waterways and finally the ocean (Alewell *et al*., 2020). Modern agriculture is dependent on additional P inputs derived from phosphate rock, which is a non-renewable resource and current global reserves may be depleted in 50 - 100 years (Cordell *et al*., 2009). Losses of P are up to an order of magnitude smaller than those of nitrogen, but P is perhaps of greater concern in terms of the ecological quality of fresh waters and may be more significant with respect to freshwater eutrophication (Withers & Lord, 2002). The peak usage of P is estimated to occur around 2030 (Cordell *et al*., 2009) and thus better P management is an urgent issue (Rufi-Salis *et al*., 2020).

As stated in Table 1, P is absorbed by plant in various protonated forms of phosphate. The four different protonated forms (H_3PO_4, $H_2PO_4^-$, HPO_4^{2-} and PO_4^{3-}) are collectively referred to as inorganic phosphate (Pi). These species exist in chemical equilibrium with one another and their ratios in solution is a function of the solution's pH. These equilibrium fractions are plotted in Fig. 3, which were calculated from the Brønsted-Lowry acid-base equilibrium equations (Kotz *et al*., 2009).

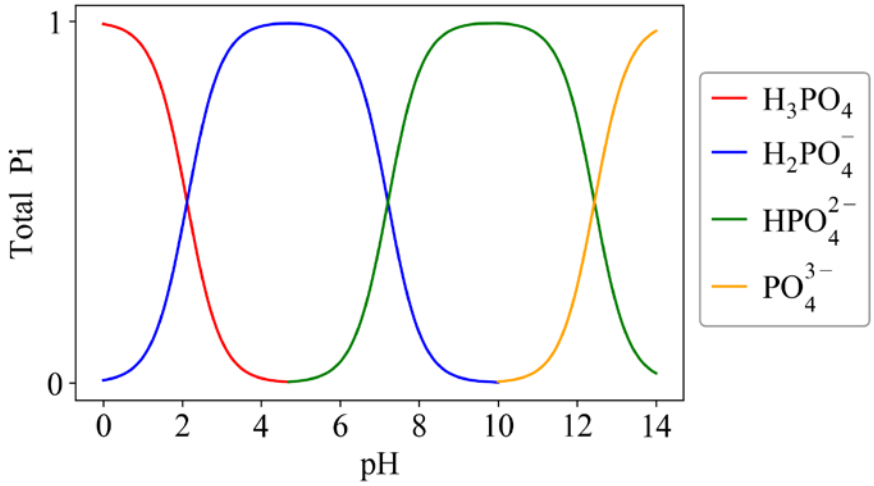

Fig. 3: Distribution of the various protonated forms of phosphate as a function of the solution's pH.

2.4 Hydroponics

The fundamental difference between conventional agriculture and hydroponics is that instead of soil cultivation, plant roots are submerged in an aqueous medium with all the required nutrients dissolved therein. In hydroponics, the plants are supported via mechanical means instead the roots being anchored in the soil. These mechanical supports may include gravel beds or foam collars which hold plant stems in place (while the roots are suspended in the liquid) (Christie, 2014). Agitation and aeration of the liquid is required to ensure sufficient mixing (to prevent diffusional limitations) and to supply dissolved oxygen to the roots. Several different hydroponic systems have been developed to meet these requirements. Common systems include the Nutrient-Film-Technique and the Ebb-and-Flow (flood-and-drain) system (Trejo Téllez & Gómez-Merino, 2012). Hydroponics offers several advantages over conventional agriculture. Most commonly, faster plant growth rates, lower water consumption, independence on fertile land, freedom from soil-borne diseases and pests, and easier control of fertiliser usage (Bradley & Marulanda, 2000; Christie, 2014; Kumar & Cho, 2014; Rufi-Salis *et al*., 2020; Seungjun & Jiyoung, 2015). Drawbacks also exist such as higher capital investments (Jensen, 1999).

The liquid medium, termed the nutrient solution, is of primary concern in hydroponic systems. Besides mixing and aeration requirements, the nutrient solution must be mildly acidic (pH ≈ 6). At pH values higher than 7, some nutrients can become unavailable or precipitate in solution, and at pH values below 4, plant roots are damaged (Bugbee, 2004). Nutrient concentrations and the amount of nutrients relative to one another are also important (Steiner, 1961). Common nutrient solution formulations are given in Table 2. These solutions were formulated based on the total nutrient concentration and the relative uptake rates of the individual nutrients. High nutrient concentrations are desired to prevent nutrient depletion which will result in nutrient deficiency symptoms and cessation of plant growth. High nutrient concentrations however mean high ionic strength since all the nutrients are present in ionic form. The ions exert a negative osmotic pressure on the nutrient solution which is an important variable to ensure healthy plant growth since water is transported in plants via osmotic pressure differences (McElrone *et al*., 2013).

Table 2: Elemental composition of common nutrient solutions as reported by (Trejo Téllez & Gómez-Merino, 2012). All values are given in ppm (mg-element L^{-1}), except for the bracketed values for N and P in Hoagland's solution.

Nutrient	Hoagland & Arnon (1938)	Hewitt (1966)	Cooper (1979)	Steiner (1984)
N	210 (15 mM)	168	200-236	168
P	31 (1 mM)	41	60	31
K	234	156	300	273
Ca	160	160	170-185	180
Mg	34	36	50	48
S	64	48	68	336
Fe	2.5	2.8	12	2-4
Cu	0.02	0.064	0.1	0.02
Zn	0.05	0.065	0.1	0.11
Mn	0.5	0.54	2	0.62
B	0.5	0.54	0.3	0.44
Mo	0.01	0.04	0.2	N/A

The total number of ions in solution is directly proportional to the osmotic pressure of the solution (for ideal solutions), according to Van 't Hoff's theory described in Equation 2 (van't Hoff, 1887).

$$\Pi = iCRT \tag{2}$$

Where, Π is the osmotic pressure of the solution (in units of force per area), i is the Van't Hoff's factor (dimensionless), C is the molar concentration of the solute, R is the ideal gas constant and T is the absolute temperature.

Numerous studies have examined the effects of osmotic pressure on hydroponic performance and optimal values are often suggested for various plant species (Sonneveld & Voogt, 2009; Sublett *et al*., 2018). These generally do not exceed that of Hoagland's solution. Diluted

Hoagland's solution is often used (half or quarter strength) when nutrient concentrations can be managed to prevent depletion. From Equation 2, the osmotic pressure is proportional to the ionic concentration, which is near-proportional to the nutrient solution's electrical conductivity (EC) (Trejo-Téllez & Gómez-Merino, 2012). The EC is easily measured, and EC probes are relatively cheap. As such, the total nutrient concentration in solution is commonly controlled using EC. Typical ECs employed in hydroponic solutions range between 1.5 dS m^{-1} and 2.5 dS m^{-1} (Hosseinzadeh *et al*., 2017).

2.5 Pollution prevention and mitigation from hydroponic systems

High osmotic pressures negatively affect the hydraulic properties of plants and therefore, nutrient concentrations generally do not exceed that of Hoagland's solution (Sonneveld & Voogt, 2009). To get an idea of how quickly plants consume the nutrients in Hoagland's solution, consider a plant cultivated in 1 L of Hoagland's solution. If the plant has a nitrogen content of 5 mg g^{-1} (fresh mass), 42 g of new biomass can be grown, which is about the size of a juvenile lettuce plant. From this calculation, it appears that limited nutrients are available in the solution, since the final harvested plant will typically be much larger than a juvenile lettuce plant (meaning that additional nutrient will be required). Although the volume of nutrient solution used per plant varies greatly between different hydroponic systems, most systems required additional nutrients during a crop cycle. The most robust approach is to replace the nutrient solution and discharge the spent solution into the environment or municipal waterways. These systems are known as open hydroponic systems, and although environmentally hazardous, have been widely employed. As water quality restrictions tighten however, efforts to reduce these pollution rates have become topical. Many studies aimed to recycle the liquid medium by adding additional nutrients to prevent depletion. These systems are known as closed hydroponic systems since they attempt to reuse to solution continuously (Kumar & Cho, 2014). This is most-commonly accomplished by measuring the nutrient solution's electrical conductivity (EC) and dosing additional nutrients in response (Christie, 2014; Domingues *et al*., 2012). The EC of the solution is a measure of the total nutrient concentration. This approach requires that nutrients are added in the same proportions to which the plants consume them, otherwise depletion of some nutrients and accumulation of others will result. Adding nutrients in the exact proportions is near-impossible since two nutrients must be added simultaneously (a single nutrient salt) and some nutrient salts are insoluble (such as calcium and magnesium phosphates, for example). Therefore, without sufficient degrees of freedom, some nutrients must be added in too low/high

proportions (resulting is accumulation of some and depletion of others at constant EC), To add nutrients in near-exact proportions, their sodium/chloride salts must be used, which causes salinity build-up.

Similar to EC, the transpiration rates of the plants have also been used (Bugbee, 2004). Plant nutrient uptake is proportional to plant size, which is proportional to the transpiration rates of the plants. Therefore, nutrients can be added to the water used to control the solution volume (top-up or refill solution). If the refill solution contains the correct amount of nutrients in correct proportions, the concentration of nutrients in the hydroponic unit can be kept constant. This approach has similar drawbacks to using EC in which nutrient imbalances are likely to result. Furthermore, plant transpiration rates are strongly affected by changes in temperature, humidity, solar radiation and windspeed (Allen *et al*., 1998), requiring different refill solution makeups. These variables must hence be controlled for this strategy to be effective.

Ion-selective-electrodes (ISE) have also been used to control individual nutrient concentrations since the EC only provides information regarding the total nutrient concentration. Nitrate, ammonium, and phosphate ISEs have been used to control these respective pollutants in solution, albeit not at significantly low concentrations (Cho *et al*., 2018; De Marco & Phan, 2003; Jung *et al*., 2019a; Jung *et al*., 2019b; Kim *et al*., 2011; Kim *et al*., 2013; Xiao *et al*., 1995). These instruments are expensive, however, and exhibit practical limitations such as signal drift, reduced accuracy over time and interference from other ions in solution (Bugbee, 2004; Christie, 2014; Jung *et al*., 2019b; Kim *et al*., 2013).

Although the nutrient solution can be recycled extensively when nutrient concentration control is employed, infinite recycling is not possible due to nutrient imbalances (discussed above) and inert build-up resulting from water addition (to compensate for transpiration) (Silberbush & Ben-Asher, 2001). Also, plants exude toxic species into the nutrient solution, which is intended to cause detrimental effects to competing species in the soil (Hosseinzadeh *et al*., 2017). In hydroponic systems however, this results in autotoxicity (known as allelopathy). Therefore, complete water treatment technologies, such as membrane filtration, are often employed. The primary membrane filtration techniques include ultrafiltration (UF), reverse osmosis (RO) and electrodialysis (ED). UF permits electrolytes and low molecular weight organic solutes to pass through; while RO membranes reject all components apart from pure water (Koide & Satta, 2004). UF and RO operate at high pressures, which is required to drive the water molecules

through the polymer membrane. ED uses the same principle of molecular filtration but employs electric potential instead of pressure as the driving force. The primary drawback of these systems is their energy requirements during operation, which impacts the environment through a different avenue. RO is most-commonly employed in industry but only a few records exist on its application to hydroponic wastewater treatment (Kumar & Cho, 2014). Rufí-Salís *et al*. (2020) used RO to treat wastewater from a rooftop greenhouse and estimated a 50 % reduction in the overall environmental impact of the system. Martin-Gorriz *et al*. (2021) used RO powered by solar energy to treat hydroponic wastewater. The overall environmental impacts reported are a 72 % reduction in eutrophication potential, 43 % increase in fossil fuel combustion, 37 % increase in global warming and 32 % increase in acidification.

Chemical precipitation has also been used as a nutrient separation technique. Precipitation of nutrients is induced by increasing the pH of the wastewater. However, only some of the nutrients can be removed with this technique. Phosphate, for example, precipitates out as calcium and magnesium phosphates at high pH but nitrates remain in solution. Saxena & Bassi (2013) reported a 97 % removal of phosphate after raising the pH to 11 with NaOH. Rufí-Salís *et al*. (2020) reported complete removal of phosphate and partial removal of magnesium.

Various biological wastewater treatment methods have also been employed. Nitrification followed by denitrification is commonly employed in municipal wastewater treatment to remove ammonium and nitrate. The ammonium is first converted to nitrite and/or nitrate by nitrifying bacteria under aerobic conditions. Subsequently, the produced nitrite/nitrate is reverted to atmospheric nitrogen by denitrifying bacteria. This second step can be carried out by either heterotrophic or autotrophic bacteria. Heterotrophic denitrification occurs anaerobically and requires organic carbon as energy source. Autotrophic denitrification uses inorganic substrates such as hydrogen gas and reduced sulphur compounds, instead of organic carbon (Di Capua *et al*., 2019). Organic carbon is typically abundant in municipal wastewater and hence heterotrophic denitrification can occur without substrate addition. Hydroponic wastewater contains little (or no) organic carbon nor enough electron donors for autotrophic denitrification. Substrate addition is thus the financial and environmental expense of employing denitrification for hydroponic wastewater treatment. This problem was addressed by Park *et al*. (2008) who constructed denitrification filters which used plant prunings as the carbon source. The authors reported nitrate removal efficiencies > 95 % at carbon to nitrogen loading rate of 3:1 (mass basis

is assumed). Yamamoto *et al*. (2000) used thiosulfate as electron donor in an autotrophic denitrification unit to treat hydroponic wastewater and reported a 90 % N removal efficiency.

The use of constructed wetlands is another biological wastewater treatment method. This treatment technique is known as phytoremediation as it essentially involves the growth of non-target crops (such as reeds) within a wetland-like biome. The wastewater flows through this artificial habitat and the organisms within it (primarily the plants) consume the nutrients in the wastewater. Prystay & Lo (2001) used a constructed wetland (planted with Bulrush) to treat effluent from an industrial-sized greenhouse. The authors reported 65 %, 54 %, and 74 % removal efficiencies for phosphate, nitrate, and ammonium, respectively. Grasselly *et al*. (2005) employed a constructed wetland which hosted plants (common reeds and Bulrush) and denitrifying bacteria (discussed in the previous section). The authors used vinery sewages as the organic substrate for the denitrifying bacteria and reported a nitrogen removal efficiency of 70 % – 100 %. Gagnon *et al*. (2010) studied the efficiency of a constructed wetland in cold climates (8 °C) using Reed canary grass and *Typha sp*. The authors reported removal rates of 4.9 g-N m^{-2} day^{-1} and 0.5 g-P m^{-2} day^{-1}. The streamlines (flow patterns) through constructed wetlands can be manipulated to allow for either aerobic or anaerobic conditions. Seo *et al*. (2008) used a combination of horizontal flow and vertical flow patterns to create regions of both aerobic (allowing nitrification) and anaerobic (allowing for denitrification) conditions. The authors also used calcite filter media which can remove nutrients via adsorption. Removal efficiencies of 68.4 % and 94.3 % for N and P were reported. Other phytoremediation technologies using phytoplankton have also been employed. Salazar *et al*. (2021) cultivated microalgae in a photobioreactor fed with hydroponic wastewater and reported 18 % – 35 % removal efficiencies of N and 40 % – 98 % for P. At around the same time, Delrue *et al*. (2021) also treated hydroponic wastewater with microalgae and reported removal efficiencies of 98 % and 87 % for N and P.

Plant autotoxicity and infections must also be addresses when extensive recycling of the nutrient solution is employed. Plants release numerous organic compounds from their roots, known as root exudates. Besides the toxic compounds mentioned earlier, these exudates primarily consist of organic acids, which introduces a carbon substrate for heterotrophic microorganisms. Various plant infections (such as root rot caused by *Pythium* infection) are intensified by the presence of organic carbon. The methods used to remove these species (other than the membrane filtration methods discussed earlier) are adsorption by activated carbon, electro-

degradation treatment and photo-catalytic treatment. Adsorption by activated carbon (AC) is the most common method (Richa *et al*., 2020). Several authors have reported significant increases in plant yield when activated carbon or charcoal was added to the nutrient solution (Asaduzzaman & Asao, 2012; Lee *et al*., 2006; Pramanik *et al*., 2000; Yu & Matsui, 1994; Asao *et al*., 2003). Electrical degradation (ED) has also been applied in which organic root exudates are oxidised to carbon dioxide by passing an electrical current through the solution. Asao *et al*. (2008) and Asaduzzaman *et al*. (2012) used ED to mitigate the effects of autotoxicity in existing hydroponic cultures. The authors reported 71 % and 99 % recovery rates, respectively. Photocatalytic treatment (PC) has also been used which, similarly to ED, also involves oxidation of the organic exudates. Electromagnetic radiation is emitted onto a semiconductor (such as UV onto TiO), which causes the semiconductor to exhibit a strong oxidation effect, thus resulting in combustion of the organic species in the solution. Several authors have reported significantly higher plant yields when employing (PC) (Miyama *et al*., 2009; Miyama *et al*., 2012; Miyama *et al*., 2013; Sunada *et al*., 2008; Qui *et al*., 2013).

Besides chemical build-up, pathogens can also become prevalent in the solution and affect plant growth. With sufficient organic carbon removal as discussed above, pathogens are minimized but plant infections can still occur, and several disinfection techniques have been suggested for the nutrient solution. Most common are UV, ozone, and hydrogen peroxide treatment methods. Choi *et al*. (2011) used UV sterilization on waste hydroponic nutrient solution and reported that harmful bacteria were removed to below acceptable limits. Zheng & Tu (2000) used to UV sterilization to remove pathogens from a nutrient solution inoculated with *Pythium aphanidermatum* (root rot) and reported significant reductions in fungal populations but no increases in plant yield. Lau and Mattson (2021) used hydrogen peroxide in organic based nutrient solutions and reported equal plant yields as compared with a synthetic nutrient solution (growth was stunned when the organic solution was used without hydrogen peroxide). Graham *et al*. (2011) used ozone in a drip irrigation system and reported no adverse effects on plant growth as significant reductions in algae populations. Msayleb *et al*. (2021) used ozone bubbling to inactivate *Fusarium oxysporum*, which causes Fusarium wilt, and reported 0 % viability of the pathogen.

2.6 pH dynamics in hydroponic systems

Plant root exudates consist of numerous chemical species. In the absence of nutrient absorption, these exudates result in an overall acidic effect due the large fraction of organic acids in the exudates (Dijkshoorn, 1962; Hosseinzadeh *et al*., 2017). These are depicted as "COO^- H^+" in Fig. 4, which summarizes the pH dynamics in hydroponic systems as discussed below. The absorption of nutrients and the reactions they undergo during assimilation also produces pH effects. Besides nitrogen, which is absorbed in the largest amount, the remaining nutrients produces an overall acidic effect (Smith & Raven, 1979). This is because most of these nutrients are positively charged as shown in Fig. 1, and the plant must in turn exude an equivalent number of protons (H^+) to maintain electrical neutrality in solution (Dijkshoorn, 1962). This is theoretical however, since nutrients are not strictly absorbed and assimilated in isolation. These pH effects are typically dwarfed by the pH effects associated with nitrogen absorption. When nitrate is absorbed as the sole nitrogen source, hydroxide exudation (or proton absorption) is required to balance the electrical charge (Dijkshoorn, 1962). Therefore, when nitrate is supplied as the sole nitrogen source, the pH of the solution rises. Similarly, if ammonium is absorbed as the sole nitrogen source, cationic exudation (H^+) is required to maintain electrical neutrality (Hachiya & Sakakibara, 2017), and the pH of the solution decreases. Raven (1985) defined the theoretical amounts of hydroxide and protons produced during the assimilation of nitrate and ammonium according to Equations 3 and 4:

$$3NH_4^+ + 45CO_2 + 32H_2O \rightarrow C_{45}H_{72}N_3O_{32} + 4H^+ + 45O_2 \quad (3)$$

$$3NO_3^- + 45CO_2 + 37H_2O \rightarrow C_{45}H_{72}N_3O_{32} + 2OH^- + 51O_2 \quad (4)$$

It follows that a ratio of nitrate to ammonium absorbed by the plant exists such that the acidic and basic effects balance (pH remains constant). This phenomenon has been used to develop various ammonium-to-nitrate feed strategies to maintain pH levels (Imsande, 1986; Pitts & Stutte, 1999)

When ammonium is present in hydroponic systems, nitrifying bacteria become established over time and generate an acidic effect. These bacteria commonly consist of two complementary groups in symbiosis, namely, ammonium oxidising bacteria and nitrite oxidising bacteria (Quinlan, 1984). The first group generate their energy requirements from the oxidation of

ammonium, which produces nitrite (NO_2^-). This reaction is highly acidic in which two protons are released per ammonium oxidised (Norton & Ouyang, 2019). The second group of bacteria oxidizes nitrite to nitrate (NO_3^-), usually at faster rates. This second reaction is pH neutral (Madigan *et al.*, 2003) and thus the overall reaction is often described as: $NH_4^+ \rightarrow NO_3^- + 2H^+$.

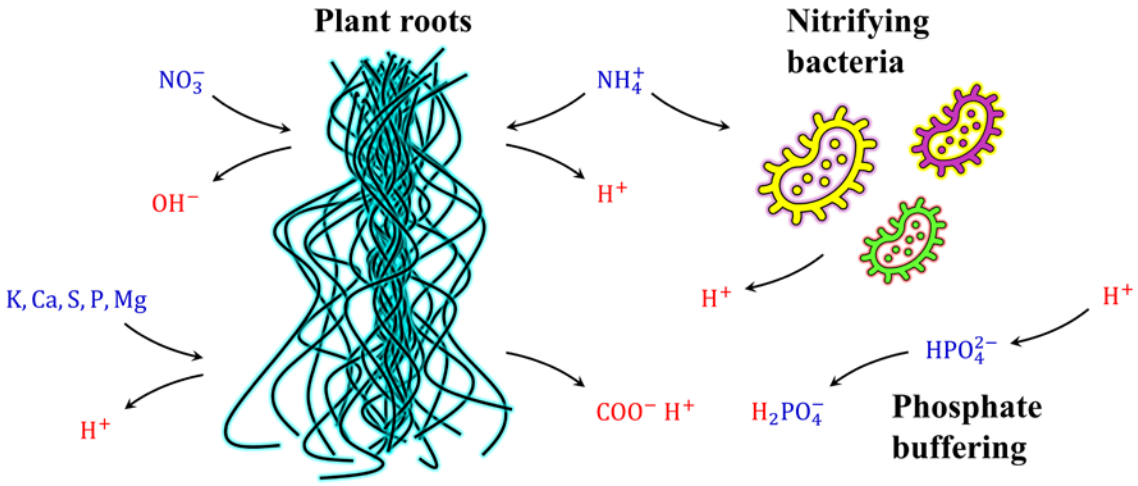

Fig 4: Illustration of pH phenomena which occur in hydroponic systems. Shown are the pH effects from plant root exudation, the pH effects associated with nutrient uptake, the pH effect of ammonium oxidation by nitrifying bacteria, and the pH buffering effects caused by the presents of phosphates.

The exudation of acidic and basic species results in the ionization of water to form hydronium and hydroxide ions: $2H_2O \leftrightharpoons H_3O^+ + OH^-$ (Kotz *et al.*, 2009). For convenience, hydronium ions (H_3O^+) are typically considered as "free protons" (H^+) in solution since the protons are loosely attached to the water molecules. Therefore, the ionization reaction is simplified to: $H_2O \leftrightharpoons H^+ + OH^-$. This reversible reaction has an equilibrium constant of 10^{-14} mol L^{-1} at 25 °C. The pH of the solution is defined as the logarithm of the amount of H^+ (hydronium) in solution ($pH = -\log[H^+]$). At a neutral pH, in which $[H^+] = [OH^-] = 10^{-7}$ mol L^{-1}, the addition of protons or hydroxide are directly reflected in the solutions pH since only a small amount ($< 10^{-7}$ mol L^{-1}) will react with the existing hydroxides/protons in solution to form water. For example, if 0.1 M HCl is added to pure water $pH = 7$ (assuming complete ionization of the HCl to form H^+ and Cl^-), the water ionization reaction will occur in reverse only to a very small extent as the added H^+ reacts with the small amount of OH^- (10^{-7}), which was initially present in the water. This small change can be neglected, and the pH will be:

$-\log(0.1) = 1$. This assumption does not hold if chemical species other than water are present that can react with the added protons. Phosphates are one such species. Consider a phosphate solution at pH of 7, it can be seen from Fig. 3 that near-equal amounts of HPO_4^{2-} and $H_2PO_4^-$ will be present in the solution. When additional protons (such as HCl) are added, a large fraction will react with HPO_4^{2-} to form more $H_2PO_4^-$, and some $H_2PO_4^-$ will react to form H_3PO_4. Therefore, less free protons (hydronium ions) will result when 0.1 mol HCl is added to 1 L of a phosphate solution as compared with the above example (pure water). Hence, the final pH will be > 1. Chemical species such as phosphate are known as pH-buffering species since they effectively resist changes in pH. The extent to which a solution resist pH changes is termed the buffering capacity (β) of the solution. β is defined as the equivalents of strong acid (mols of protons) or base added to the solution, divided by the corresponding change in pH and the solution volume, as shown in Equation 5 (Michałowska-Kaczmarczyk & Michałowski, 2015). β also depends on the absolute pH of the solution as buffering species typically buffer the pH only within specific pH ranges. Phosphates, for example, are good pH buffers around a pH of 7, but not at very low or high pH values. Therefore, ΔpH is often standardised at an initial pH value.

$$\beta = \frac{\Delta H^+}{\Delta pH\, V} \tag{5}$$

Where β is the buffering capacity, ΔH^+ is the number of protons added to the solution, ΔpH is the corresponding change in pH and V is the solution volume.

CHAPTER 3 Experimental

3.1 Experimental setup

The setup consisted of four independent hydroponic units, each designed to host a single plant. A photo of the setup, and a simplified process-flow-and-instrumentation diagram (of one of the four systems) is shown in Fig. 5 and Fig. 6, respectively. Each system was equipped with two peristaltic dosing pumps (P1 and P2 in Fig. 6) and two dosing reservoirs (D1 and D2) for accurate chemical addition, a water addition pump (P3) for liquid level control, and a pH probe. The controller (Arduino™, labelled "C" in Fig. 6) enabled online pH measurements and autonomous pump actuations. The liquid level was controlled automatically at a setpoint which corresponded to a liquid volume of 1.8 L in each system. An ebb-and-flow type hydroponic system was selected in which the flood-and-drain mechanism was induced by switching P4 on for 25 min (flood) and off for 5 min (drain), continuously. When P4 is on, liquid flows into the plant vessel and biofilter (open connection between the two units). The "free drain" outlet shown in Fig. 6 exhibits a lower flowrate (controlled by appropriate tube diameter selection) than the incoming flowrate from P4. Therefore, the plant vessel and biofilter continue to fill until the liquid level reaches the overflow connection of the plant vessel. The excess liquid flows back into the reservoir via the overflow and thus a stead state flooding of the plant vessel and biofilter is realized. After 25 min, P4 is switched off and both units drain via the "free drain" outlet. For each experiment (run), all four systems were operated in parallel under the same conditions, which essentially represented a quadruplicate (four repeat runs). Kale (*Brassica oleracea* var. *Sabellica*) was used as the model plant in all experiments. The biofilter shown in Fig. 5 and Fig. 6 contained inert packing for microbial attachment. The biofilter was initially included as an optional feature and only served a purpose in the last two chapters of this dissertation.

3.2 Apparatus and instruments

An Arduino Mega 2560™ was employed as the controller platform which controlled all four systems simultaneously. HAOSHI™ pH probes ("pH meter Pro") were used for online pH measurements. Kamoer© peristaltic pumps ("Precision Peristaltic Pump + Intelligent Stepper Controller") were used for dosing chemicals such as acids and bases. DFrobot™ peristaltic pumps ("digital peristaltic pump") were used for automated water addition.

Fig. 5: Annotated photo of the experimental setup showing four independent hydroponic systems. In each experiment, all four systems were operated in parallel under the same conditions (thus yielding four repeats). Each system is labelled "system 1" to "system 4" (from right to left) in the subsequent data reports.

All chemicals/nutrients were purchased from Merck™ (BioXtra©, ≥ 99.0 %). For plant lighting, four Mars Hydro™ 400 W blue/red LED lights (Mars II 400 LED Grow Light©) were

used, producing 10 000 Lux at the canopy. Kale seeds (*Brassica oleracea* var. *Sabellica* or Vate's Blue Curled Kale) were purchased from Raw™. The main recirculation pumps (responsible for the ebb-and-flow mechanism) were purchased from Xylem™ ("Flojet Diaphragm Electric Operated Positive Displacement Pump, 3.8 L min^{-1}, 2.5 bar, 12 V DC"). For seedling propagation, aeroponic systems (Aeroponic Cloner) purchased from hydroponic.co.za™ were used. DoPhin® "14 in 1 nitrifying bacteria" was used as an inoculum. Evolution Aqua Kaldnes® K1 Media was used for biofilter packing. Four Regent® 9500 air pumps were used for sparging. Chemical analysis of the nutrient solution was done via liquid samples of 2 mL taken daily. Phosphate, nitrate, nitrite, and/or ammonium analysis was done on these samples (depending on the aims of the run) using Merck™ photometric cell tests (phosphate test: PMB 0.0025 − 5.00 mg/l PO_4-P, Spectroquant© nitrate test: DMP 0.10 - 25.0 mg/l NO_3-N, nitrite test: 0.002 - 1.00 mg/l NO_2-N, and ammonium test: 2.0 - 150 mg/l NH_4-N Spectroquant®). The absorbance was measured in a spectrophotometer (Agilent Technologies™, Cary 60 UV-Vis, G6860A) at 690, 340, 525, and 690 nm for phosphate, nitrate, nitrite, and ammonium.

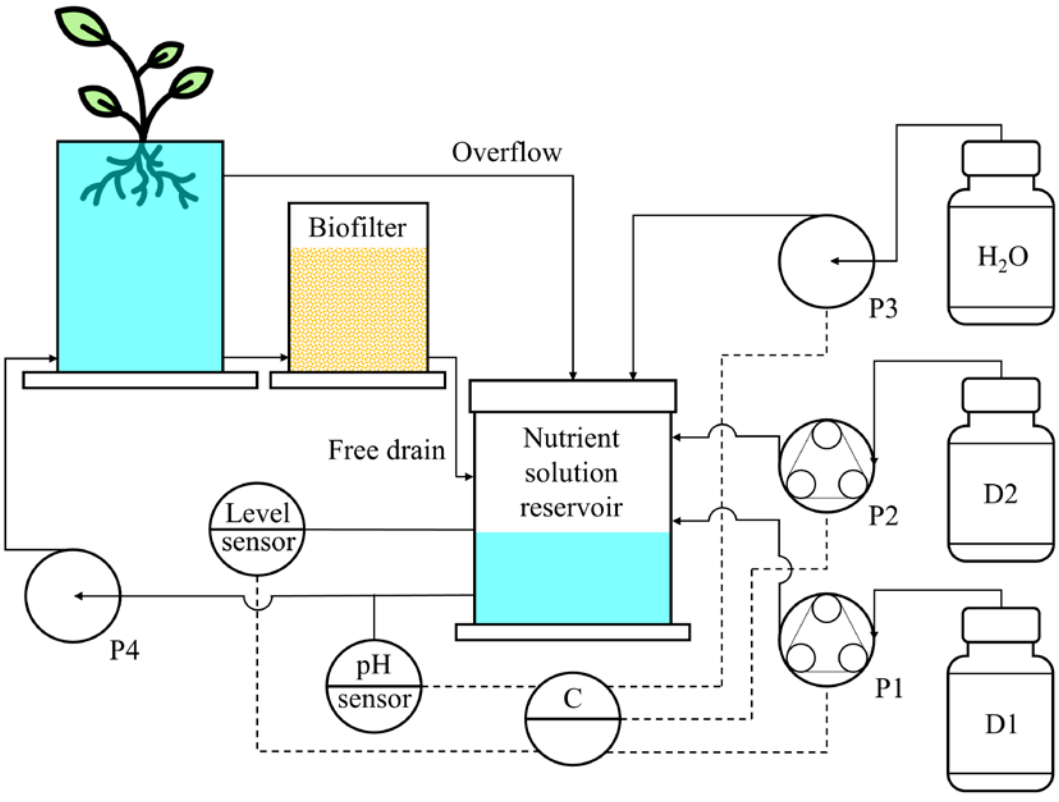

Fig. 6: Simplified process flow and instrumentation diagram of the experimental setup (one of the four) showing major control elements (controller "C", sensors, and pumps), vessels (plant vessel, biofilter and nutrient solution reservoir), and dosing reservoirs (D1, D2, H_2O).

CHAPTER 4 Phosphate

4.1 Introduction

Although inorganic phosphate (Pi) is supplied in much lower quantities than N (Fig. 1), the environmental impacts resulting from Pi pollution are near-equal in magnitude to those of N pollution. This is particularly true for fresh-water ecosystems in which Pi is often the limiting nutrient (Schindler & Vallentyne, 2008). The addition of Pi into the hydrosphere results in eutrophication (most commonly), which is the unrestricted growth of phytoplankton such as algae. The algae consume dissolved oxygen in the water which results in the death of fish and other organism's dependent on dissolved oxygen (Horrigan, *et al*., 2002). Also, toxic compound from the algal blooms makes their way up the food chain resulting in further mortality (Anderson, 1994).

Although Pi can be removed from hydroponic wastewater via the methods discussed in Section 2.5, these wastewater treatment technologies also incur environmental costs from energy consumption (likely fossil fuel) or occupation of space (constructed wetlands). Therefore, for environmentally friendly usage of Pi in hydroponic systems, the discharge rate of Pi from the hydroponic unit must be minimized (R_i from Equation 1). This will reduce pollution in open hydroponic systems proportionally and reduce the load on wastewater treatment units in closed systems. The total nutrient concentration is typically controlled using the solution's EC as discussed in Section 2.5. With nutrient concentration control employed, Q in Equation 1 is minimized since the nutrient solution can be recycled more extensively. Therefore, to minimize R_i, the concentration of Pi in solution must be controlled at the minimum level (at which adequate plant growth is maintained).

Pi concentration control can be accomplished using EC, transpiration rates or ISEs, as discussed in Section 2.5. Given the drawbacks of these methods (also discussed in Section 2.5), a pH-based control system was developed. Pi solutions are good pH buffers as explained in Section 2.6. If Hoagland's solution is supplied (with nitrate as the sole nitrogen source) the pH rises, and acid dosing is required for pH homeostasis. Therefore, this acid dosing and the corresponding changes in pH upon dosing can be used to calculate the buffering capacity (β) online. The premise of this chapter is that the buffering capacity can be used as an inferential measurement of the Pi concentration in solution. Pi concentration control can therefore be accomplished by dosing additional Pi in response to the inferred value. For example, a small amount of additional Pi can be dosed when the inferred concentration is below a specified setpoint.

4.2 Method

All runs were conducted for a period of ten days without solution replacement and under 24-hour light (no night cycle to avoid fluctuations in ∇pH, see nomenclature). Seedlings were cultivated in separate systems (aeroponic cloners) and were transplanted to the main experimental setup when they weighed around 10 g, followed by commencement of the respective run. Seedlings were selected randomly in part, with preference given to visually large and healthy plants. Plants were cultivated in modified Hoagland's solution (Hoagland & Arnon, 1938) composed of deionised water with 5 mM KNO_3, 5 mM $Ca(NO_3)_2{\cdot}4H_2O$, 2 mM $MgSO_4{\cdot}7H_2O$, 6 mg L^{-1} NaOH, 7.5 mg L^{-1} Fe-EDTA, 0.05 mg L^{-1} Cu-EDTA, 2.9 mg L^{-1} H_3BO_3, 1.8 mg L^{-1} $MnCl_2{\cdot}4H_2O$, 0.2 mg L^{-1} $ZnSO_4{\cdot}7H_2O$ and 0.1 mg L^{-1} $Na_2MoO_4{\cdot}2H_2O$. Different amounts of Pi were charged initially (as KH_2PO_4) depending on the aims of each run. Liquid samples were taken daily and analysed for Pi concentration. Besides Pi, all other nutrient concentrations were kept high via relative addition (Hellgren & Ingestad, 1996).

Run 1 was performed to establish the relationship between Pi concentration and β during plant growth. Using this relationship, Pi concentration control at lower levels was attempted in runs 2 and 3 by controlling β at a setpoint corresponding to low Pi concentrations. This was accomplished by dosing an additional amount of Pi (0.02 mmol L^{-1} per instance) when β fell below the respective setpoint. The Pi dosing solution (D1 in Fig. 6) contained 0.1 M KH_2PO_4 which and was raised to a pH of 6.1 using NaOH. The pH of the system was controlled with an acid

solution (0.03 M HCl) which was dosed from the second dosing reservoir (D2 in Fig. 6). Lastly, to determine whether any variation in physiological properties occurred at the lower Pi concentrations employed, run 4 was conducted in which Pi was controlled at high concentrations to represent standard protocol. The Pi concentration was kept high by employing a high β setpoint in the control algorithm.

4.3 Results and discussion

4.3.1 Establishing a relationship between Pi and β in Hoagland's solution

Hydroponic solutions contain other buffering species such as BO_3^{3-} and EDTA, although these are typically present in much lower quantities than Pi. To determine the degree to which Pi dominates the solution's buffering capacity, a simple experiment was performed in which the buffering capacity of deionised water, Hoagland's solution without Pi, and Hoagland's solution with various amounts of Pi was measured. In each experiment, 0.1 mmol of HCl was added to 2 L of each solution and the resulting drop in pH was used to calculate the buffering capacity from Equation 5. The initial pH of the different solutions (prior to adding the 0.1 mmol HCl) was adjusted to 6.1 using NaOH and HCl. Subsequently, the 0.1 mmol HCL was added to each solution and the resulting drop in pH was recorded. The results are reported in Fig. 7 in which the pH drops (ΔpH) are given as bars in subplot (a) and the corresponding buffering capacities are plotted in subplot (b). The results show that Hoagland's solution without Pi has a practically identical buffering capacity to deionised water when compared with Hoagland's solution containing Pi. Thus, regarding the nutrients only, it may be concluded that Pi dominates the solution's buffering capacity within the pH range investigated. Furthermore, from Fig. 7 (b), a linear relationship is observed between β and the Pi concentration in Hoagland's solution.

4.3.2 Inferring Pi concentration from β during plant growth

Some plant root exudated such as organic acids are also known as good buffers (Hosseinzadeh *et al*., 2017). To determine if these or other plant growth phenomena contribute to the nutrient solution's buffering capacity, run 1 was performed in the main setup (Fig. 5 and Fig. 6) in which the buffering capacity was calculated online during plant growth.

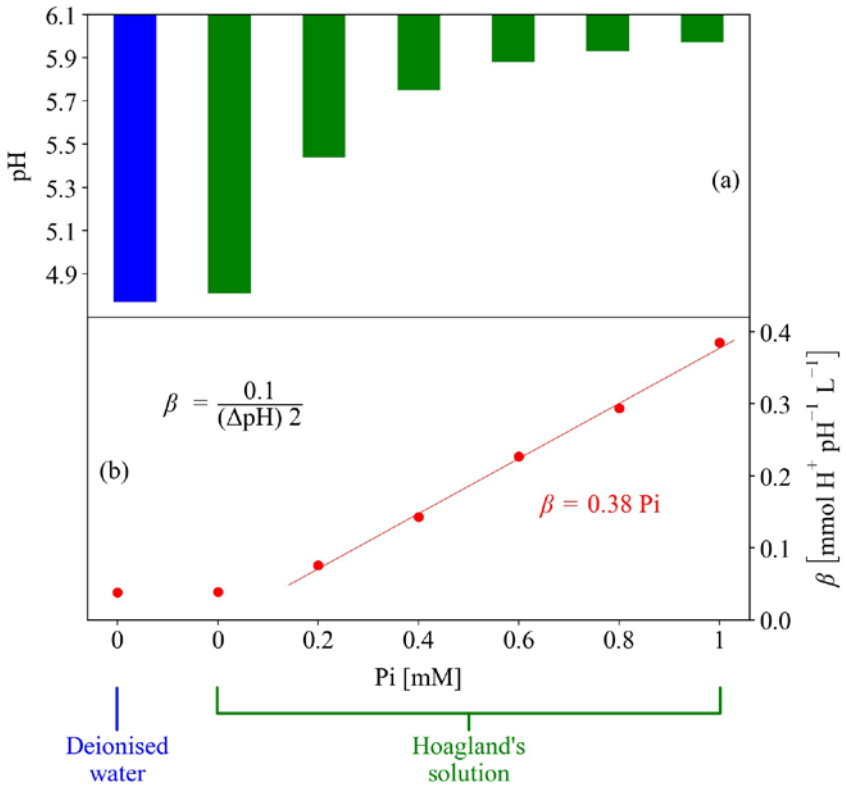

Fig. 7: Results from measuring the buffering capacity of deionised water and Hoagland's solution with various concentrations of Pi. The initial pH of the solutions were adjusted to 6.1 using NaOH and HCl. Subsequently, 0.1 mmol HCL was added to 2 L of each solution. The resulting drop in pH is reported as bars in subplot (a) and the corresponding buffering capacities are plotted in subplot (b).

Standard Hoagland's solution was charged, and Pi was allowed to deplete (no additional Pi was dosed) while all other macronutrient concentrations were kept constant via relative addition. β was calculated online from the acid dosing instances (required for pH control) and the corresponding changes in pH according to Equation 5. However, β was difficult to measure accurately, specifically ΔpH, due to slow mixing of the nutrient solution relative to the changes in pH as caused by the plants. Noisy measurements resulted and thus, an alternative strategy for measuring β was employed in which the changes in pH as caused by the plants were used instead of the changes in pH as caused by acid dosing. This is demonstrated in Fig. 8, which shows that this strategy holds if the upper limit of the pH remains constant, such that the drop in pH caused by acid dosing is equal in magnitude to the rise in pH as caused by the plant before the next acid dosing instance. The upper limit of the pH profile (blue line) was kept constant at an average value of 6.1 ($\sigma = 0.03$ as measured in a trial run). This was achieved by manipulation of the acid dosing rate (D_{H^+}) via proportional-integral-differential (PID) control.

As shown in Fig. 8, acid dosing was automated to occur every hour (the amount dosed was determined by the PID control algorithm) as indicated in green text, which results in a sudden drop in pH. From this low pH (after complete mixing), until the next acid dosing instance, the change in pH (increase) is caused solely by the plant. If the upper limit of the pH profile remains constant (achieved using PID control), the change in pH as caused by the plant between acid dosing instances is equal in magnitude to the drop in pH caused by acid dosing. Thus, using the rate variables instead (dividing the numerator and denominator of Equation 5 by Δt), β is equal to the acid dosing rate (D_{H^+}) divided by the rate of change of pH as caused by the plant ($\nabla \mathrm{pH} = \frac{\Delta \mathrm{pH}}{\Delta t}$), as shown in Fig. 8.

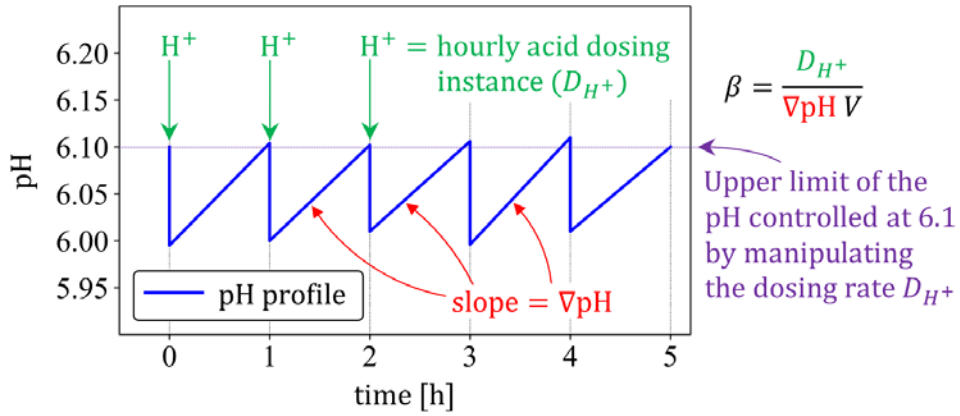

Fig. 8: Illustration of variables used in calculating β from online pH measurements. Shown is a section of a pH profile which is used as an example. Acid dosing occurs every hour (at $t = 0, 1, 2, 3$ ...). The upper limit of the pH profile is accurately controlled at 6.1 by manipulating the acid dosing rate (amount dosed every hour) using PID control. Under these conditions, the change in pH caused by acid dosing (ΔpH in Equation 5) is equal in magnitude to the change in pH caused by the plant between acid dosing instances, thus allowing for ∇pH to be used in calculating β.

The results from run 1 are given in Fig. 9. Subplot (a) reports the Pi concentrations as measured via analysis of liquid samples. Subplots (b) and (c) report the corresponding acid dosing rates required for pH control (D_{H^+}) and the rates of pH increase as caused by the plants (∇pH). The increasing nature of the plots is the result of increasing plant size. The exceptionally high increase in the ∇pH plot is due to increasing plant size as well as the reduction in β resulting from decreasing Pi concentration. β is plotted in subplot (d), in which a clear reduction in β is observed with decreasing Pi concentration. Subplot (e) is a plot of the Pi concentration vs. β

(Fig. 9 (a) vs. (d)) which indicates a linear relationship between the Pi concentration and β. Fig. 9 (e) is in good agreement with Fig. 7 (b) which shows that Pi dominates the buffering capacity of the solution during plant growth. Therefore, it has been demonstrated that the Pi concentration in the hydroponic solution can be inferred from measurement of the solution's buffering capacity.

Oscillations in the acid dosing rates (Fig. 9 (b)) repeating every 24-hours are observed. The oscillations appear in sync between plants even though all four systems were operated independently, sharing only the control platform (a single Arduino™) and the laboratory environment. As continuous plant lighting was employed (no night cycle), constant plant metabolism (smooth dosing curves) was expected. However, the seedlings received a 4-hour night cycle prior to commencement of the runs, the oscillations are thus assumed to be the result of the circadian rhythm of the plants, in which the plants anticipate the previously employed day-night cycle (McClung, 2006).

4.3.3 Controlling the Pi concentration at various levels

Results from the above experiments show that the Pi concentration in solution can be inferred from β. From Fig. 9 (e) it can be seen that β (in units of mmol H^+ pH^{-1} L^{-1}) is approximately half of the Pi concentration in the solution (in units of mM), which agrees with the results shown in Fig. 7 (in which $\beta = 0.38$ Pi). Thus, to control the Pi concentration at lower levels, additional Pi dosing can be automated in response to β as measured online. A simple control algorithm was implemented which caused 0.02 mmol L^{-1} of additional Pi to be dosed if β was lower than a specified setpoint. The Pi dosing reservoir (D2 in Fig. 6) contained 1 M KH_2PO_4 at a pH of 6.1 (raised with NaOH). The same acid dosing solution from run 1 (0.03 M HCl. D1 in Fig. 6) was used for pH control. Run 2 was hence performed in which a β value setpoint of 0.1 mmol H^+ pH^{-1} L^{-1} was specified, which corresponds to a Pi concentration between 0.1 and 0.2 mM as seen in Fig. 7 (e). The results from run 2 are given in Fig. 10, which conveys Pi concentration control around 0.2 mM ($\sigma = 0.03$ mM, $n = 40$). Subplots (a) to (d) report the Pi concentrations (as blue dots with magnitudes on the left vertical axis) for each of the four plants. Relatively constant profiles around 0.2 mM Pi are observed with slight variation between plants. The corresponding β values are plotted as red dots on the right vertical axis. Vertical, green-dashed lines indicate Pi dosing instances which typically occurred in succession

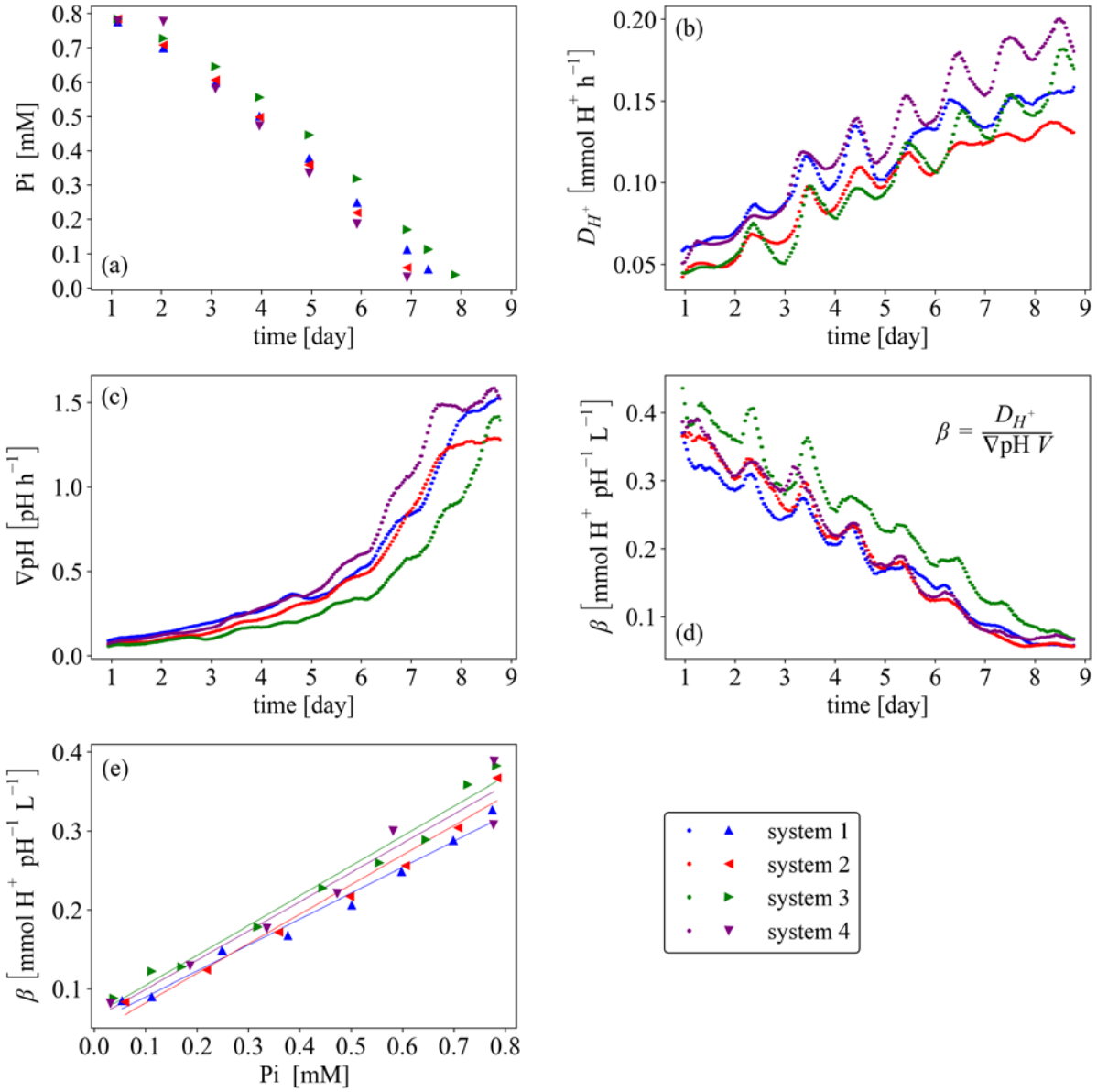

Fig. 9: Results from run 1 using standard Hoagland's solution. Pi could deplete (no additional Pi was dosed), and all other macro-nutrient concentrations were kept constant via relative addition. Pi concentration (a), acid dosing rate (b), and rate of pH increase as caused by the plants (c) are shown. Subplot (d) shows β as measured online. Subplot (e) is a plot of the Pi concentration vs. β, which indicates a linear relationship between the two variables.

(hence some appear thicker/thinner). After dosing, an increase in β is observed after a period of lag-time. Subplots (e) and (f) report the acid dosing rates required for pH control and the rates of pH increase as caused by the plants.

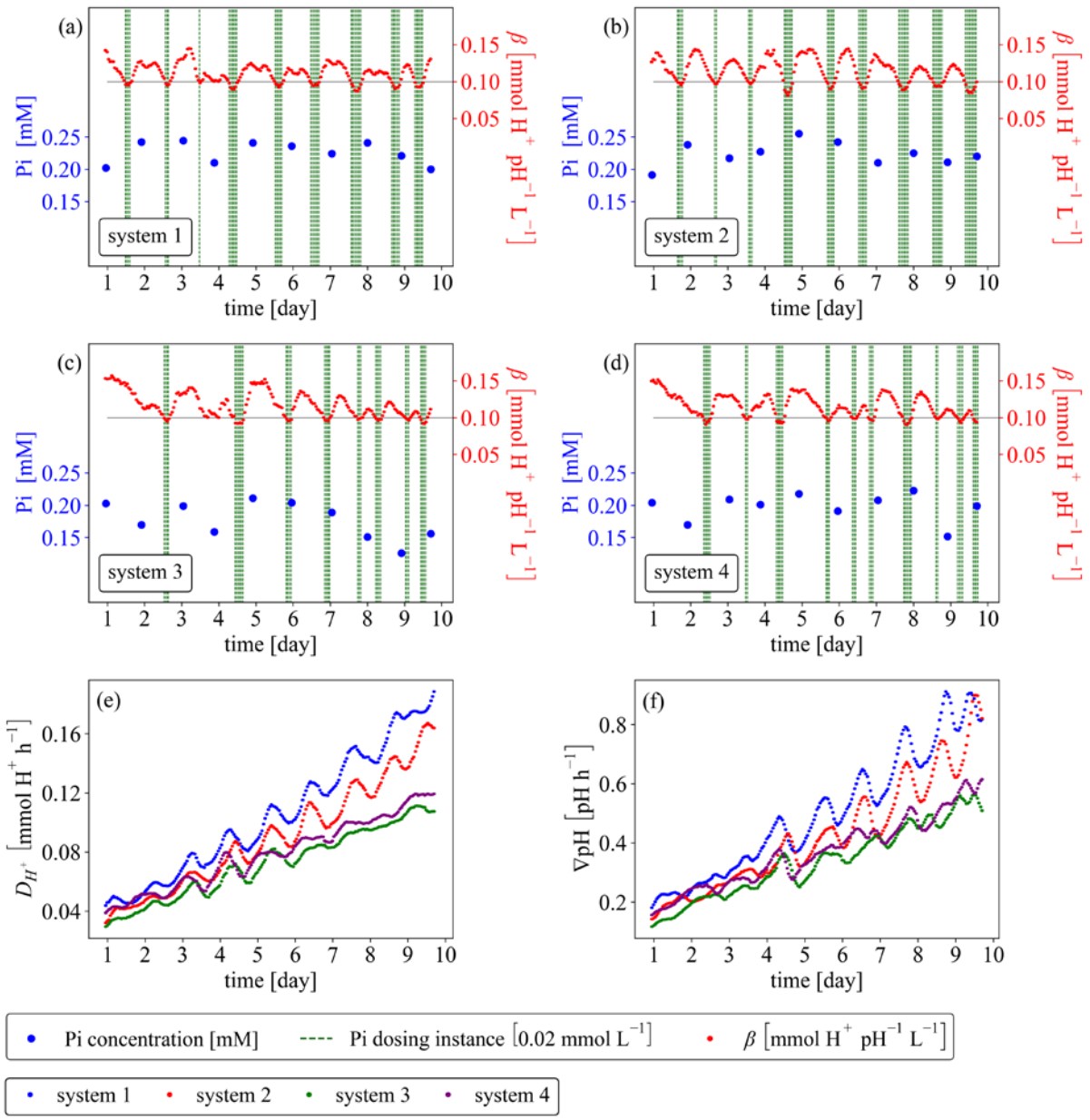

Fig. 10: Results from run 2 in which the Pi concentration was controlled around 0.2 mM. Note that the top legend concerns subplots (a) – (d) and the bottom legend concerns (e) and (f). Concentration control was achieved by dosing additional Pi when β fell below a setpoint value of 0.1 mmol H^+ pH^{-1} L^{-1}. Subplots (a) to (d) show the Pi concentrations in solution as blue dots (with magnitudes on the left vertical axis) and online β measurements as red dots (with magnitudes on the right vertical axis) for each of the four plant systems. Green, vertical-dashed lines indicate Pi dosing instances of 0.02 mmol L^{-1} (usually occurring in succession). Subplots (e) and (f) show the acid dosing rates and rates of pH increase (as caused by the plants) for each of the four plant systems.

Considering that Pi extinction corresponds to a β value around 0.05 mmol H^+ pH^{-1} L^{-1}, as seen in Fig. 7 (b) and Fig. 9 (e), a β value setpoint of 0.08 mmol H^+ pH^{-1} L^{-1} was employed in run 3 in an attempt to minimize the Pi operating concentration. The results from run 3 are given in Fig. 11 which conveys Pi concentration control at around 0.1 M ($\sigma = 0.03$ mM, $n = 40$), with slight variation between plants. Considering that the Pi concentration dropped to below 0.05 mM at one instance (Fig. 11 (d), day 9) and that the variation in Pi concentration is more sensitive to changes in the β setpoint at low Pi concentrations (as can be seen in Fig. 7), an operating concentration of 0.1 mM is believed to be the lowest possible operating concentration with minimal risk of Pi extinction given the standard deviation ($\sigma = 0.03$ mM, $n = 40$). This concentration is an order of magnitude lower than the concentration in Hoagland's solution.

In Figs. 11 (a) to (d), a slight decrease in the phosphate concentration is observed over time. This may be due to a slight increase in the buffering capacity of the solution resulting from root exudation, observable only at the low Pi concentrations employed. The almost imperceptible decrease in the Pi concentration, however, indicates that these exudates are in much smaller quantities than Pi.

To determine whether plant growth was affected at the low Pi concentrations employed, run 4 was performed under standard hydroponic conditions (high Pi concentrations) where the Pi concentration was controlled using the same control strategy but specifying a high β value setpoint of 0.38 mmol H^+ pH^{-1} L^{-1} which corresponds to a Pi concentration of 1 mM (concentration in Hoagland's solution) from Fig. 7. The results are reported in Fig. 12 in the same way as reported for runs 2 and 3 (Fig. 10 and Fig. 11) and convey Pi concentration control around 1 mM ($\sigma = 0.08$ mM, $n = 40$).

Higher variation in β is observed in run 4 as compared to runs 2 and 3, which indicates that the Pi concentration is more accurately inferred at lower β values. This is also seen in Fig. 9 (d) where more stable β profiles result as Pi decreases. This is believed to be due to the accuracy of the pH probes employed (± 0.01 pH units) in which small differences in pH (low ΔpH corresponds to high β values) are less accurately measured as compared with large differences in pH. This is substantiated in Fig. 12 (f), in which the ∇pH curves are "less smooth" as compared with those in Fig. 10 (f) and Fig. 11 (f).

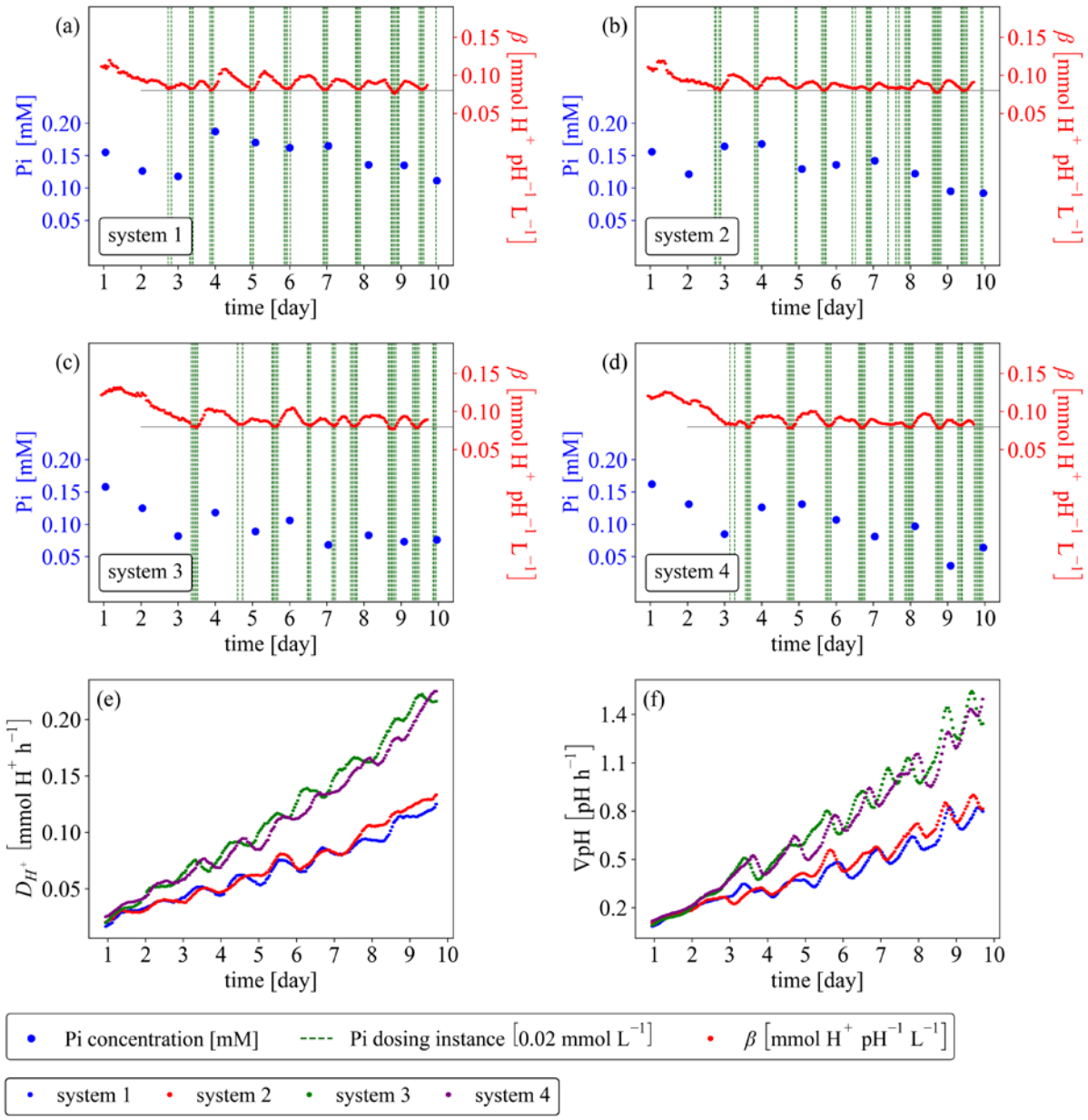

Fig. 11: Results from run 3 where the Pi concentration was controlled around 0.1 mM. Note that the top legend concerns subplots (a) – (d) and the bottom legend concerns (e) and (f). Concentration control was achieved by dosing additional Pi when β fell below a setpoint value of 0.08 mmol H^+ pH^{-1} L^{-1}. Subplots (a) to (d) show the Pi concentrations in solution as blue dots (with magnitudes on the left vertical axis) and online β measurements as red dots (with magnitudes on the right vertical axis) for each of the four plant systems. Green, vertical-dashed lines indicate Pi dosing instances of 0.02 mmol L^{-1} (usually occurring in succession). Subplots (e) and (f) show the acid dosing rates and rates of pH increase (as caused by the plants) for each of the four plant systems.

Variation in the average phosphate concentration between systems (systems 1 to 4) is observed in runs 2 to 4, which is believed to be due to experimental variation (such as errors in dosing pump calibration) and not due to variations in plant make-up. This can be seen in Fig. 10 to Fig. 12 where consistently higher phosphate concentrations occur in systems 1 and 2 as compared with systems 3 and 4.

To compare plant growth characteristics between the runs, relative plant growth rates (RGR) were calculated from the initial and final plant fresh mass. Leaf mass fraction (LMF) was calculated from the final dry mass of the plants. From the total amount of Pi dosed, the initial and final Pi concentrations, and the change in plant fresh mass, the total plant P content (TPC) could be calculated. The above parameters, including the initial and final plant fresh mass are reported in Table 3. No significant variation in RGR (ANOVA, $p = 0.58$) or LMF (ANOVA, $p = 0.5$) is observed between runs. However, a significant increase in the TPC (ANOVA, $p = 0.002$) of the plants in run 4 (as compared with plants from runs 2 and 3) is observed. The lower Pi content found in plants cultivated under lower Pi concentrations does not necessarily indicate that plant nutrition was adversely affected. To the contrary, excessive Pi uptake has been reported to occur at 0.5 mM or higher operating concentrations (half that of Hoagland's solution), which can induce iron and zinc deficiencies (Chaney & Coulombe, 1982). Accordingly, strategies to operate at lower Pi concentrations have been suggested (Bugbee, 2004). Therefore, the nutritional properties of the plants cultivated under the lower Pi concentrations of runs 2 and 3 may be more desirable than those cultivated under standard conditions.

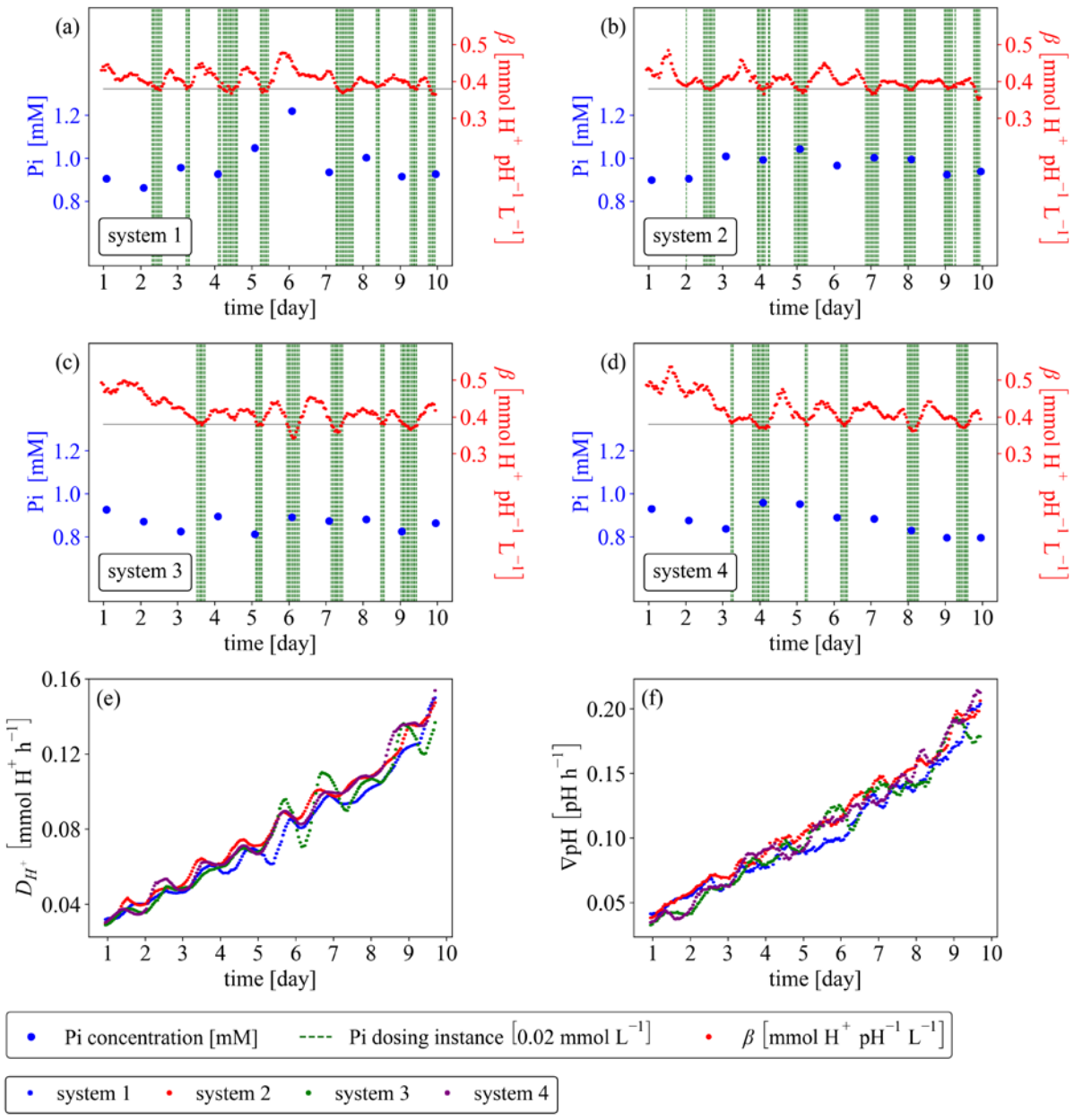

Fig. 12: Results from run 4 using Hoagland's solution. All nutrients were kept constant at high concentrations and thus run 4 represents a control run. Note that the top legend concerns sub-plots (a) – (d) and the bottom legend concerns (e) and (f). The Pi concentration was controlled around 1 mM by dosing additional Pi when β fell below a setpoint value of 0.38 mmol H^+ pH^{-1} L^{-1}. Subplots (a) to (d) show the Pi concentrations in solution as blue dots (with magnitudes on the left vertical axis) and online β measurements as red dots (with magnitudes on the right vertical axis) for each of the four plant systems. Green, vertical-dashed lines indicate Pi dosing instances of 0.02 mmol L^{-1} (usually occurring in succession). Subplots (e) and (f) show the acid dosing rates and rates of pH increase (as caused by the plants) for each of the four plant systems.

Table 3: Growth characteristics of runs 2, 3 and 4 where the Pi concentration was controlled at various levels per run. Initial and final plant fresh mass (IFM and FFM), relative growth rate based on fresh mass (RGR), total plant phosphorous content per fresh plant mass in mg-P g^{-1} (TPC), and leaf mass fraction on a dry mass basis (LMF) are tabulated.

	System #	IFM [g]	FFM [g]	RGR [day^{-1}]	TPC [mg g^{-1}]	LMF [g g^{-1}]
	1	9.83	90.62	0.22	0.65	0.86
Run 2	**2**	10.32	107.49	0.24	0.57	0.84
0.2 mM Pi	**3**	8.59	74.81	0.22	0.61	0.85
	4	11.26	85.58	0.20	0.60	0.85
	1	10.23	81.84	0.21	0.60	0.85
Run 3	**2**	8.98	89.36	0.23	0.62	0.83
0.1 mM Pi	**3**	9.34	95.68	0.23	0.56	0.86
	4	9.72	116.11	0.25	0.54	0.82
	1	10.55	100.41	0.23	0.69	0.85
Run 4	**2**	11.20	102.03	0.22	0.70	0.86
1 mM Pi	**3**	8.88	82.63	0.22	0.73	0.83
	4	10.09	86.82	0.22	0.66	0.87

4.4 Conclusions

It was shown that the Pi concentration in a hydroponic system can be controlled at much lower levels compared to the standard protocol using pH as the sole measured variable, without sacrificing plant growth characteristics. This was accomplished by online calculation of β which was shown to be a good inferential measurement of the Pi concentration in solution. Thus, automated dosing of additional Pi could be implemented to maintain β (and hence the Pi concentration) at a setpoint. This strategy was successful at controlling the Pi concentration at an order of magnitude lower than the typical operating concentrations (and hence discharge concentrations). Therefore, the load of Pi pollution (or the load which must be removed in a wastewater treatment unit) can be reduced by an order of magnitude when employing the proposed control system.

CHAPTER 5 Nitrate

5.1 Introduction

Plants can absorb nitrogen in the form of nitrate and/or ammonium. In hydroponic systems, optimal growth is often achieved when nitrate is supplied as the primary nitrogen source and many nutrient solutions are formulated with nitrate as the sole nitrogen source (Cooper,1988; Hewitt, 1996; Hoagland & Arnon, 1938; Steiner, 1984). This is partly because high ammonium fractions can be detrimental to hydroponic plants due to their high ammonium affinity, resulting in excessive amounts of ammonium being absorbed (Pitts & Stutte, 1999). Also, the anionic nature of nitrate results in more-equivalent charge uptake (see Fig. 1), thus promoting balanced nutrient uptake and requiring less cation exudation to maintain electrical neutrality (Bugbee, 2000; Le Bot, 1998). This chapter considers nitrate when supplied as the sole nitrogen source. A pH-based control algorithm was developed to control the nitrate concentration at low levels in solution. As discussed in Section 2.6, nitrate uptake is accompanied by hydroxide exudation which requires acid dosing to control the solution's pH. The premise of this chapter is that a relationship exists between the acid dosing rate required for pH homeostasis and the nitrate uptake rate of the plant. Similar to the approach used by Bugbee (2004) in which the plants' transpiration rates were used to infer the nutrient uptake rates (see Section 2.6), here the proton (acid) dosing rates are used to infer the nitrate uptake rates. With an established relationship, the nitrate concentration can be controlled by dosing additional nitrate at an equal rate to the inferred uptake rates. Since the nitrate concentration is not measured directly, drift in the nitrate concentration (slow accumulation/depletion) is bound to occur. As such, the control scheme was calibrated to effect slow depletion of nitrate in solution. Since depletion ultimately results in extinction, a nitrate extinction prevention algorithm was included, in which nitrate extinction

was inferred from a reduction in the rate of change of pH (∇pH), which upon detection, actuated additional nitrate dosing.

5.2 Method

Seedlings were cultivated in separate systems (aeroponic cloners) and were transplanted to the main experimental setup when they weighed around 10 g, followed by commencement of each respective run. Seedlings were selected randomly in part, with preference given to visually large and healthy plants. Run 1 was conducted for a period of 10 without solution replacement. Runs 2 to 4 were conducted for 13 days with solution replacement on days 5, 9 and 11. Run 5 was conducted for 11 days with solution replacement on day 7. In run 5, an initial nitrate concentration of 5 mM was charged. Nitrate extinction did not occur until after the solution had been replaced on day 7 with a nitrate concentration of 0.5 mM. A day/night cycle was implemented with 20 h light and 4 h dark in all runs except run 5, where 24 h light was employed to avoid fluctuations in ∇pH.

Run 1 was performed to establish a relationship between proton dosing and nitrate uptake. This was accomplished by cultivating plants in standard Hoagland's solution (5 mM KNO_3, 5 mM $Ca(NO_3)_2{\cdot}4H_2O$, 1 mM KH_2PO_4, 2 mM $MgSO_4{\cdot}7H_2O$, 6 mg L^{-1} NaOH, 7.5 mg L^{-1} Fe-EDTA, 0.05 mg L^{-1} Cu-EDTA, 2.9 mg L^{-1} H_3BO_3, 1.8 mg L^{-1} $MnCl_2{\cdot}4H_2O$, 0.2 mg L^{-1} $ZnSO_4{\cdot}7H_2O$ and 0.1 mg L^{-1} $Na_2MoO_4{\cdot}2H_2O$) and controlling the pH with HCl (1 M). The solution was replaced regularly to maintain a solution strength > 2/3 full Hoagland's solution (according to EC measurements). A simple control algorithm was employed which dosed a small amount of acid (0.15 mmol) when the pH rose above a setpoint of 6.1. Nitrate uptake was calculated from nitrate concentration measurements obtained from analysis of liquid samples.

Runs 2 to 4 employed the relationship obtained in run 1 to control the nitrate concentration at various levels. This relationship and the resulting control strategies are described in the following section. A nitrogen-free (except for EDTA) solution was used, which was simply Hoagland's solution but substituting 5 mM KNO_3 with 2.5 mM K_2SO_4 and 5 mM $Ca(NO_3)_2{\cdot}4H_2O$ with 5 mM $CaCl_2{\cdot}2H_2O$. Different amounts of nitrate (depending on the aims of each run) were added as KNO_3. In run 5, a nitrate extinction prevention algorithm was implemented, in which nitrate extinction was inferred from a reduction in ∇pH (discussed in the following section).

5.3 Results and discussion

5.3.1. Relating nitrate absorption to proton dosing

Run 1 was conducted using standard Hoagland's solution (high nitrate concentration). The results are given in Fig. 13, in which the hypothetical nitrate concentrations, and proton dosing rates (required for pH homeostasis) are plotted. The hypothetical concentrations are the actual (measured) concentration minus the added amounts of nitrate (manually with a pipette to maintain high concentrations). Fig.13 (c) is a plot of the ratio of HCl dosing to nitrate absorption (η_1, see Nomenclature), which indicates a constant ratio of proton dosing required for pH homoeostasis and nitrate absorbed by the plant ($\eta_1 \approx 0.5$ mol mol^{-1}). This relationship provides the means of inferring the nitrate absorption rate from the proton dosing rate.

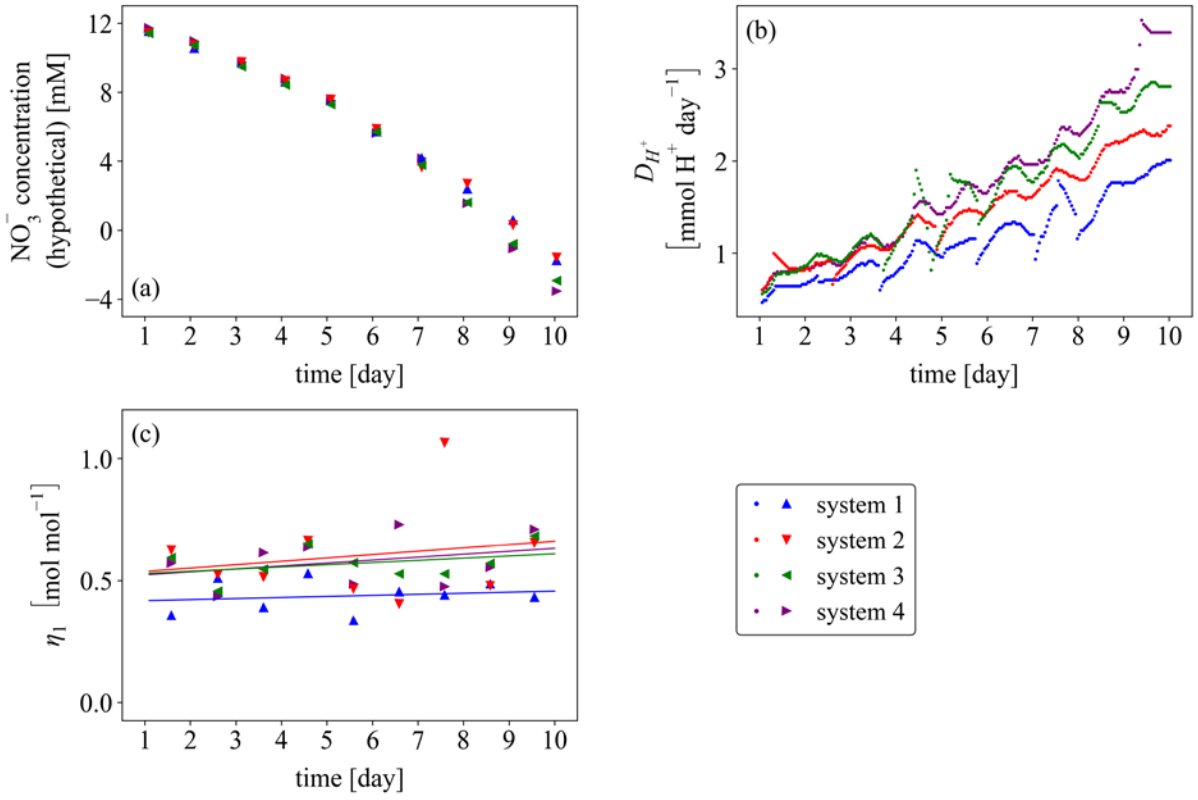

Fig. 13: Results from run 1 in which plants were cultivated in standard Hoagland's solution (nitrate as the sole nitrogen source). The pH was controlled at an average value of 6.1 ($\sigma = 0.07$, $n = 997$). The hypothetical nitrate concentrations (a) and the HCl dosing rates required for pH homeostasis (b), are shown. The hypothetical concentrations are the actual (measured) concentrations minus the added amounts of nitrate (manually with a pipette to maintain high concentrations). Subplot (c) plots the ratio of proton dosing to nitrate absorption (ratio of (a) to (b)), in which a fitted value of $\eta_1 \approx 0.5$ mol mol^{-1} is obtained.

5.3.2 Controlling the nitrate concentration at various levels

Provided that for every mol of nitrate absorbed, 0.5 mols of protons need to be dosed to maintain the solution's pH, if the acid dosing solution (D1 in Fig. 6) used to control the pH is composed of the same proton-to-nitrate ratio (for example, 0.5 M HNO_3 and 0.5 M $NaNO_3$), controlling the pH will indirectly control the nitrate concentration since the absorbed nitrate is constantly replaced by the acid dosing. Runs 2, 3 and 4 employed this strategy to control the nitrate concentration at approximately 11 mM, 1 mM and 0.5 mM, respectively.

It was observed in trial experiments (not reported) that a proton-to-nitrate ratio of 0.5 mol mol^{-1} ($= \eta_1$) in the acid dosing reservoir resulted in slow accumulation of nitrate in solution, whereas a ratio of 0.6 mol mol^{-1} resulted in slow depletion of nitrate. Inevitable variation in η_1, due to genetics or changes in plant growth stage, or errors in composing the acid dosing solution, will result in either accumulation or depletion of nitrate in solution. Thus, conceding that drift in the nitrate concentration is inevitable, a proton-to-nitrate ratio of 0.6 mol mol^{-1} in the acid dosing solution (allowing for slow depletion of nitrate in solution) was employed in runs 2, 3 and 4. Nitrate drift was prevented by small manual additions of $NaNO_3$ in runs 3 and 4.

Fig. 14 (a) to (c) gives the nitrate concentrations (as triangles with magnitudes on the left vertical axis) for runs 2 to 4, respectively. Vertical dotted lines indicate the times at which the solution was replaced. A common/bulk dosing solution was used in all three runs. Thus, variation in the rate of nitrate depletion in solution is due to variation in η_1. Relatively constant nitrate concentration profiles are observed. For run 2, with an initial nitrate concentration of 11.5 mM, no additional nitrate was added manually. A slight decrease in nitrate concentration can be observed between solution replacements, indicating that the proton-to-nitrate ratio in the dosing solution is larger than the plant's η_1 value. In runs 3 and 4, additional nitrate was added manually to correct for the gradual decrease in concentration. Manually added amounts are plotted as bars in Fig. 14 with magnitudes on the right vertical axis. Given the manual additions as well as the quantified automatic dosages of nitrate, the total nitrate consumed could be calculated. It was found that manual dosing accounted for 8 % (± 4 %) of the total nitrate absorbed. Therefore, the control strategy performed well to supply most of the nitrogen needed. The calculated η_1 values varied between 0.52 and 0.57, with an average value of 0.55 for the eight plants.

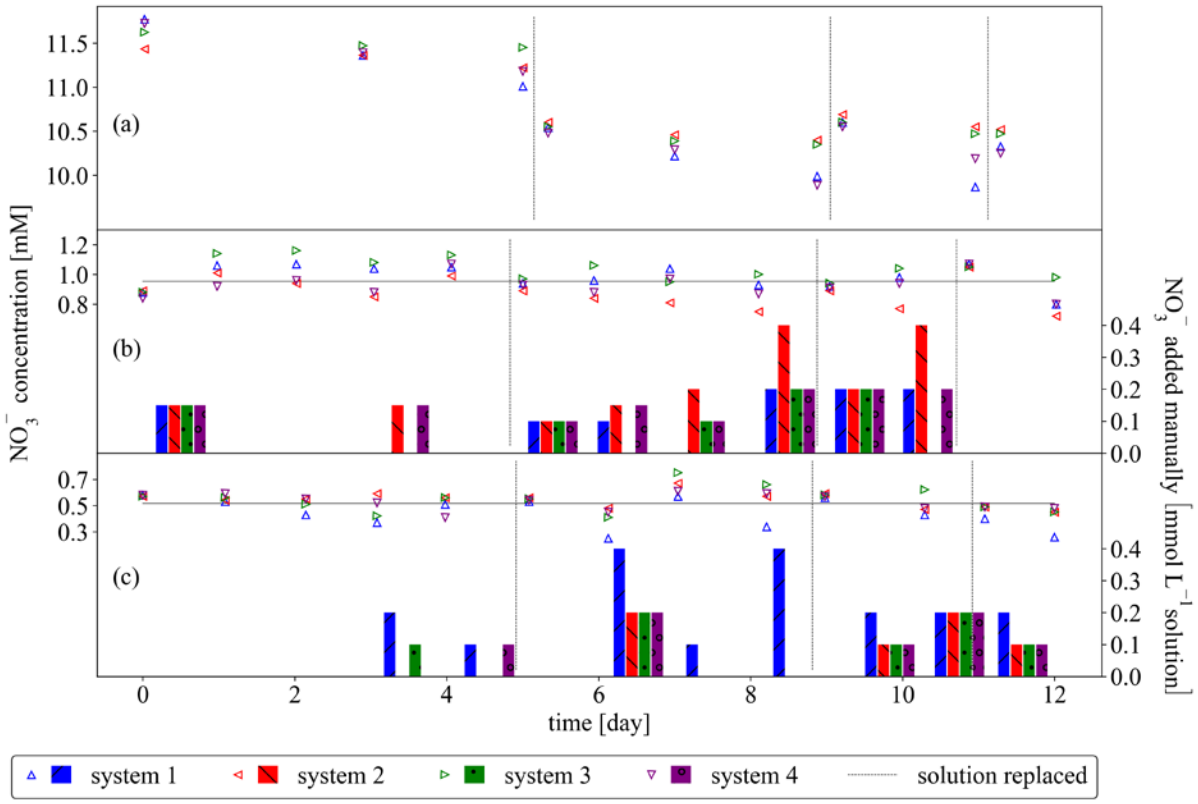

Fig. 14: Results from runs 2 to 4 in subplots (a) to (c), respectively. The nitrate concentration was controlled at approximately 11 mM, 1 mM, and 0.5 mM for runs 2, 3 and 4, respectively. All runs used the same dosing solution composed of 0.3 M $HNO_3$and 0.2 M $NaNO_3$. For runs 3 and 4 manual corrections were made by adding $NaNO_3$ (manual pipetting) as indicated by bar plots in (b) and (c). Vertical dotted lines indicate solution replacement.

Given that the same dosing solution was used during runs 2 to 4, from Fig. 14 it can be seen that η_1 varied between plants. For example, in run 3, the plant cultivated in system 2 had the lowest η_1 value (as more nitrate had to be added manually), whereas in run 4, plant 1 had the lowest η_1 value. Thus, it is clear that η_1 varies slightly between plants, which may be due to genetic differences in nutrient uptake characteristics.

Fig. 15 (a), (b) and (c) gives the nitrate dosing rates $\left(D_{NO_3^-}\right)$ for runs 2 to 4, in which the natural logarithm is used to linearise the growth curves. It can be shown from the population growth equation that the slopes of the fitted lines equal the relative dosing rates (RDR) (Hellgren & Ingestad, 1996; Raistrick, 1999). Practically identical relative dosing rates are observed, which agree with the relative growth rates (RGR) given in Fig. 15 (d). Thus, no reduction in growth rate or nitrogen uptake rate is apparent with decreasing nitrate concentration. To the contrary,

there appears to be a slight increase in the growth parameters. Fig. 15 (d) compares the average growth parameters (RGR and RDR) of the three runs as reported in subplots (a) to (c). The relative growth rates (RGR) are higher than the relative dosing rates (RDR), which indicates that less nitrogen per plant mass is absorbed with increasing plant size. This can be attributed to a decreasing η_1 value with plant size (fewer protons need to be dosed to maintain the pH per nitrate absorbed). However, no evidence of this has been found in the data. Instead, it is assumed that the nitrogen content in the plants decrease with plant size, which is corroborated by Le Bot *et al*. (1998).

5.3.3. Automatic nitrate extinction prevention

For run 5, nitrate addition was fully automated (no manual addition as in runs 3 and 4). In addition to the nitrate control strategy used in runs 2 to 4, where the nitrate concentration was controlled by controlling the pH with a mixture of acid and nitrate, a second dosing pump (P2 in Fig. 6) and a dosing solution containing $NaNO_3$ only (D2 in Fig. 6) was utilized, the purpose of which was to dose automatically the extra required nitrate which previously had to be added manually.

It was noted in trial experiments that the rate of change of pH (∇pH) decreased as the nitrate concentration reached zero. This can be attributed to a reduction in the nitrate assimilation rate when nitrate concentrations are critically low. Thus, nitrate extinction may be inferred from a reduction in ∇pH, which upon detection, can actuate the second dosing pump P2. This is similar to an approach which has been used in the microbial nitrification of wastewater, where ammonia extinction is inferred from a reduction in ∇pH (Andreottola *et al*., 2001; Hajsardar *et al*., 2016; Kim & Hao, 2001). The extra nitrate will then only be added upon extinction of nitrate in the solution. Provided that the nitrate concentrations are not critically low for any significant period, this strategy should satisfy the plant's nitrogen requirements while maintaining low nitrogen concentrations. This control strategy is designed to operate in conjunction with the strategy in the previous section. Slow nitrate depletion is employed through calibration of the proton-to-nitrate ration in the acid dosing solution, and upon nitrate extinction, a set amount of additional nitrate is dosed. This complete control algorithm is given in Fig. 16. Results from the last four days of run 5 (which employed the control strategy outlined in Fig. 16) are given

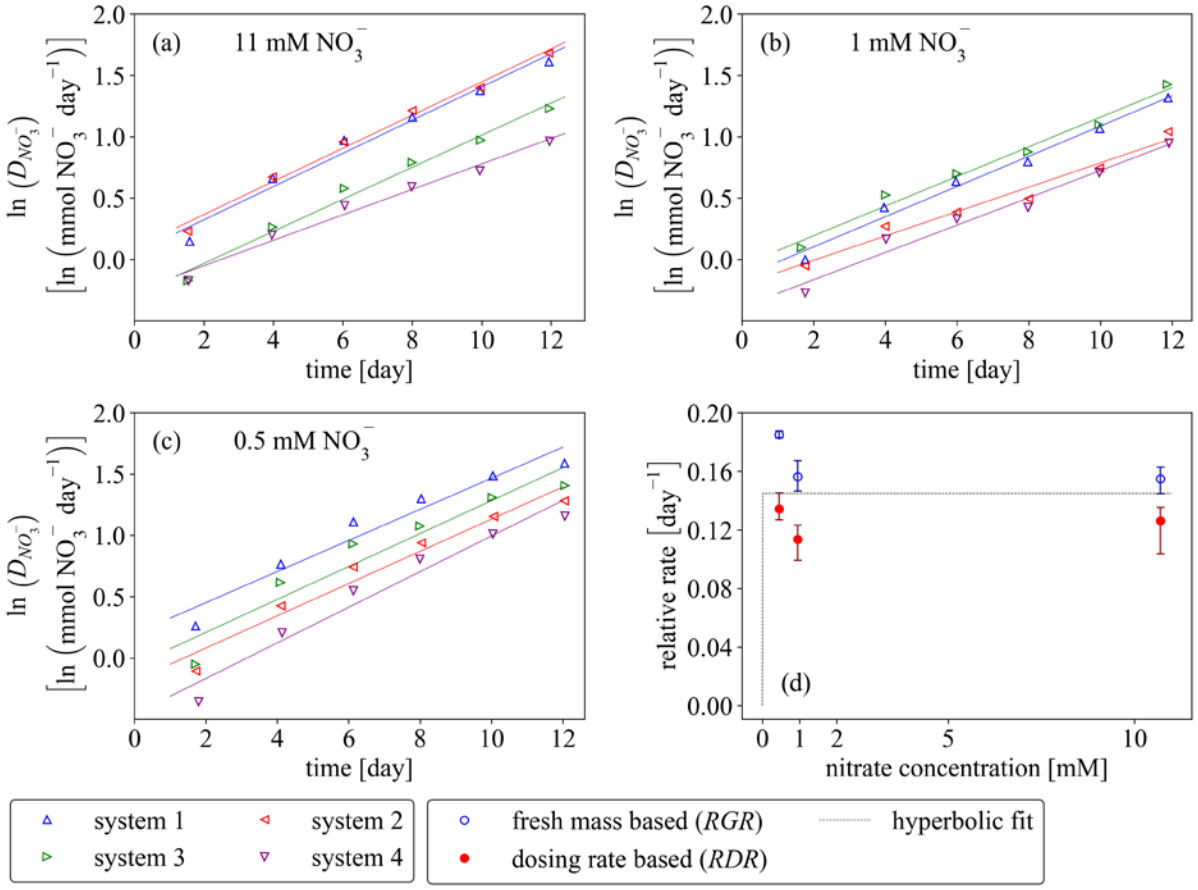

Fig. 15: Subplots (a), (b) and (c) provide logarithmic plots of the dosing rates $\left(D_{NO_3^-}\right)$ for runs 2 to 4. The slopes of the fitted lines equal the RDR values. Subplot (d) gives the average RDR and RGR values of each run as a function of the nitrate operating concentration. Error bars span the data range (min. ↔ max.) of the four plants.

in Fig. 17 (no nitrate extinction occurred prior to this), which shows how ∇pH decreases when nitrate becomes extinct. This is conveyed by plotting the nitrate concentrations together with the relative ∇pH measurements. The relative ∇pH measurements are the ratios of the instantaneous ∇pH measurements to the running average of the ∇pH measurements (average over the past 6 hours). As shown in Fig. 16, the controller doses additional nitrate when this ratio falls below 0.7, *i.e.*, a 30 % reduction in ∇pH. Consistent dosing occurring approximately every 6 hours is observed, which shows that the strategy works well to provide the extra required nitrogen which previously had to be added manually in runs 3 and 4. Furthermore, a favourably fast response is observed where an increase in ∇pH (recovery) is apparent immediately after dosing. As shown in Fig. 17, the nitrate concentrations varied between 0 and 0.2 mM, which is two orders of magnitude lower than the standard protocol.

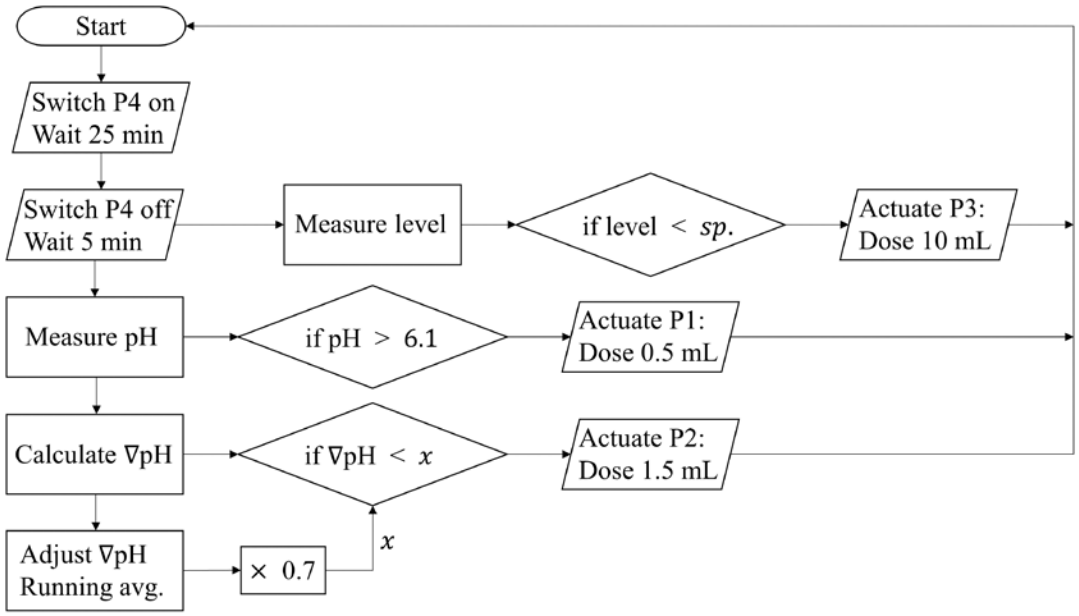

Fig. 16: Sequential function chart of the control algorithm responsible for the flood-and-drain mechanism (switching P4 on and off), liquid level control (first horizontal branch), pH control (second branch) and nitrate extinction prevention (bottom branch). "*sp*." corresponds to a liquid volume of 1.8 L.

Run 5 employed 24-hour light whereas all previous runs received a 4-hour night cycle. As such, the RGRs and RDRs cannot be accurately compared. Nonetheless, the average RGR for runs 2 to 4 (of 12 plants) was 0.17 day^{-1} (± 0.016) and the average RDR for the 3 runs was 0.12 day^{-1} (± 0.013). These agree with the average RGR (for 4 plants) and RDR for run 5, which equals 0.21 day^{-1} (± 0.012) and 0.16 day^{-1} (± 0.016), which are around 20 % higher with 20 % more light. Although no reduction in growth rate was observed, the critically low nitrogen concentrations (0.1 mM) were in effect for 4 days only (nitrate extinction did not occur prior to this). As such, the effects of cultivating under these low concentrations (2 orders of magnitude lower than the standard protocol) for an entire crop lifecycle should be investigated prior to application. The extinction prevention algorithm should perhaps be activated less frequently, *i.e.*, larger amounts of $NaNO_3$ should be dosed upon nitrate extinction (higher overall operating concentration) and should rather exists as a fail-safe mechanism.

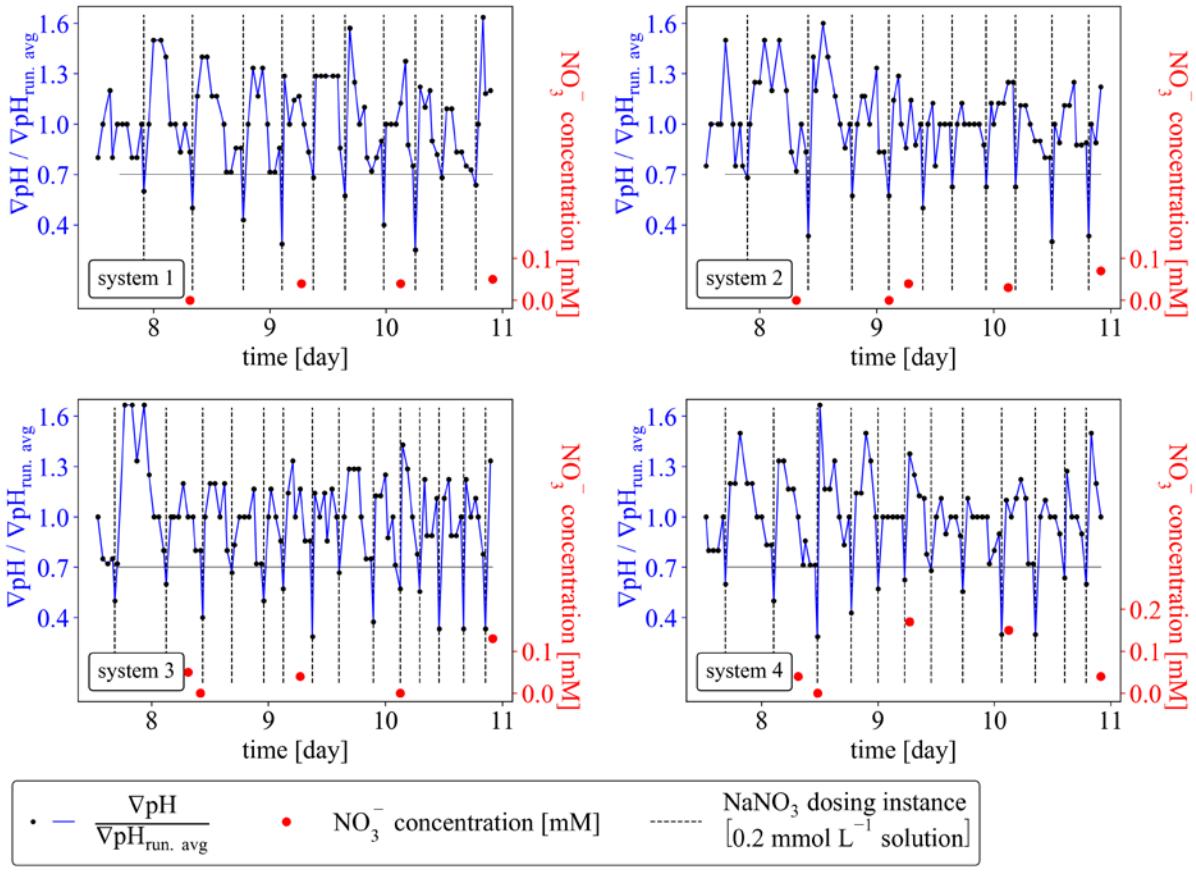

Fig. 17: Results from run 5 in which an automatic nitrate extinction prevention algorithm was included. Shown are profiles of ∇pH divided by the running average of ∇pH. As described in Fig. 16, $NaNO_3$ dosing occurs when there is a 30 % reduction in ∇pH, whereupon 0.2 mmol $NaNO_3$ L^{-1} solution is dosed. Also shown, are the measured nitrate concentrations in solution.

5.4 Conclusions

It was shown that the nitrate concentration in a hydroponic system can be controlled at much lower levels compared with the standard protocol using pH as the sole measured variable, without sacrificing plant growth rate. This was accomplished by employing a proton-to-nitrate ratio in the acid dosing solution that is slightly higher than the plant's proton-to-nitrate uptake ratio (η_1), which allows for a slow nitrate depletion rate in solution. As depletion ultimately results in extinction, an automatic nitrate addition strategy was included where nitrate extinction was inferred from a reduction in the rate of change of pH. The combined control strategy worked well to control the nitrate concentration at low levels with minimal risk of nitrate extinction in solution. Thus, the discharge rate of nitrogen from the system (R_i in Equation 1) was successfully minimized.

CHAPTER 6 Ammonium

6.1 Introduction

High ammonium fractions can be detrimental to hydroponic crops, but small fractions (relative to nitrate) often improve plant growth (Cytryn *et al*., 2012; Tabatabaei *et al*., 2006; Hachiya & Sakakibara, 2017; Neal & Wilkie, 2014; Pelayo Lind *et al*., 2021; Pitts & Stutte, 1999). Since nitrate-only nutrient solutions are generally adequate, ammonium is of interest primarily from an environmental perspective. Organic and wastewater-based fertilizers typically contain large fractions of ammonium. On such a fertilizer is biogas digestate, which is a waste stream from the anaerobic-digestion process (which primarily produces methane) (Möller & Müller, 2012; Weiland, 2010). The ammonium concentrations in the digestate often reaches concentrations as high as several hundred mM (Svehla *et al*., 2017). This liquid fertilizer has been applied in conventional agriculture as it is rich in all the essential nutrients required for plant growth (Koszel & Lorencowicz, 2015). Its liquid form, however, is apt for the hydroponic industry (Bergstrand *et al*., 2020; Stiles *et al*., 2018; Stoknes *et al*., 2016).

It was stated that pollution can be minimized by minimizing R_i in Equation 1. However, a bonus would be to use already-recycled nutrients rather than synthetic nutrients. The remaining two chapters are therefore devoted to the utilization of ammonium wastewaters as hydroponic nutrient solutions. Biogas digestate will be used as the model ammonium rich fertilizer in the current chapter. A similar approach to the previous chapter (“Nitrate”) is used, in which the proton uptake/exudation characteristics resulting from nitrogen absorption are exploited. Other than plant nitrogen uptake, an additional nitrogen flux must be accounted for. This flux involves the microbial oxidation of ammonium to nitrate. These microbes, known as nitrifying bacteria, are abundant and will naturally establish in aerobic environments where ammonium

is present (Tyson *et al*., 2007). Since high ammonium fractions can be detrimental to hydroponic crops, these bacteria are favourable and commonly employed (Pelayo Lind *et al*., 2021). Nitrification is highly acidic (see Section 2.6) and hence this process cannot be neglected in pH-based control systems.

Analogous to the previous chapters, this chapter surrounds nitrogen concentration control at low levels in hydroponic systems in which ammonium (digestate) is fed. Three effects dominate the solution's pH, namely, nitrate absorption by the plant (since nitrate is produced by the nitrifying bacteria), ammonium absorption by the plant, and ammonium oxidation by the nitrifying bacteria. These effects are depicted in Fig. 18, which were discussed in Section 2.6. In the previous chapter, the only pH effect was that of nitrate absorption (which releases η_1 OH^-), In this chapter, the same approach will be used but accounting for all three pH effects to control the nitrogen concentration (ammonium and nitrate) at low levels, thereby minimizing R_i in Equation 1.

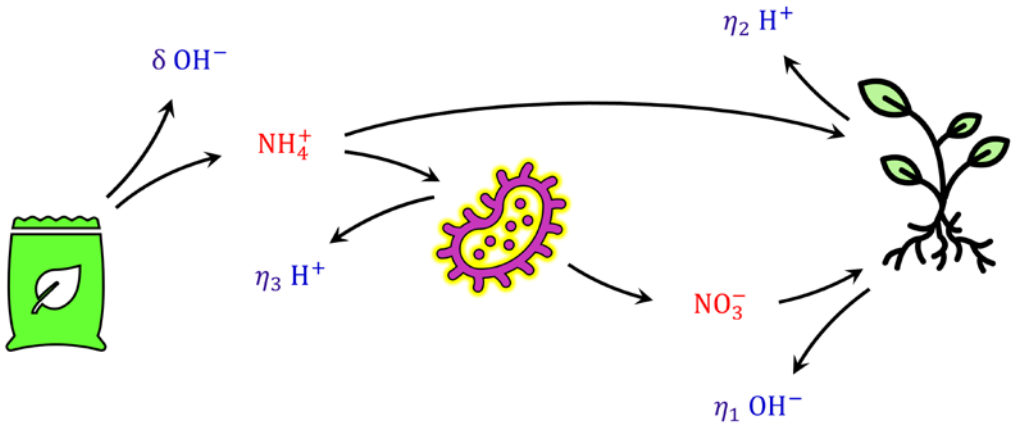

Fig. 18: Illustration of the pH effects caused by ammonium oxidation (proton excretion), ammonium absorption by the plant (proton excretion) and nitrate absorption by the plant (hydroxide excretion). Assuming digestate is used as ammonium fertilizer, which is typically alkaline, it is depicted as releasing hydroxide ions upon addition to the solution. δ is the hydroxide-to-ammonium ratio in the digestate (see Nomenclature) and η is the respective proton-to-nitrogen (or hydroxide-to-nitrogen) exudation characteristics of each organism in mol mol^{-1}. It is assumed that all nitrite is oxidised to nitrate.

6.2 Method

Seedlings were cultivated in separate systems (aeroponic cloners) and were transplanted to the main experimental setup when they weighed around 10 g, followed by commencement of the respective run. Seedlings were selected randomly in part, with preference given to visually large and healthy plants. To exploit the three pH effects described in Fig. 18, η_1, η_2 and η_3 had to be established. η_1 has already been established in the previous chapter (0.5 mol mol^{-1}) and thus η_2 and η_3 was determined in runs 1 and 2 (of this Chapter), respectively. In run 1, plants were cultivated under standard hydroponic conditions with ammonium as the sole nitrogen source and controlling the pH with 0.03 M NaOH. The nutrient solution was composed of 5 mM $(NH_4)_2SO_4$, 4 mM $CaCl_2{\cdot}2H_2O$, 2 mM K_2SO_4, 2 mM $MgSO_4{\cdot}7H_2O$, 1 mM KH_2PO_4, 6 mg L^{-1} NaOH, 7.5 mg L^{-1} Fe-EDTA, 0.05 mg L^{-1} Cu-EDTA, 2.9 mg L^{-1} H_3BO_3, 1.8 mg L^{-1} $MnCl_2{\cdot}4H_2O$, 0.2 mg L^{-1} $ZnSO_4{\cdot}7H_2O$ and 0.1 mg L^{-1} $Na_2MoO_4{\cdot}2H_2O$. The experimental setup had never-before been charged with ammonium and no additional aeration was employed. Therefore, it is assumed that no nitrifying bacteria established during the run (given their significantly slow growth rates). This was confirmed by nitrate analysis of liquid samples in which no nitrate was detected. Run 2 entailed the cultivation of nitrifying bacteria in the biofilters depicted in Fig. 5 and 6 (without plants). The experimental conditions were near-identical to those of run 2. The same nutrient solution formulation was charged except that 10 mM $(NH_4)_2SO_4$ was charged instead of 5 mM. The pH was controlled at 6.5 using KOH instead of NaOH (to minimize inert build-up in future plant growth runs). Additional aeration was employed (sparging) and a large nitrification bacterial inoculum was supplied which had previously been activated. Daily sampling commenced two weeks after inoculation and ammonium, nitrite and nitrate analysis was undertaken. The total cultivation period was 12 weeks, after which time run 3 was performed which introduced plants together with the established biofilter.

Based on the data obtained from runs 1 and 2, a nitrogen concentration control strategy was developed (explained in subsequent sections). Run 3 was performed to test the proposed control strategy. In run 3, a similar nutrient solution as in runs 1 and 2 was charged but with nitrate as the sole nitrogen source. This nutrient solution was composed of 4 M $Ca(NO_3)_2{\cdot}4H_2O$, 2 mM $MgSO_4{\cdot}7H_2O$, 1 mM KH_2PO_4, 6 mg L^{-1} NaOH, 7.5 mg L^{-1} Fe-EDTA, 0.05 mg L^{-1} Cu-EDTA, 2.9 mg L^{-1} H_3BO_3, 1.8 mg L^{-1} $MnCl_2{\cdot}4H_2O$, 0.2 mg L^{-1} $ZnSO_4{\cdot}7H_2O$ and 0.1 mg L^{-1}

$Na_2MoO_4 \cdot 2H_2O$. Run 4 was essentially a repeat of run 3 but at a lower initial nitrate concentration of 1 mM (and hence operating concentration). The nutrient solution was composed of 0.5 mM $Ca(NO_3)_2 \cdot 4H_2O$, 4 mM $CaCl_2 \cdot 2H_2O$, 2 mM $MgSO_4 \cdot 7H_2O$, 1 mM KH_2PO_4, 6 mg L^{-1} NaOH, 7.5 mg L^{-1} Fe-EDTA, 0.05 mg L^{-1} Cu-EDTA, 2.9 mg L^{-1} H_3BO_3, 1.8 mg L^{-1} $MnCl_2 \cdot 4H_2O$, 0.2 mg L^{-1} $ZnSO_4 \cdot 7H_2O$ and 0.1 mg L^{-1} $Na_2MoO_4 \cdot 2H_2O$.

6.3 Results and discussion

6.3.1 Determining η_2 and η_3

Run 1 was performed to establish η_2 by cultivating plants (without nitrifying bacteria) under standard hydroponic conditions with ammonium as the sole nitrogen source and controlling the pH with automated hydroxide dosing. Run 2 was performed to establish η_3 by cultivating nitrifying bacteria under near-identical conditions to run 1 (without plants). Additional aeration (sparging) was employed, and a large bacterial inoculum was supplied. The results of the two runs are given in Fig. 19, reported in the same format as in Fig. 13. From Fig. 19 (c) and (f), it can be seen than η remains constant with $\eta_2 \approx 1$ and $\eta_3 \approx 2$ (mol mol^{-1}). Therefore, the assumption made in Fig. 18 of constant nitrogen to proton uptake/exudation characteristics is valid and will thus form the basis of the control scheme developed in the following sections.

6.3.2 Controlling the nitrogen concentration using pH

From Fig. 19, it can be seen that the ammonium uptake rate by the plants is similar to the ammonium oxidation rate by the bacteria. However, the ammonium oxidation rates continued to increase in the months after run 2 commenced. By the time run 3 was performed (about two months later), the ammonium oxidation rates were around ten times faster than the average nitrogen absorption rates of the plants. Under these conditions, it was postulated that the pH could be controlled by dosing ammonium to the system containing a nitrate-based nutrient solution initially (pre-nitrified digestate). For example, since ammonium oxidation occurs rapidly (relative to plant nitrogen uptake), the near-immediate effect of dosing ammonium will be acidic since most of the dosed ammonium is oxidised by the bacteria (releasing η_3 protons). Therefore, if nitrate is the predominant nitrogen source in the nutrient solution, the pH rises, and ammonium dosing can be used to control the pH. i.e., the same conditions as in run 1 Chapter 5 are employed (standard hydroponic conditions) but substituting HCl for ammonium.

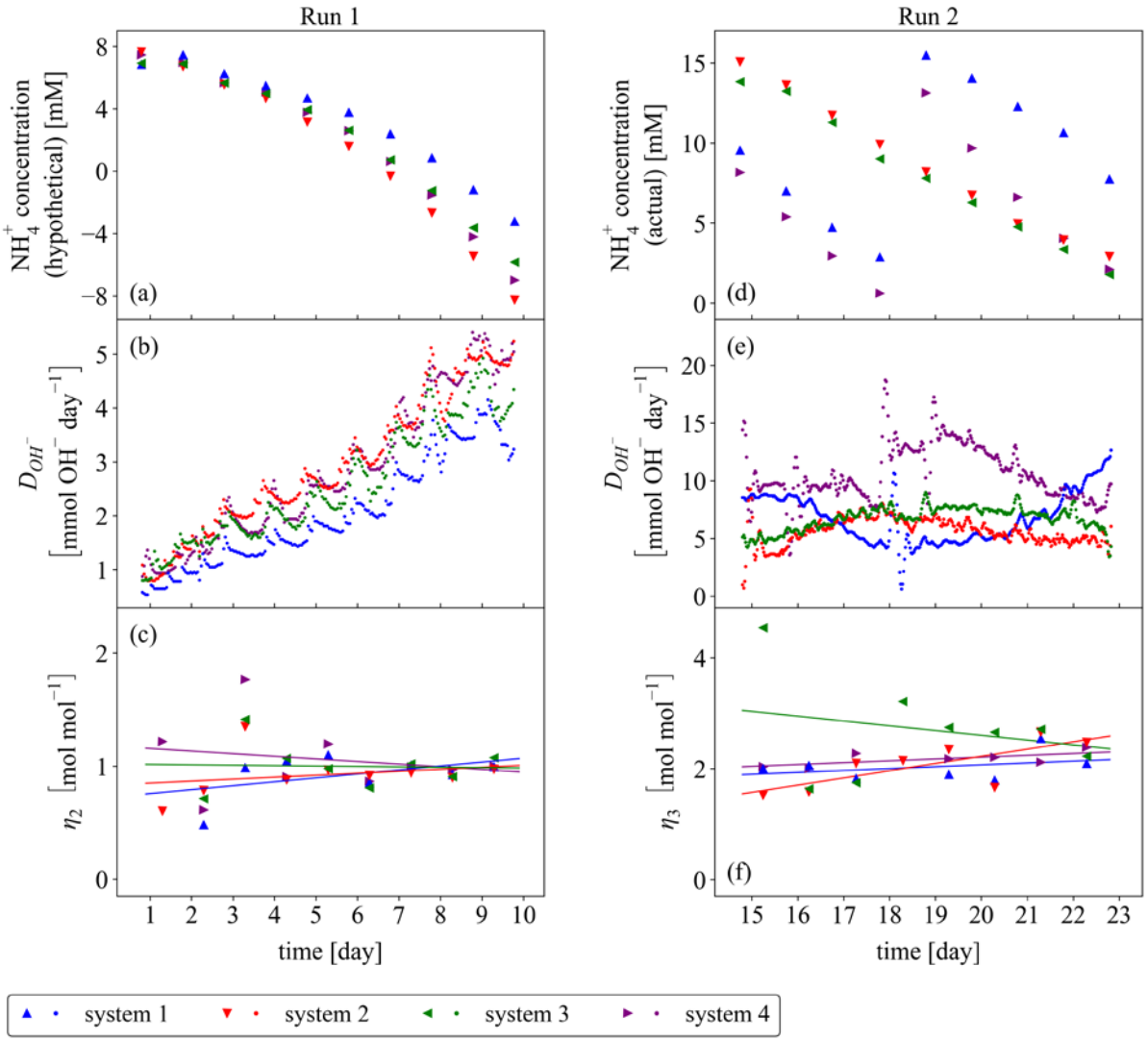

Fig. 19: Results from runs 1 and 2 reported in columns 1 and 2. In run 1 (subplots (a) to (c)), plants were cultivated in standard Hoagland's solution with ammonium as the sole nitrogen source. The hypothetical ammonium concentrations are given in (a), which are the actual (measured) concentration minus the added amounts of ammonium (manually with a pipette to prevent depletion). The pH was controlled via automatic hydroxide dosing, the rates of which are given in (b). The ratio of the hydroxide dosing rates to the ammonium uptake rates (η_2) are given in (c). No significant amounts of nitrifying bacteria are assumed to have established during the run. In run 2, nitrifying bacteria were cultivated without plants by supplying the same ammonium solution formulation used in run 1. Additional aeration (sparging) was employed, and a large bacterial inoculum (previously activated) was charged. Data was recorded after two weeks, which is reported in the same format as run 1 in subplots (d) to (f).

If this ammonium dosing strategy is used, it can be deduced from Fig. 18 that the ammonium dosing rate will be 25 % of the nitrate uptake rate by the plant (by doing a proton balance). This is assuming that $\eta_1 = 0.5$ and $\eta_3 = 2$ according to Fig. 13 and 19, and that negligible amounts of ammonium is absorbed by the plant due to high ammonium oxidation rates. As a result, the nitrate concentration in the solution will decrease over time. Consider however, if instead of dosing ammonium only, a mixture of hydroxide and ammonium was dosed. If the ratio of hydroxide-to-ammonium (δ) does not exceed the value of η_3 (≈ 2), the effect of dosing will remain acidic but higher dosing rates will be realized since the effect is less acidic. Therefore, the decrease in the nitrate concentration in solution will be slower with increasing δ values. It can hence be deduced from Fig. 18 that a δ value of 1.5 will result in ammonium dosing rates being equal to plant nitrate uptake rates. Since all ammonium is converted to nitrate, the nitrate concentration will remain constant (assuming all ammonium dosed is rapidly oxidized).

Run 3 was performed to test this control strategy. Plants were cultivated in the system together with the established biofilter. The pH was controlled by dosing ammonium and hydroxide in a ratio of 1.5 mol mol^{-1}. Ammonium as $(NH_4)_2SO_4$ and hydroxide as KOH was dosed individually from separate dosing reservoirs (D1 and D2 in Fig. 5 and 6). Hoagland's solution was charged initially with nitrate as the sole nitrogen source. A sequential function chart is given in Fig. 20 to convey the control algorithm. From trial runs, it was found that a constant feed of ammonium was required to maintain the vitality of the nitrifying bacteria. Therefore, the controller dosed 1 mmol day^{-1} ammonium and 1.5 mmol day^{-1} hydroxide at 30 min intervals (thus, 1/48 mmol ammonium per instance), regardless of the pH. This is shown as "Low" at the bottom of Fig. 20 in which $D_{NH_4^+}$ is the ammonium dosing rate and D_{OH^-} is the hydroxide dosing rate. When the pH rose above the specified setpoint SP, higher amounts of ammonium and hydroxide was dosed (still in a ratio of 1.5). These rates are abbreviated as "High" in Fig. 20. The "Low" nitrogen dosing rate (1 mmol day^{-1}) is equal to the nitrogen uptake rate of a small Kale plant weighing about 10 g. Therefore, larger plants (as compared with runs 1 and 2) were employed to better observe the control action. The two outermost branches at SP_L and SP_H were added primarily as safety features in case of disturbances or biofilter inactivity. These branches did not play a significant role in the upcoming runs and can thus be neglected, but they are nonetheless recommended.

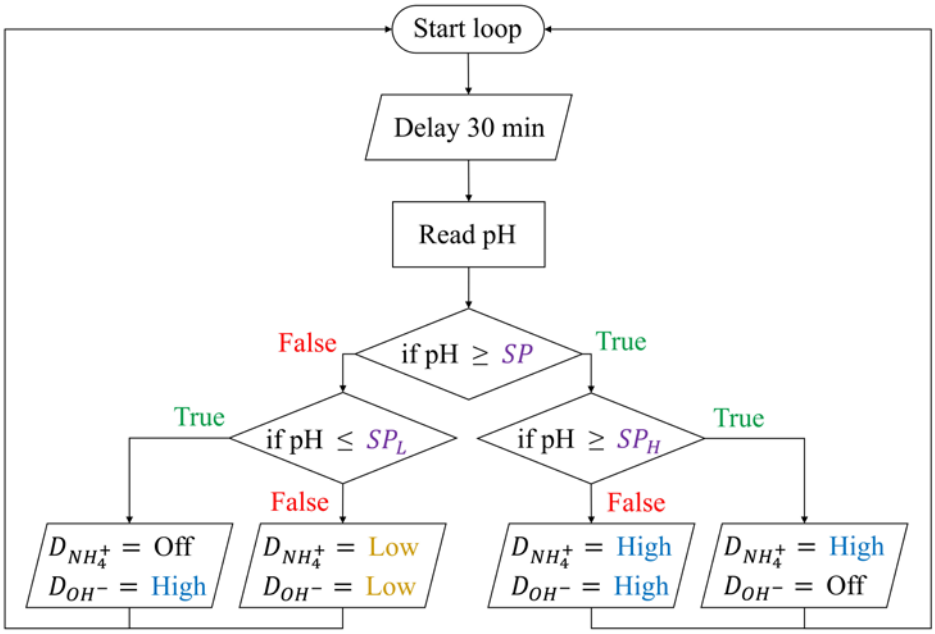

Fig. 20: Sequential function chart of the control algorithm. Online pH measurements were taken every 30 min as shown. High dosing rates of both chemicals were actuated in the constant ratio of 1.5 mol mol^{-1} (as discussed in Section 3.2) when the pH was above the setpoint value $SP = 6.1$, but below a higher setpoint value $SP_H = 6.4$. The "High" dosing rates were proportional to the setpoint error (proportional control action), specifically, $D_{NH_4^+}$ = "High" = $30 \times (\text{pH} - 6.1) + 1$ mmol day^{-1} and $D_{OH^-} = 1.5 \times D_{NH_4^+}$. If the pH rose above SP_H (safety feature), hydroxide dosing was halted and $D_{NH_4^+}$ was dosed at a high rate of 7 mmol day^{-1}. If the pH was below $SP = 6.1$ but not as low as $SP_L = 5.8$, low dosing rates were actuated (also in the constant ratio of 1.5). This was necessary to maintain the vitality of the bacteria and prevent inactivation. $D_{NH_4^+}$ = "Low" = 1 mmol day^{-1} and D_{OH^-} = "Low" = 1.5 mmol day^{-1}. If the pH was below $SP_L = 5.8$ (another safety feature), ammonium dosing was halted, and high hydroxide rates were actuated (also proportional control), specifically, $D_{OH^-} = 20 \times (5.8 - \text{pH}) + 5$ mmol day^{-1}.

The results of run 3 are reported in Fig. 21. Subplot (a) gives the nitrate concentrations of the four systems (triangle markers). No ammonium was detected in the solution (measurements were at the calibration error of 0.1 mM), thus rapid ammonium oxidation was confirmed. The highest measured nitrite concentration was 0.002 mM; hence ammonia oxidation remained the rate limiting step during nitrification. A slow downward drift in the nitrate concentration profiles is observed. The nitrate depletion rate is around 19 % (± 6 %) of the rate in run 1 Chapter

5 (Fig. 13), in which no additional nitrogen was added/dosed (hence 81 % of the plant's nitrogen in run 3 was dosed as ammonium). Predictions of the nitrate concentrations, if no additional nitrogen was dosed, is also shown for comparison. These predictions are based on exponential fits of the nitrate concentrations in run 1 Chapter 5 (standardised based on initial plant mass). A higher δ value may be employed to reduce the downward drift in the nitrate concentrations of run 3. However, inevitable drift (either up or down) is expected because small errors in pump calibration and genetic variations in the plants and bacteria (regarding the proton/hydroxide to nitrogen uptake characteristics) are bound to exist (Van Rooyen & Nicol, 2021). These parameters are likely dependent on the system and plant species. Therefore, calibration would be required if implemented. Subplot (b) shows the pH profiles for each system. Tight pH control is observed indicating the success of the control strategy. The ammonium and hydroxide dosing rates increased with plant plants size. The results shows that the nitrate concentration in nitrification-hydroponic systems can be maintained at relatively constant levels by controlling the pH with an alkaline ammonium solution at a specific hydroxide-to-ammonium ratio. Similarly, for an ammonium solution at the same pH as that of the hydroponic system, 1.5 mol of hydroxide must be dosed together with 1 mol of ammonium. As an added benefit, this strategy reduces the amount of base required (hence cation build-up) compared to using pre-nitrified ammonium fertilizer only (nitrification occurring in an external unit from the plant growth unit), which requires 2 mol of hydroxide to oxidise one mol of ammonium. In addition, feeding this pre-nitrified solution to the hydroponic system would require additional acid dosing (hence anion build-up) to control the pH.

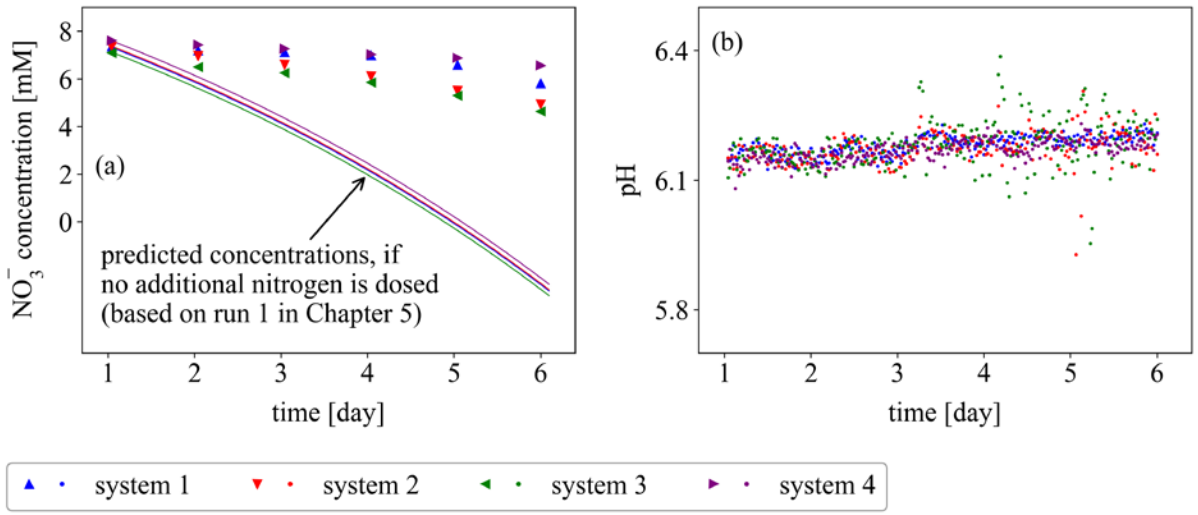

Fig. 21: Results from run 3 in which the nitrate concentration was controlled by controlling the pH with ammonium and hydroxide dosing in a ratio of 1.5 (mol hydroxide per mol ammonium). An overview of the control algorithm is given in Fig. 20. Subplot (a) shows the nitrate concentrations in solution (triangle markers) together with predicted concentrations (based on run 1 Chapter 5, Fig. 13) if no additional nitrogen was dosed. Subplot (b) shows the online pH measurements (raw) for each of the four systems. All ammonium and nitrite measurements were at the calibration limits of the analytical tests (0.1 mM and 0.001 mM, respectively), which confirms rapid ammonium oxidation and complete nitrification (all ammonium is converted to nitrate).

6.3.3 Controlling the nitrogen concentration at lower levels

Since the nitrogen concentration can be maintained at a relatively constant value (given a slow downward drift in concentration when $\delta = 1.5$), lower operating concentrations may be employed (thus minimizing R_i in Equation 1). Lower nitrogen concentrations can be employed without affecting plant growth or nutrition (discussed in Chapter 1), but lower nitrogen levels mean higher risk of nitrogen extinction in solution. Therefore, good controller performance and robustness is required. Run 4 was performed to determine the feasibility of operating at lower nitrogen concentrations using the proposed control strategy outlined in Fig. 20. Run 4 was conducted under the same conditions as run 3 (also employing a δ value of 1.5), except for charging a lower initial nitrate concentration of 1 mM. The results are reported in Fig. 22 in the same format as in Fig. 21. Like run 3, no ammonium or nitrite was detected.

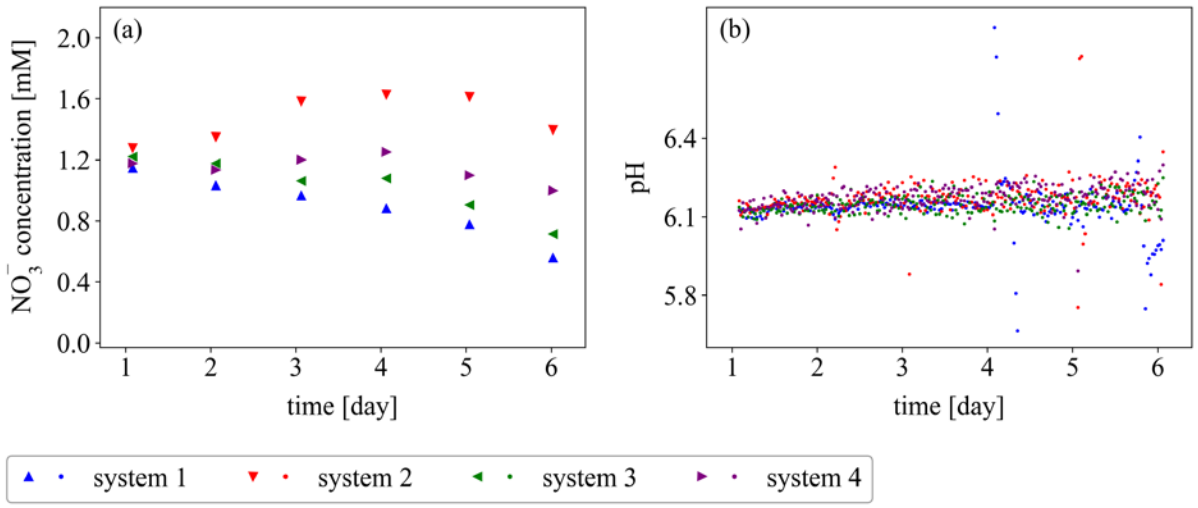

Fig. 22: Results from run 4 in which the nitrate concentration was controlled by controlling the pH with ammonium and hydroxide dosing in a ratio of 1.5 (mol hydroxide per mol ammonium). An overview of the control algorithm is given in Fig 20. Subplot (a) shows the nitrate concentrations in solution (triangle markers). Subplot (b) shows the online pH measurements (raw). All ammonium and nitrite measurements were at the calibration limits of the analytical tests (0.1 mM and 0.001 mM, respectively), which confirms rapid ammonium oxidation and complete nitrification (all ammonium is converted to nitrate).

Similar to run 3, a slow depletion rate in the nitrate concentrations is observed (with a small initial increase in system 2). However, the depletion rates are 3 % (± 3 %) of those in run 1 in Chapter 5 (Fig. 13) which are significantly slower than those of run 3 (which were 19 % (± 6 %) of run 1 in Chapter 5). These rates are reported in Fig. 23 which is intended to compare the growth characteristics between the runs. The relative growth rates (RGR) and nitrogen content of the plants are also compared in Fig. 23. As can be seen from Fig. 23, all the $RGRs$ are around 0.2 day^{-1}. A significant decrease in the plant nitrogen content is observed for run 5 (ANOVA, $p = 0.06$), which is believed to be due to the low nitrogen concentrations employed. When comparing the nitrate depletion rates of runs 4 and 5, the rates appear to decrease with the nitrate concentration in solution (ANOVA, $p = 0.006$). To explain this phaenomenon, mathematical modelling of the flux model depicted in Fig. 18 was undertaken. The model and simulation results are given in the following section, which agrees with the observed phenomenon in which the rate of nitrate depletion decreases with the nitrate concentration. The simulation predicts a steady state nitrate concentration which demonstrates controller robustness. This steady state concentration was not achieved in the current system, however, which is believed to be due to imperfect mixing and system instabilities as observed in the pH and dosing profiles

of the previous runs. However, it was shown that the control strategy effectively safeguards against nitrate extinction in solution.

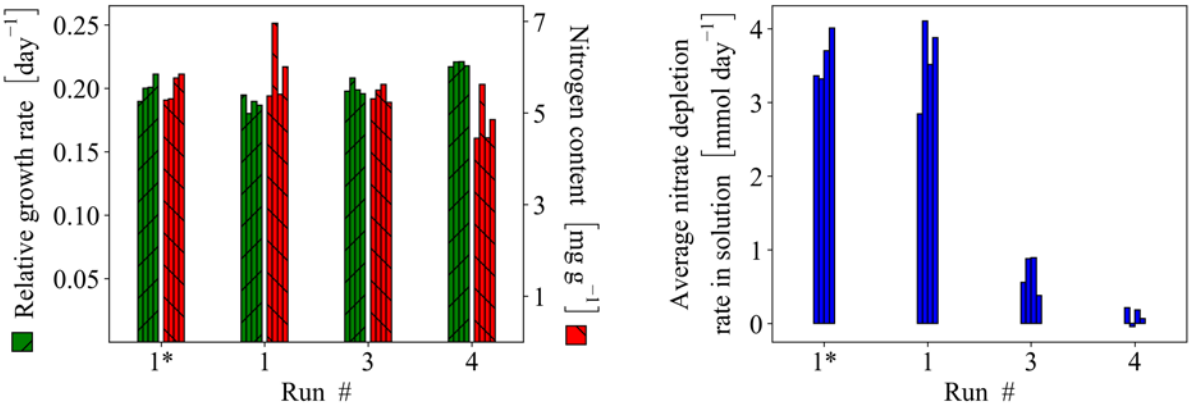

Fig. 23: Comparison of the relative growth rates (RGR) of the plants, the nitrogen content of the plants, and the average nitrate depletion rates in solution between runs. Run 1* is from Chapter 5 (Fig. 13) and runs 1, 3 and 4 are from this chapter. The average nitrate depletion rates are standardized based on initial plant mass. The nitrogen content was calculated from a nitrogen mass-balance over the solution and change in plant fresh mass (thus units of mg elemental nitrogen per change in plant fresh mass).

From Fig. 23, it can be seen that plants in runs 1* (Chapter 5) and 1 (this chapter) had similar nitrogen contents. The only difference between the runs was the nitrogen source, with nitrate being supplied in run 1* and ammonium in run 1. This shows that the influx of total nitrogen is regulated by the plant, rather than separate uptake mechanisms for nitrate and ammonium. If the influx of total nitrogen was not regulated by the plant, double the amount of plant nitrogen content would be expected if both nitrate and ammonium is supplied in sufficiently high concentrations. Therefore, efforts to model plant nitrogen uptake should consider the total nitrogen concentration in solution rather than model nitrate and ammonium uptake separately. A suggested correlation is given in the following section (Equation 10), which is intended to explain the observed phenomenon of slower nitrate depletion rates at lower nitrate concentrations.

6.4 Mathematical modelling and simulation

It was shown in the previous section that the rate of nitrate depletion is related to the concentration of nitrate in solution. This may be the result of higher ammonium uptake rates by the plants at lower nitrate concentrations (since the ammonium-to-nitrate concentration ratio in the

solution is higher). To demonstrate, consider the conditions employed in run 3. A δ value of 1.5 resulted in slow depletion of nitrate in solution while the ammonium concentrations remained low. As ammonium uptake relative to nitrate is related to the concentration ratio of ammonium-to-nitrate in solution (Imsande, 1986), higher ammonium uptake rates by the plants are expected when the nitrate concentration approaches that of ammonium. From Fig. 18, it can be shown that if the pH and nitrogen concentrations remain constant: $\delta = (\eta_1 + \eta_2 - \eta_3)F^P_{NH_4^+} + (\eta_3 - \eta_1)$. Where, $F^P_{NH_4^+}$ is the fraction of the total ammonium dosed which is absorbed by the plant (the rest being taken by the bacteria). This function is plotted in Fig. 24 (a) in which $\eta_1 = 0.5$, $\eta_2 = 1$, and $\eta_3 = 2$. Since ammonium and hydroxide dosing is intended to produce an acidic effect (lowering the pH when it rises above a setpoint), high δ values will result in nitrate accumulation and low δ values will lead to nitrate depletion in solution. Therefore, if the δ required for constant nitrate concentration is lower than the actual δ being dosed, nitrate will accumulate in solution and vice versa. So as the nitrate concentration decreases, $F^P_{NH_4^+}$ increases and the employed δ becomes "too high" which tends towards nitrate accumulation. This may be difficult to conceptualize initially and thus it is shown mathematically below by modelling the flux diagram depicted in Fig. 18.

The nitrate balance over the solution at constant volume, assuming all ammonium consumed by the bacteria is converted to nitrate (zero nitrite accumulates and negligible amounts of nitrogen is used to produce bacterial biomass):

$$V\frac{d[\mathrm{NO_3^-}]}{dt} = r^B_{NH_4^+} - r^P_{NO_3^-} \tag{6}$$

Where, $[\mathrm{NO_3^-}]$ is the concentration of nitrate in solution (mM), $r^B_{NH_4^+}$ is the ammonium oxidation rate by the bacteria which is assumed equal to the nitrate production rate by the bacteria (mmol day^{-1}), $r^P_{NO_3^-}$ is the nitrate uptake rate by the plant (mmol day^{-1}) and V is the solution volume (L) (assumed constant).

The ammonium balance over the solution at constant volume:

$$V\frac{d[\mathrm{NH_4^+}]}{dt} = D_{NH_4^+} - r^B_{NH_4^+} - r^P_{NH_4^+} \tag{7}$$

Where, $[NH_4^+]$ is the concentration of ammonium in solution, $D_{NH_4^+}$ is the rate of ammonium dosed to the solution (mmol day^{-1}), $r_{NH_4^+}^B$ is the ammonium oxidation rate by the bacteria (mmol day^{-1}) and $r_{NH_4^+}^P$ is the ammonium consumption rate by the plant (mmol day^{-1}).

The proton balance becomes (assuming hydroxide exudation is equivalent to proton uptake):

$$\frac{d\mathrm{H}^+}{dt} = -\delta\, D_{NH_4^+} - \eta_1\, r_{NO_3^-}^P + \eta_2\, r_{NH_4^+}^P + \eta_3\, r_{NH_4^+}^B \tag{8}$$

The total nitrogen uptake rate by the plant (r_N^P) in mmol day^{-1}:

$$r_N^P = r_{NO_3^-}^P + r_{NH_4^+}^P \tag{9}$$

The total nitrogen content of the plants in run 1 from Chapter 5 (nitrate only) was equal to the nitrogen content of the plants from run 1 in this chapter (ammonium only), which was shown in Fig. 23. This result shows that r_N^P is constant (at a specific plant size) and independent of the nitrogen source (nitrate or ammonium). Therefore, nitrate and ammonium uptake cannot be modelled separately since the total amount of nitrogen absorbed is constant. Although an affinity often exists for a particular nitrogen source (which is dependent on plant species and environmental conditions), the uptake rates of each nitrogen source will depend on its availability relative to the other (ammonium-to-nitrate ratio in solution). As a preliminary assumption, a linear relationship is assumed between the nitrate uptake rate and the concentration fraction of nitrate-to-ammonium in solution (no affinity). When an affinity exists, a non-linearity is introduced, α, which is the affinity of the plant to absorb ammonium over nitrate. Assuming $\alpha = 1$, *i.e.*, the plant has equal affinity for both nitrogen sources:

$$r_{NO_3^-}^P = r_N^P \left(\frac{[\mathrm{NO_3^-}]}{[\mathrm{NO_3^-}] + [\mathrm{NH_4^+}]} \right)^{\alpha} \tag{10}$$

Equation 10 simply states the nitrate uptake rate is equal to the fraction of nitrate in solution, multiplied by the total nitrogen uptake rate by the plant (when $\alpha = 1$, zero affinity). At higher nitrate affinity, $\alpha < 1$, and at higher ammonium affinity, $\alpha > 1$.

With the pH controlled, $d\mathrm{H}^+ \approx 0$. Also, assuming all the ammonium dosed is immediately consumed, $d[\mathrm{NH}_4^+] \approx 0$ (and letting $\alpha = 1$), substitution of equations 7, 8, 9 and 10 into 6 followed by algebraic manipulation yields:

$$V\frac{d[\mathrm{NO}_3^-]}{dt} = -r_N^P \frac{(\delta + \eta_1 - \eta_3)[\mathrm{NO}_3^-] + (\delta - \eta_2)[\mathrm{NH}_4^+]}{(\delta - \eta_3)([\mathrm{NO}_3^-] + [\mathrm{NH}_4^+])} \tag{11}$$

Let, $\delta = 1.25$ (allowing for nitrate depletion in solution), $\eta_1 = 0.5$, $\eta_2 = 1$, $\eta_3 = 2$ (from results shown in Fig. 19), $r_N^P = 1$ (unit nitrogen uptake, at specific plant size), $V = 1$, $\mathrm{NH}_4^+ = 0.1$ mM (assuming the ammonium concentrations remain low and constant). With and an initial nitrate concentration of 1 mM and 0 mM (2 separate cases), integration of equation 11 yields the two profiles shown in Fig. 24 (b), for each of the initial nitrate concentrations. Fig. 24 (b) conveys a decrease in the nitrate depletion rate as the nitrate concentration approaches that of ammonium from a higher concentration, which was observed in run 4. This demonstrates that nitrate extinction is effectively inhibited. Also, a steady state nitrate concentration is predicted.

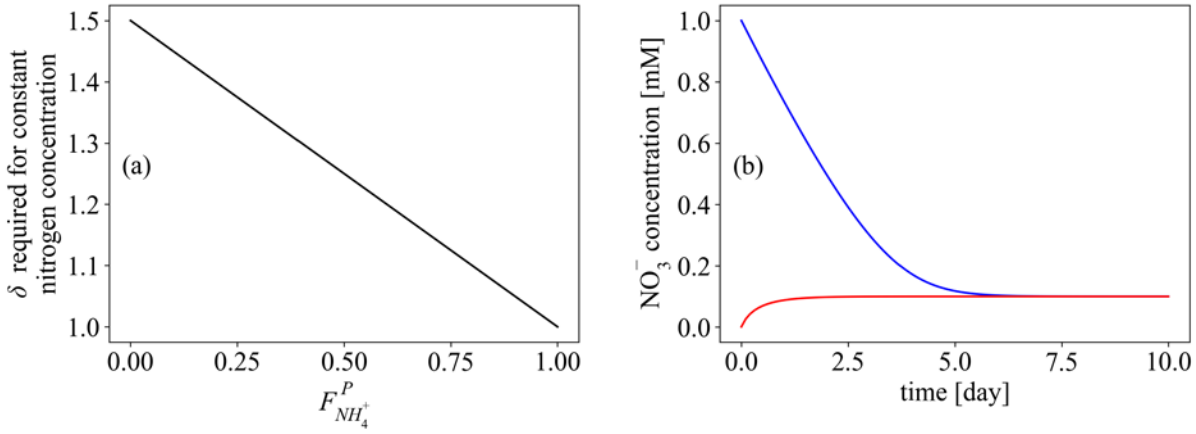

Fig. 24: Mathematical predictions of the flux model shown in Fig. 18. Subplot (a) shows the relationship between the hydroxide-to-ammonium ratio (δ) in the ammonium dosing solution (which is dosed to control the pH), and required to maintain the nitrate concentration at a constant value, versus the fraction of the dosed ammonium which is absorbed by the plant (the rest being absorbed by the bacteria). As the nitrate concentration decreases and approaches that of ammonium, a higher fraction of ammonium is absorbed by the plant and δ decreases as seen in (a). If this δ is lower than the actual δ being dosed, nitrate will accumulate in solution and vice versa. This is demonstrated in Subplot (b) in which equation 11 was integrated at a constant $\delta = 1.25$ (actual being dosed).

6.5 Conclusions

It was shown that the nitrogen concentration can be controlled at various levels in nitrification-hydroponic systems using online pH measurement only. This was accomplished by controlling the pH of a nitrate rich medium by dosing hydroxide and ammonium in a constant ratio of 1.5 mol mol^{-1}. This demonstrates that when digestate is used to control the pH of the nutrient solution, the nitrogen concentration can be controlled simultaneously if the pH of the digestate is adjusted such that the same ratio of hydroxide-to-ammonium (1.5 mol mol^{-1}) exists in the digestate. It was also shown that the control strategy effectively inhibits nitrogen extinction in the medium, allowing for low nitrogen concentrations to be employed at low risk of nitrogen extinction. The results demonstrate that good nitrogen use efficiency can be achieved in these systems and that nitrogen pollution can be reduced proportionally.

CHAPTER 7 Ammonium extended

7.1 Introduction

Using recycled nutrients (such as digestate) to compose hydroponic solutions, which was done in Chapter 6 “Ammonium”, is attractive from an environmental perspective. A second chapter is therefore devoted to digestate. In Chapter 6, the nitrogen concentration was controlled in a dual nitrification-hydroponic unit. These systems are known as *internal* nitrification-hydroponic systems (since nitrification occurs within the hydroponic unit). Alternatively, nitrification may occur separately from the hydroponic unit. These systems are known as *external* nitrification-hydroponic systems. Advantages and disadvantages exist for both configurations. For example, nitrification performs better at higher temperatures and pH levels as compared to hydroponic units, and therefore external nitrification allows for each unit to be optimized separately. Disadvantages of external nitrification are higher inert build-up due to additional acid and base dosing requirements to control pH (see end of Section 6.3.2). The choice between internal or external nitrification thus depends on process variables. The aim of this chapter is to develop pH-based control algorithms for efficient nitrification in *external* systems.

Since 2 protons are releases per ammonium oxidised to nitrate (as established in Chapter 6), the hydroxide dosing rate resulting from the pH controller must be double the rate of ammonium oxidation by the bacteria:

$$D_{OH^-} = 2\, r^B_{NH_4^+} \tag{12}$$

Where, $r^B_{NH_4^+}$ is the ammonium oxidation rate by the bacteria (molar) and D_{OH^-} is the hydroxide dosing rate required for pH homeostasis.

The relationship given in Equation 12 provides the means to develop pH-based nitrification control systems. The objectives of these control systems would be: (1) to maintain operation at the microbial maximum nitrification rate (υ_{max}), (2) achieve high conversion of ammonia to nitrate, and (3) adapt accordingly to accommodate variations in microbial activity (robustness). Nitrification can be carried out in various reactor types and the choice depends again on process variables. Therefore, control algorithms were designed for three common reactor types, namely, batch, fed-batch and continuous reactors.

7.2 Method

The main experimental setup shown in Fig. 5 and 6 was used for all experiments. No plants were cultivated since nitrification is considered in isolation (independent of plant growth). The same microbial culture (initially cultivated in Chapter 6) was used. One of the four units failed during run 1 and thus the remaining 3 were used in all remaining experiments. Thus, triplicates are presented instead of quadruplicates as in the previous chapters. The dosing reservoirs, D1 and D2, shown in Fig. 5 and 6 contained 0.2 mM $(NH_4)_2SO_4$ (representing digestate) and 0.3 M KOH, respectively. A drain pump (not shown in Fig. 5 and 6) was incorporated to each system to allow for a continuous liquid throughput (CSTR configuration), which was employed in the Section 7.3.3.

Run 1 involved nitrification control in a batch setup with a proposed control strategy (discussed in the following section). The same nutrient solution used in runs 1 and 2 of Chapter 6 was charged, except for $(NH_4)_2SO_4$, where 4 mM was charged initially. The pH was controlled autonomously (at 6.5) by dosing hydroxide from the 0.3 mM KOH reservoir via proportional-integral (PI) control (from online pH measurements taken every 30 mins). Run 2 employed a different control strategy in a fed-batch system. The same nutrient solution was supplied with zero $(NH_4)_2SO_4$ initially. Ammonium was dosed at a calculated value according to a second proposed control strategy. The pH was also controlled autonomously via PI control. Run 3 was near-identical to run 2, but instead, a constant throughput of deionised water was employed at a dilution rate of 1 day^{-1} (thus, operation in a CSRT instead of a fed-batch).

7.3 Results and discussion

7.3.1 Batch nitrification

Batch systems have the advantage of operating at υ_{max} (objective 1) since substrate (ammonium) is consistently available in the bulk solution. Also, complete conversion can be achieved (objective 2). To maintain high production rates, draining and refilling the of the batch system is required soon after complete consumption of ammonium. This is also necessary to maintain the health (maintenance energy) of the microbial community. If the reactor is devoid of ammonium for an extended period, high death rates can be expected. Therefore, control systems able to detect ammonium extinction and drain-and-replace the medium quickly (or dose additional ammonium) are central to batch nitrification units.

Since the hydroxide dosing rates are an inferential measurement of the ammonium oxidation rates, ammonium extinction will be accompanied by a cessation in hydroxide dosing. This provides an online indication of ammonium extinction and enables the controller to take immediate action. This is similar to the approach used in Section 5.3.3, where nitrate extinction was inferred from a reduction in the rate of change of pH. As mentioned in Section 5.3.3, this approach has also been used in wastewater nitrification (Andreottola *et al*., 2001; Hajsardar *et al*., 2016; Kim & Hao, 2001). However, in these systems, the pH is not controlled at a set point and oscillates due to alternating nitrification/denitrification processes. Relatively low ammonium concentrations are dealt with (a few mM) and hence changes in pH are sufficiently small as not to affect microbial performance. Digestate, however, contains high ammonium concentrations (often over 100 mM) which would result in critically low pH levels well before complete ammonium conversion. Therefore, the pH must be controlled to achieve efficient nitrification. Thus, the pH remains constant, and the hydroxide dosing rates (resulting from the pH control system) may provide information regarding the ammonium oxidation kinetics instead of changes in the measured pH values.

This control hypothesis was investigated in run 1. Each of the 3 systems was charged with 4 mM ammonium and the pH was controlled at 6.5 via feedback proportional-integral control. More specifically, hydroxide is constantly dosed to the system but the rate at which it is dosed is adjusted (increased/decreased) by the pH controller every 30 min. This adjustment is based on the error signal received by the controller (difference between the pH reading and the pH setpoint). The control algorithm is given in the Sequential-Function-Chart shown in Fig. 25.

The degree of reduction in the hydroxide dosing rate (indication of ammonium extinction) was determined by comparing the recent dosing rate (average over the past 3 hours to reduce noise) to the maximum dosing rate (maximum of all past dosing rates), as described in Fig. 25. Ammonium extinction was assumed from a 50 % or larger reduction in the recent dosing rate compared to the maximum dosing rate, which upon detection, actuated additional ammonium dosing.

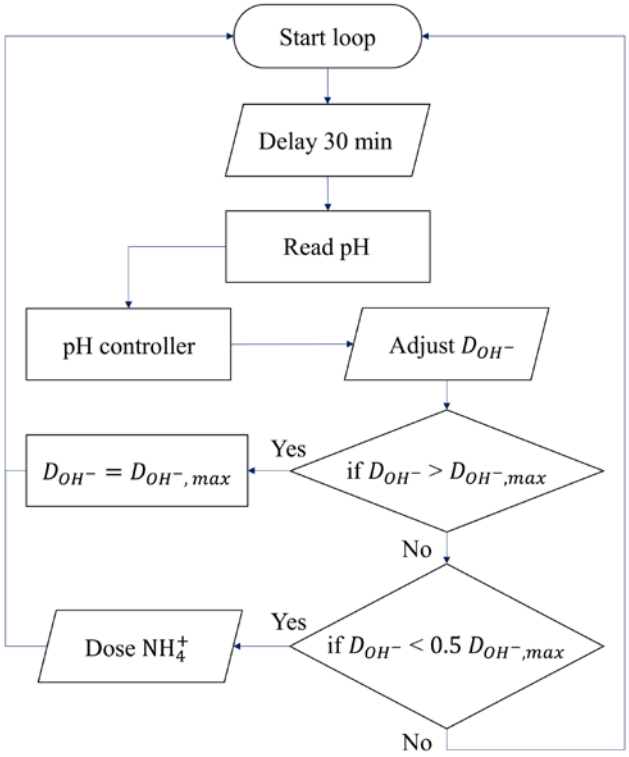

Fig. 25: Sequential-Function-Chart of the batch control algorithm designed to infer ammonium extinction from a 50 % reduction in the hydroxide dosing rate. The pH controller is a feedback proportional-integral controller. $D_{OH^-,max}$ is the maximum D_{OH^-} value since the start of the run. To reduce experimental noise, a six-point running average of the dosing rates were used (average over 3 hours) in the two "if" statements shown in the diamond boxes.

The results from run 1 are given in Fig. 26 for each of the 3 systems. Sharp declines in the hydroxide dosing rates (blue lines) are observed at ammonium extinction, which is confirmed by ammonium concentration measurements (red dots). Vertical green dashed-lines indicate ammonium dosing instances, which were actuated when a 50 % reduction in the ammonium dosing rates occurred. Fast recovery (increase in the hydroxide dosing rates) is observed after

the ammonium dosing instances. Note that the dosing rates are running averages over the past 3 hours (6 points), which was required to prevent false extinction readings resulting from experimental noise. This however caused ammonium dosing to occur in succession since the running average of the dosing rates took longer to increase (slower response time) than the immediate dosing rates. The immediate dosing rates dropped to zero soon after ammonium extinction and returned to their original values equally soon after additional ammonium was dosed.

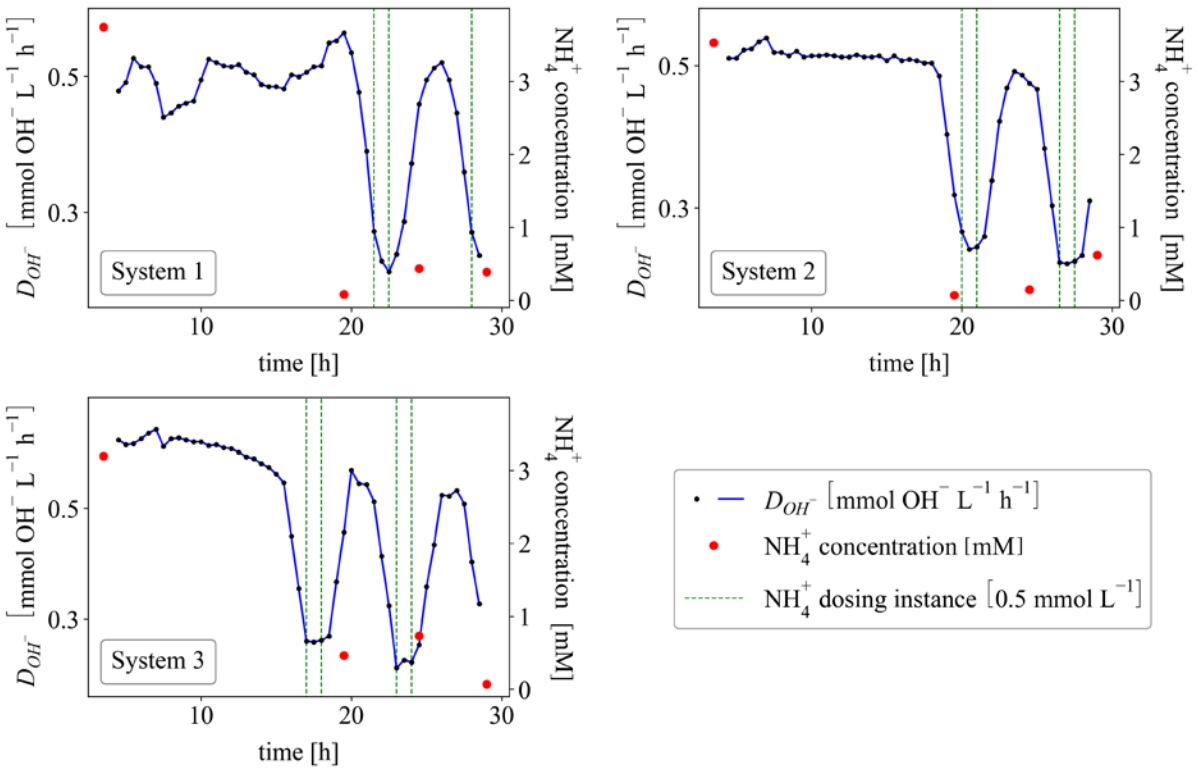

Fig. 26: Results from run 1 in a batch setup. Ammonium extinction was inferred from a 50 % reduction in the hydroxide dosing rates (6 point running average). This was accomplished with the control algorithm presented in Fig. 25. The hydroxide dosing rates are given as blue lines for each of the 3 systems. Ammonium dosing instances are shown as vertical green dashed-lines (which occurred upon a 50 % reduction in the hydroxide dosing rate). Ammonium extinction was confirmed by measurement of the ammonium concentrations in solution (red dots).

Maximum nitrification rates were maintained, and complete conversion was achieved in the batch setup. Controller adaptability (objective 3) is not applicable since ammonium is constantly available in the liquid, and thus variations in microbial activity do not affect controller performance. Although all objectives were satisfied, drawbacks to the batch setup exist. One such drawback is a potential false-alarm of ammonium extinction. For example, if a drop in

temperature occurred such that a 50 % reduction in the nitrification rates resulted, the controller would mistake this as an ammonium extinction event. If large variations in microbial activity are expected, the control strategy can be modified to guard against this by comparing the current dosing rate (which is the average over a 3-hour window) against a longer running average (such as over a 12-hour window), instead of comparing the current dosing rate to the maxing dosing rate over the whole time-span. Inferring ammonium extinction from a reduction in the more-recent dosing rate, compared to all past dosing rates will prevent false ammonium extinction readings if nitrification rates decrease relatively slowly.

7.3.2 Fed-batch systems

Although the batch control system satisfied all the objectives laid out in Section 7.1, other reactor configurations may be desired based on production specifications and drawbacks associated with batch systems, such as substrate inhibition (Kim *et al*., 2006). Thus, a control algorithm was designed for fed-batch systems next. To meet objective 2 (which is to operate at υ_{max}) a control strategy is required which feeds ammonium at υ_{max} under conditions in which υ_{max} varies (objective 3 of adaptability). To understand the mechanism of such a control strategy, consider Fig. 27 which plots the ammonium dosing rate ($D_{NH_4^+}$) against the corresponding hydroxide dosing rate (D_{OH^-}) required to control the pH. The 'kink' in the curve is the point at which the ammonium dosing rate equals υ_{max}. Left of this point, ammonium is fed at a slower rate than υ_{max} and thus the hydroxide dosing rate is 2 times the ammonium feed rate (Equation 12), since all ammonium is consumed. To the right of this point, ammonium is fed at a faster rate than the bacteria can consume it. Under these conditions, ammonium is still oxidized at υ_{max} and the hydroxide dosing rate remains constant at $2\upsilon_{max}$. Therefore, if the controller doses an arbitrary amount of ammonium, the resulting hydroxide dosing rate provides information regarding the region of operation (either to the left or right of the targeting operating point). Specifically, if $D_{OH^-}/D_{NH_4^+} < 2$, the ammonium dosing rate is too large and must be reduced (operation is to the right of the target operating point). Alternatively, if $D_{OH^-}/D_{NH_4^+} = 2$, ammonium dosing is less than or equal to υ_{max}. In this case, no information exists regarding how much lower the ammonium dosing rate is than υ_{max} and thus ammonium dosing should be increased to prevent drifting away from the target operating point. This control strategy is conveyed in Fig. 28, in which the ammonium dosing rates are adjusted incrementally based on the operating regime. Note that a specification of $D_{OH^-}/D_{NH_4^+} < 1.9$ is

employed instead of $D_{OH^-}/D_{NH_4^+} < 2$. This is required to account for experimental errors such as pump calibrations or dosing solution concentrations. If, for example, this specified constant is larger than the actual value (for example, if 2.1 was specified, when the actual value is 2), the controller would continue to decrease the ammonium dosing rates until the ammonium dosing rates equal zero. Therefore, to safeguard against this, the specified constant (1.9 in this case) should be slightly below the calibrated value to allow for errors. Operation will thus occur slightly to the right of the target operating point in Fig. 27. This will result in slow accumulation of ammonium in solution but can be minimized through accurate calibration.

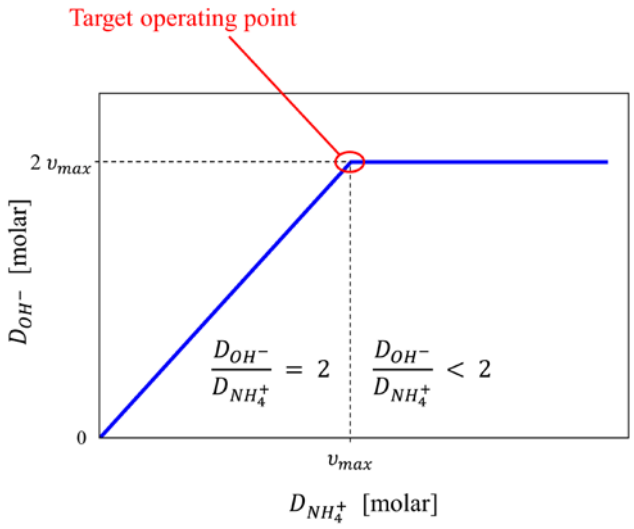

Fig. 27: Plot of the hydroxide dosing rate (D_{OH^-}) required for pH control as a function of the ammonium dosing rate ($D_{NH_4^+}$). At lower ammonium dosing rates, which are below υ_{max}, the hydroxide dosing rate is double the ammonium dosing rate (see Equation 12) since all the ammonium dosed is consumed. When the ammonium dosing rate is higher than υ_{max}, the hydroxide dosing rate remains constant at $2\upsilon_{max}$ regardless of $D_{NH_4^+}$.

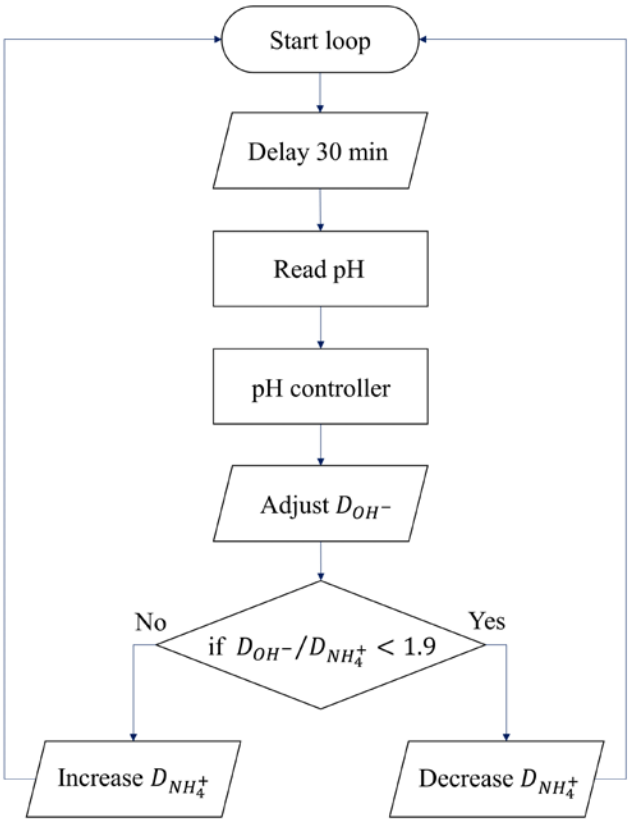

Fig. 28: Sequential function chart of the control algorithm used in the fed-batch system. Designed to operate slightly to the right of "Target operating point" shown in Fig. 27, the ammonium dosing rate is decreased when it is larger than υ_{max} and increased when its smaller than υ_{max}. A constant of 1.9 is specified (instead of 2) to account for calibration errors as discussed in the text.

Run 2 was conducted to test this control strategy in which the control algorithm shown in Fig. 28 was employed in a fed-batch system with zero ammonium initially. An arbitrary amount of ammonium was dosed by the controller to "kick-start" the algorithm. The results are given in Fig. 29 for each of the three systems. It can be seen that the ammonium dosing rates (red lines) "follow" the hydroxide dosing rates (blue lines). Slow accumulation of ammonium in solution occurred indicating that operation was maintained slightly to the right of the "Target operating point" shown in Fig. 27 (ammonium dosing was slightly higher than υ_{max}). The cumulative amounts of ammonium dosed per litre solution (not shown) were around 10 times higher than the ammonium concentrations in solution (thus, around 90 % conversion was achieved). These results show that nitrification can be accomplished at maximum production rates with 90 % conversion under adaptable control. Thus, all objectives were satisfied. However, the

accumulation of ammonium may become significant if the solution is not replaced regularly. To address this problem, the same control strategy was employed in a CSTR setup.

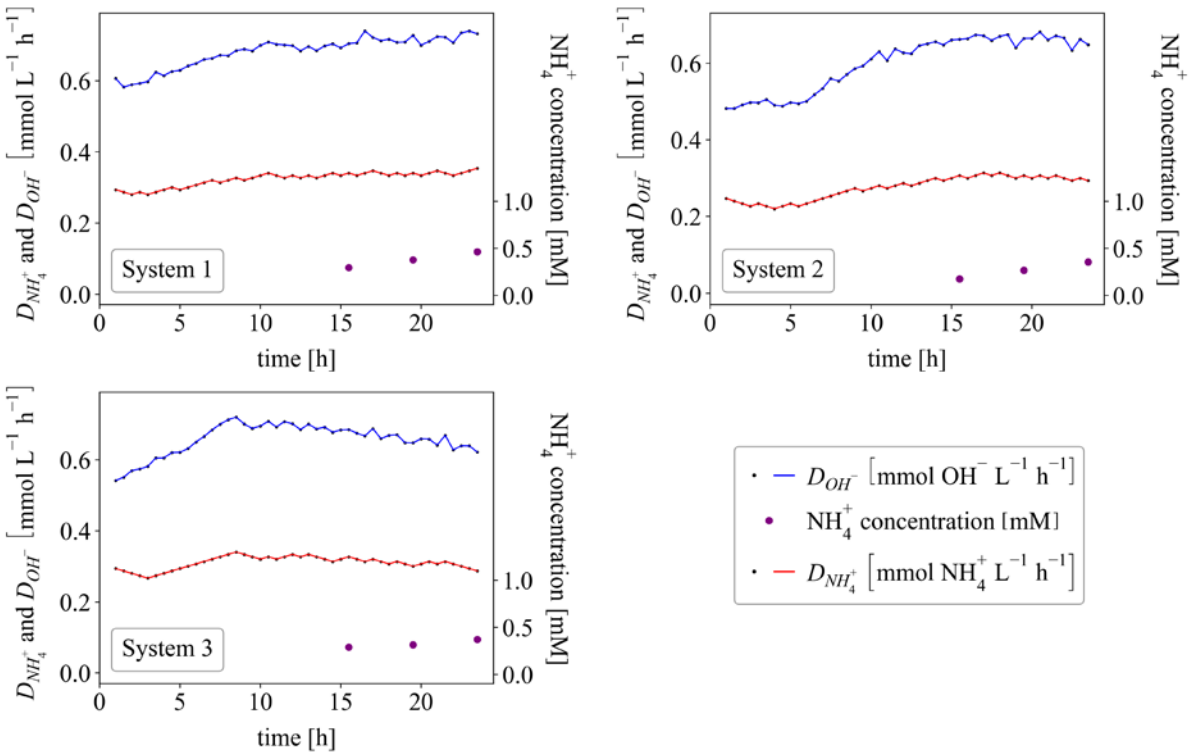

Fig. 29: Results from the control strategy shown in Fig. 28, employed in a fed-batch system (Run 2). Hydroxide dosing rates are shown as blue lines and the ammonium dosing rates are show as red lines. The ammonium concentrations in solution were measured and shown as purple dots.

7.3.3 Continuous systems

To eliminate ammonium accumulation, a dilution rate of 1 day^{-1} was employed (using deionised water), thus converting the fed-batch reactor into a CSTR. Run 3 was performed to test the control algorithm presented in Fig. 28 in the CSTR. The results are shown in Fig. 30, reported in the same format as in Fig. 29 but including the nitrate concentrations in the reactor/effluent (measured via analysis of liquid samples). Ammonium concentrations stabilized at values below 1 mM and nitrate concentrations at around 7 mM. This corresponded to a conversion of 93 % (± 1 %). The control algorithm performed well to consistently feed ammonium at just above υ_{max}, under varying υ_{max} conditions (adaptable control).

The ammonium-to-nitrate ratio in solution has great agricultural significance and an optimum ratio typically exists for each plant species (Cytryn *et al.*, 2012). This ratio is often around 1/3 molar, thus requiring a 75 % conversion of ammonium to nitrate (Tabatabaei *et al.*, 2006). As such, if a higher ammonium-to-nitrate ratio is desired, operation should occur further to the right of the "Target operating point" shown in Fig. 27. This can be accomplished by decreasing the constant in the "if statement" of Fig. 28 (currently equal to 1.9).

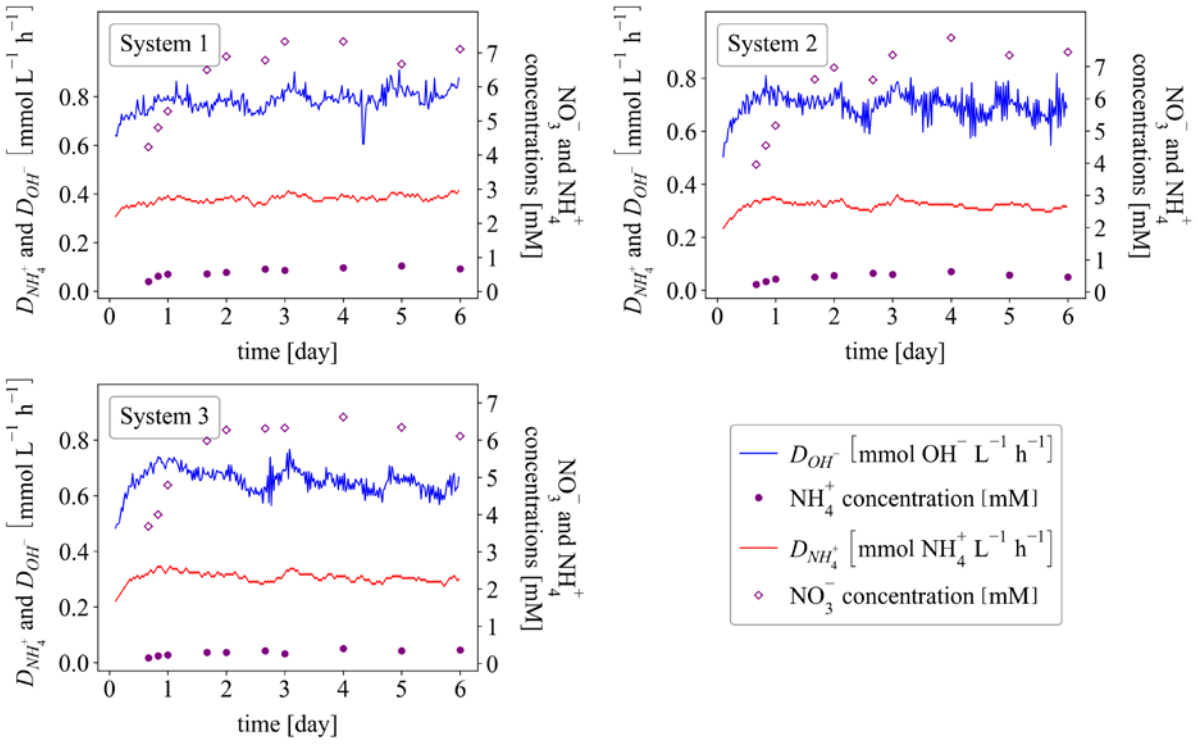

Fig. 30: Results from the control strategy shown in Fig. 28 employed in a CSTR setup with a dilution rate of 1 day^{-1}. Hydroxide dosing rates are shown as blue lines and the ammonium dosing rates are show as red lines. The ammonium and nitrate concentrations in solution were measured and are shown as purple dots and diamond markers, respectively.

The CSTR setup requires knowledge of the ammonium concentration in the feed. If this concentration is unknown or varies during production, the batch control scheme may be a better alternative. The solution in the batch system can be drained and replaced immediately upon ammonium extinction, thus realising a semi-continuous process.

7.4 Conclusions

The objectives specified in Section 7.1, namely, operation at v_{max}, high conversion and controller adaptability was satisfied using the presented control schemes in batch, fed-batch and CSTR units. Although all the objectives were satisfied in all three reactor configurations, the CSTR system appeared as the most attractive method since seamless production of a high nitrate (93 %) liquid-fertilizer was realised. Drawbacks of each setup was discussed and thus the choice of system will depend on process specifications.

CHAPTER 8 General discussion and conclusions

It was shown that N and P discharge from hydroponic systems can be reduced by around an order of magnitude using the presented control strategies with pH as the sole measured variable. This was accomplished by controlling the N and P concentrations at lower levels and incorporating recycled nutrients (digestate) as feed. Although plant growth rates were maintained, slight decreases in plant N and P content were observed. Stress responses to low nutrient concentrations are typically dependent on plant species and thus the choice of operating concentration should consider the crops being cultivated.

Using EC as the measured variable is the traditional approach to control nutrient concentrations. Although EC has many merits, the drawbacks of using EC (discussed in Section 2.5) may be problematic in some cases (if the feed has a high salinity content, like digestate, for example). pH-based control systems may therefore serve as a much-needed alternative. In general, better nutrient management can likely be achieved by using a combination of EC and pH as input variables to a controller. This work has introduced the use of pH as a new method of nutrient concentration control to the literature. Since pH is routinely measured and controlled in hydroponic systems, pH-based control systems will likely find practical application for better management of fertilizer nutrients.

Although N and P were focused on (given their pollution potential), other nutrient levels could also be controlled using pH. This was accomplished using the same approach as in Chapters 5 and 6, where a constant proton-to-nitrate ratio of around 0.5 mol mol^{-1} was utilized to control the nitrate concentration. Since plant nutrients are generally absorbed in proportion to one another, other nutrients could be added together with nitrate in proportional amounts. For example, in Chapter 5, the nitrate concentration was controlled by controlling the pH with an acid

solution consisting of a proton-to-nitrate ratio of around 0.5 mol mol^{-1}. If it is known that the plant's potassium uptake rate is 1/3 of its nitrogen uptake rate, then the potassium concentration will also be controlled if the acid dosing solution consists of a potassium to nitrate ratio of 1/3. As a rough starting point, Hoagland's solution may be composed with additional HCl at a proton to nitrate ratio of 0.5 mol mol^{-1}. Using this solution as the acid dosing solution for pH control will result in total nutrient concentration control (to some degree of accuracy). It was found that for the model plant used (*Brassica oleracea* var. *Sabellica*), an acid dosing solution composed of a proton-to-nutrient ratio of [0.5 : 1 : 0.3 : 0.2 : 0.1 : 0.075 : 0.05] molar parts [H^+ : NO_3 : K : Ca : SO_4 : PO_4 : Mg] resulted in constant EC over a 10-day run. An advantage of this approach is the chemical stability of the acid dosing solution. The acidic conditions conveniently prevented any nutrients from precipitating (at an acid strength of 0.1 M H^+) and inhibited any microorganism infections such as algae. Disadvantages (as compared to EC) include the absence of an online estimate of the total nutrient concentration. A combination of this pH-based approach and the EC method is likely to yield the best results if total nutrient concentration is opted for.

Emphasis has been placed on ammonium wastewaters (digestate in particular) as feed (chapters 6 and 7) since the use of recycled nutrients is attractive from an environmental perspective. Only nitrogen management was investigated even though digestate consists of all the nutrients required for plant growth. If digestate is supplied as the sole fertilizer, N must be the limiting nutrient else other nutrients (the limiting ones) will deplete in solution. However, if N is the limiting nutrient, the other nutrients will accumulate in solution to some extent. This is particularly concerning for P, since the aim is to minimize N and P. To control N and P simultaneously, P must be the limiting nutrient and N the second-most limiting nutrient. If the N concentration is controlled (using the strategy in Chapter 6, for example), P will deplete in solution over time and additional P must be added, while the remaining nutrients (other than N) will remain in excess. As demonstrated in Chapter 4, P can be inferred from the pH-buffering capacity of the solution. Although the rate of change of pH as caused by the plant was used, the system can be configured differently such that the buffering capacity is measured independent of plant growth or nutrient uptake (since the buffering capacity is inherently independent of the plants). Therefore, N can be controlled using the strategy presented in Chapter 6 (or a combination of the strategies in Chapter 7 and 5) using a digestate in which P is limiting relative to N, and the P concentration can then be maintained by dosing additional P (synthetic) in response the solution's pH-buffering capacity, thereby controlling N and P simultaneously. This

however requires that P dominates the buffering capacity of the solution. It was shown in Chapter 4 that P dominated the buffering capacity of Hoagland's solution (synthetic), but this may not be the case for digestate. As such, the degree to which P dominates the buffering capacity of a digestate which is intended to be used as feed should be determined prior to application.

REFERENCES

Akhtar, M. S., Oki, Y., Adachi, T., Murata, Y., & Khan, M. H. R. (2007). Relative phosphorus utilization efficiency, growth response, and phosphorus uptake kinetics of brassica cultivars under a phosphorus stress environment. *Communications in Soil Science and Plant Analysis*, *38*(7–8), 1061–1085. https://doi.org/10.1080/00103620701280266

Alewell, C., Ringeval, B., Ballabio, C., Robinson, D. A., Panagos, P., & Borrelli, P. (2020). Global phosphorus shortage will be aggravated by soil erosion. *Nature Communications*, *11*(1). https://doi.org/10.1038/s41467-020-18326-7

Allen, R. G., Pereira, L. S., Raes, D., & Smith, M. (1998). Crop evapotranspiration: Guidelines for computing crop requirements. *Irrigation and Drainage Paper No. 56, FAO*, (56), 300. https://doi.org/10.1016/j.eja.2010.12.001

Anderson, D. M. (1994). Red tides. *Scientific American*. https://doi.org/10.1038/scientificamerican0894-62

Andreottola, G., Foladori, P., & Ragazzi, M. (2001). On-line control of a SBR system for nitrogen removal from industrial wastewater. In *Water Science and Technology* (Vol. 43, pp. 93–100). IWA Publishing. https://doi.org/10.2166/wst.2001.0123

Asaduzzaman, M., & Asao, T. (2012). Autotoxicity in beans and their allelochemicals. *Scientia Horticulturae*, *134*, 26–31. https://doi.org/10.1016/j.scienta.2011.11.035

Asaduzzaman, M., Kobayashi, Y., Isogami, K., Tokura, M., Tokumasa, K., & Asao, T. (2012). Growth and yield recovery in strawberry plants under autotoxicity through electrodegradation. *European Journal of Horticultural Science*, *77*(2), 58–67.

Asao, T., Hasegawa, K., Sueda, Y., Tomita, K., Taniguchi, K., Hosoki, T., … Matsui, Y. (2003). Autotoxicity of root exudates from taro. *Scientia Horticulturae*, *97*(3–4), 389–396. https://doi.org/10.1016/S0304-4238(02)00197-8

Asao, T., Kitazawa, H., Ban, T., Pramanik, M. H. R., & Tokumasa, K. (2008). Electrodegradation of Root Exudates to Mitigate Autotoxicity in Hydroponically Grown Strawberry (Fragaria xananassa Duch.) Plants. *HortScience*, *43*(7), 2034–2038. https://doi.org/10.21273/hortsci.43.7.2034

Bergstrand, K. J., Asp, H., & Hultberg, M. (2020). Utilizing anaerobic digestates as nutrient solutions in hydroponic production systems. *Sustainability (Switzerland)*, *12*(23), 1–12. https://doi.org/10.3390/su122310076

Boneta, A., Rufí-Salís, M., Ercilla-Montserrat, M., Gabarrell, X., & Rieradevall, J. (2019). Agronomic and environmental assessment of a polyculture rooftop soilless urban home garden in a mediterranean city. *Frontiers in Plant Science*, *10*. https://doi.org/10.3389/fpls.2019.00341

Bradley, P. & Marulanda, C. (2000). Simplified Hydroponics to Reduce Global Hunger. *Acta Horticulturae*, *554*: 289–296.

Brown, P. H., Welch, R. M., & Cary, E. E. (1987). Nickel: A Micronutrient Essential for Higher Plants. *Plant Physiology 85*, 801–803. https://doi.org/10.1104/pp.85.3.801

Bugbee, B. (2000). Long-Term Effects of NH4+/NO3- Ratios on Growth and Nitrification in Hydroponic Culture. Hydroponics/Soilless Media. Paper 4. https://digitalcommons.usu.edu/cpl_hydroponics/4

Bugbee, B. (2004). Nutrient management in recirculating hydroponic culture. In *Acta Horticulturae* (Vol. 648, pp. 99–112). International Society for Horticultural Science. https://doi.org/10.17660/ActaHortic.2004.648.12

Burris, R. H. (2001). Nitrogen fixation. University of Wisconsin-Madison, Madison, Wisconsin, USA

Chan-Pacheco, C. R., Valenzuela, E. I., Cervantes, F. J., & Quijano, G. (2021, November 25). Novel biotechnologies for nitrogen removal and their coupling with gas emissions abatement in wastewater treatment facilities. *Science of the Total Environment*. Elsevier B.V. https://doi.org/10.1016/j.scitotenv.2021.149228

Chaney, R. L., & Coulombe, B. A. (1982). Effect of Phosphate on Regulation of Fe-Stress Response in Soybean and Peanut. Journal of Plant Nutrition, *5*(4–7), 469–487. https://doi.org/10.1080/01904168209362975

Cho, W. J., Kim, H. J., Jung, D. H., Kim, D. W., Ahn, T. I., & Son, J. E. (2018). On-site ion monitoring system for precision hydroponic nutrient management. *Computers and Electronics in Agriculture*, *146*, 51–58. https://doi.org/10.1016/j.compag.2018.01.019

Choi, B.-S., Lee, S.-S., Awad, Y. M., & Ok, Y.-S. (2011). Feasibility of Reclaimed Wastewater and Waste Nutrient Solution for Crop Production in Korea. *Korean Journal of Environmental Agriculture*, *30*(2), 118–124. https://doi.org/10.5338/kjea.2011.30.2.118

Christie E., 2014. Water and nutrient reuse within closed hydroponic systems. PhD thesis, Georgia Southern University.

Cordell, D., Drangert, J. O., & White, S. (2009). The story of phosphorus: Global food security and food for thought. *Global Environmental Change*, *19*(2), 292–305. https://doi.org/10.1016/j.gloenvcha.2008.10.009

Cooper, A., 1988. “1. The system. 2. Operation of the system”. In: Grower Books (Ed.), The ABC of NFT. Nutrient Film Technique, 3-123, Nexus Media, London.

Cytryn, E., Levkovitch, I., Negreanu, Y., Dowd, S., Frenk, S., & Silber, A. (2012). Impact of short-term acidification on nitrification and nitrifying bacterial community dynamics in soilless cultivation media. *Applied and Environmental Microbiology*, *78*(18), 6576–6582. https://doi.org/10.1128/AEM.01545-12

De Marco, R., & Phan, C. (2003). Determination of phosphate in hydroponic nutrient solutions using flow injection potentiometry and a cobalt-wire phosphate ion-selective electrode. *Talanta*, *60*(6), 1215–1221. https://doi.org/10.1016/S0039-9140(03)00229-7

De Wit, C. T., Dijkshoorn, W., & Noggle, J. C. (1962). *Ionic balance and growth of plants*. *Verslagen van Landbouwkundige Onderzoekingen* (p. 68). Wageningen: Centrum voor landbouwpublikaties en landbouwdocumentatie.

Di Capua, F., Pirozzi, F., Lens, P. N. L., & Esposito, G. (2019, April 15). Electron donors for autotrophic denitrification. *Chemical Engineering Journal*. Elsevier B.V. https://doi.org/10.1016/j.cej.2019.01.069

Dickson, R. W., Fisher, P. R., Argo, W. R., Jacques, D. J., Sartain, J. B., Trenholm, L. E., & Yeager, T. H. (2016). Solution Ammonium: Nitrate ratio and cation/anion uptake affect acidity or basicity with floriculture species in hydroponics. *Scientia Horticulturae*, *200*, 36–44. https://doi.org/10.1016/j.scienta.2015.12.034

Dijkshoorn, W. (1962). Metabolic regulation of the alkaline effect of nitrate utilization in plants. *Nature International Journal of Science*, *196*, 165–167. https://doi.org/10.1038/194165a0

Domingues, D. S., Takahashi, H. W., Camara, C. A. P., & Nixdorf, S. L. (2012). Automated system developed to control pH and concentration of nutrient solution evaluated in hydroponic lettuce production. *Computers and Electronics in Agriculture*, *84*, 53–61. https://doi.org/10.1016/j.compag.2012.02.006

Eldor, A. (2015). Soil microbiology, ecology, and biochemistry (4th ed.). Chapter 14, Amsterdam: Elsevier.

Erisman, J. W., Sutton, M. A., Galloway, J., Klimont, Z., & Winiwarter, W. (2008). How a century of ammonia synthesis changed the world. *Nature Geoscience*, *1*(10), 636–639. https://doi.org/10.1038/ngeo325

Galloway, J. N., Townsend, A. R., Erisman, J. W., Bekunda, M., Cai, Z., Freney, J. R., … Sutton, M. A. (2008, May 16). Transformation of the nitrogen cycle: Recent trends, questions, and potential solutions. *Science*. https://doi.org/10.1126/science.1136674

Gagnon, V., Maltais-Landry, G., Puigagut, J., Chazarenc, F., & Brisson, J. (2010). Treatment of hydroponics wastewater using constructed wetlands in winter conditions. *Water, Air, and Soil Pollution*, *212*(1–4), 483–490. https://doi.org/10.1007/s11270-010-0362-8

Graham, T., Zhang, P., Woyzbun, E., Dixon, M., (2011). Response of hydroponic tomato to daily applications of aqueous ozone via drip irrigation Scientia Horticulturae, *129*(3), 464–471, https://doi.org/10.1016/j.scienta.2011.04.019

Grand View Research (2020). Hydroponics Market Size, Share & Trends Analysis Report By Type (Aggregate Systems, Liquid Systems), By Crops (Tomatoes, Lettuce, Peppers, Cucumbers, Herbs), By Region, And Segment Forecasts, 2019 – 2025. https://www.grandviewresearch.com/industry-analysis/hydroponics-market

Grasselly, D., Merlin, G., Sédilot, C., Vanel, F., Dufour, G., & Rosso, L. (2005). Denitrification of soilless tomato crops run-off water by horizontal subsurface constructed wetlands. In *Acta Horticulturae* (Vol. 691, pp. 329–332). International Society for Horticultural Science. https://doi.org/10.17660/ActaHortic.2005.691.38

Guignard, M. S., Leitch, A. R., Acquisti, C., Eizaguirre, C., Elser, J. J., Hessen, D. O., … Leitch, I. J. (2017, July 6). Impacts of nitrogen and phosphorus: From genomes to natural ecosystems and agriculture. *Frontiers in Ecology and Evolution*. Frontiers Media S. A. https://doi.org/10.3389/fevo.2017.00070

Hachiya, T., & Sakakibara, H. (2017, May 1). Interactions between nitrate and ammonium in their uptake, allocation, assimilation, and signaling in plants. *Journal of Experimental Botany*. Oxford University Press. https://doi.org/10.1093/jxb/erw449

Hajsardar, M., Borghei, S. M., Hassani, A. H., & Takdastan, A. (2016). Simultaneous ammonium and nitrate removal by a modified intermittently aerated sequencing batch reactor (SBR) with multiple filling events. *Polish Journal of Chemical Technology*, *18*(3), 72–80. https://doi.org/10.1515/pjct-2016-0051

Hellgren, O., & Ingestad, T. (1996). A comparison between methods used to control nutrient supply. *Journal of Experimental Botany*. Oxford University Press. https://doi.org/10.1093/jxb/47.1.117

Hewitt, E. J., 1996. Sand and water culture methods used in the study of plant nutrition. Technical Communication No. 22. Commonwealth Bureau of Horticulture and Plantation Crops, East Malling, Maidstone, Kent, England.

Hoagland, D. R., & Arnon, D. I. (1938). The water-culture method for growing plants without soil. Berkeley, Calif: University of California, College of Agriculture, Agricultural Experiment Station.

Horrigan, L., Lawrence, R. S., & Walker, P. (2002). How Sustainable Agriculture Can Address the Environmental and Human Health Harms of Industrial Agriculture. *Environmental Health Perspectives*, *110*(5), 445–456.

Hosseinzadeh, S., Verheust, Y., Bonarrigo, G., & Van Hulle, S. (2017, March 1). Closed hydroponic systems: operational parameters, root exudates occurrence and related water treatment. *Reviews in Environmental Science and Biotechnology*. Springer Netherlands. https://doi.org/10.1007/s11157-016-9418-6

Imsande, J. (1986). Nitrate-ammonium ratio required for ph homeostasis in hydroponically grown soybean. *Journal of Experimental Botany*, *37*(3), 341–347. https://doi.org/10.1093/jxb/37.3.341

Jensen, M. (1999). Hydroponics Worldwide. *Acta Horticulturae*, 719–729.

Jung, D. H., Kim, H. J., Cho, W. J., Park, S. H., & Yang, S. H. (2019a). Validation testing of an ion-specific sensing and control system for precision hydroponic macronutrient management. *Computers and Electronics in Agriculture*, *156*, 660–668. https://doi.org/10.1016/j.compag.2018.12.025

Jung, D. H., Kim, H. J., Kim, H. S., Choi, J., Kim, J. D., & Park, S. H. (2019b). Fusion of spectroscopy and cobalt electrochemistry data for estimating phosphate concentration in hydroponic solution. *Sensors (Switzerland)*, *19*(11). https://doi.org/10.3390/s19112596

Kanter, D. R., Bartolini, F., Kugelberg, S., Leip, A., Oenema, O., & Uwizeye, A. (2020, January 1). Nitrogen pollution policy beyond the farm. *Nature Food*. Springer Nature. https://doi.org/10.1038/s43016-019-0001-5

Kim, D. J., Lee, D. I., & Keller, J. (2006). Effect of temperature and free ammonia on nitrification and nitrite accumulation in landfill leachate and analysis of its nitrifying bacterial community by FISH. *Bioresource Technology*, *97*(3), 459–468. https://doi.org/10.1016/j.biortech.2005.03.032

Kim, H., & Hao, O. J. (2001). pH and Oxidation-Reduction Potential Control Strategy for Optimization of Nitrogen Removal in an Alternating Aerobic-Anoxic System All use subject to JSTOR Terms and Conditions pH and Control Nitrogen Strategy Removal Potential of for Optimization in an A. *Water Environment Research*, *73*(1), 95–102.

Kim, H.-J., Son, D.-W., Kwon, S.-G., Roh, M.-Y., Kang, C.-I., & Jung, H.-S. (2011). Determination of Inorganic Phosphate in Paprika Hydroponic Solution using a Laboratory-made Automated Test Stand with Cobalt-based Electrodes. *Journal of Biosystems Engineering*, *36*(5), 326–333. https://doi.org/10.5307/jbe.2011.36.5.326

Kim, H. J., Kim, W. K., Roh, M. Y., Kang, C. I., Park, J. M., & Sudduth, K. A. (2013). Automated sensing of hydroponic macronutrients using a computer-controlled system with an array of ion-selective electrodes. *Computers and Electronics in Agriculture*, *93*, 46–54. https://doi.org/10.1016/j.compag.2013.01.011

Koide, S., & Satta, N. (2004). Separation Performance of Ion-exchange Membranes for Electrolytes in Drainage Nutrient Solutions subjected to Electrodialysis. *Biosystems Engineering*, *87*(1), 89–97. https://doi.org/10.1016/j.biosystemseng.2003.09.005

Koszel, M., & Lorencowicz, E. (2015). Agricultural Use of Biogas Digestate as a Replacement Fertilizers. *Agriculture and Agricultural Science Procedia*, *7*, 119–124. https://doi.org/10.1016/j.aaspro.2015.12.004

Kotz, J., Treichel, P., Townsend, J., 2009. Chemistry and Chemical Reactivity, Seventh Edition. Thomson Brooks Cole, Cengage Learning

Kumar, R. R., & Cho, J. Y. (2014). Reuse of hydroponic waste solution. *Environmental Science and Pollution Research*. Springer Verlag. https://doi.org/10.1007/s11356-014-3024-3

Kuzyakov, Y., & Xu, X. (2013, April). Competition between roots and microorganisms for nitrogen: Mechanisms and ecological relevance. *New Phytologist*. https://doi.org/10.1111/nph.12235

Lau, V., & Mattson, N. (2021). Effects of hydrogen peroxide on organically fertilized hydroponic lettuce (Lactuca sativa l.). *Horticulturae*, *7*(5). https://doi.org/10.3390/horticulturae7050106

Le Bot, J., Adamowicz, S., & Robin, P. (1998). Modelling plant nutrition of horticultural crops: A review. *Scientia Horticulturae*, *74*(1–2), 47–82. https://doi.org/10.1016/S0304-4238(98)00082-X

Le Deunff, E., Malagoli, P., & Decau, M. L. (2019). Modelling nitrogen uptake in plants and phytoplankton: Advantages of integrating flexibility into the spatial and temporal dynamics of nitrate absorption. *Agronomy*. MDPI AG. https://doi.org/10.3390/agronomy9030116

Lee, J. G., Lee, B. Y., & Lee, H. J. (2006). Accumulation of phytotoxic organic acids in re-used nutrient solution during hydroponic cultivation of lettuce (Lactuca sativa L.). *Scientia Horticulturae*, *110*(2), 119–128. https://doi.org/10.1016/j.scienta.2006.06.013

Lefebvre, D. D., Duff, S. M. G., Fife, C. A., Julien-Inalsingh, C., & Plaxton, W. C. (1990). Response to phosphate deprivation in Brassica nigra suspension cells: Enhancement of intracellular, cell surface, and secreted phosphatase activities compared to increases in Pi-absorption rate. *Plant Physiology*, *93*(2), 504–511. https://doi.org/10.1104/pp.93.2.504

Lin, X. (2010). Soil Microbial Research Principle and Method, High Education Press, Beijing.

Madigan, M. T., J.M. Martinko, and J. Parker. 2003 *Brock Biology of Microorganisms*, 10th Edition: 1019 pgs. Pearson Education, Inc.: Upper Saddle River, New Jersey.

Mahler, R. L. (2004). Nutrients plants require. *College of Agricultural and Life Sciences, CIS 1124*, 1–4.

Martin-Gorriz, B., Maestre-Valero, J. F., Gallego-Elvira, B., Marín-Membrive, P., Terrero, P., & Martínez-Alvarez, V. (2021). Recycling drainage effluents using reverse osmosis powered by photovoltaic solar energy in hydroponic tomato production: Environmental footprint analysis. *Journal of Environmental Management*, *297*. https://doi.org/10.1016/j.jenvman.2021.113326

McClung, C. R. (2006, April). Plant circadian rhythms. *Plant Cell*. https://doi.org/10.1105/tpc.106.040980

McElrone, A. J., Choat, B., Gambetta, G. A., & Brodersen, C. R. (2013). Water Uptake and Transport in Vascular Plants. *Nature Education Knowledge* 4(5):6

Michałowska-Kaczmarczyk, A. M., & Michałowski, T. (2015). Dynamic Buffer Capacity in Acid-Base Systems. Journal of Solution Chemistry, 44(6), 1256–1266. https://doi.org/10.1007/s10953-015-0342-0

Möller, K., & Müller, T. (2012, June). Effects of anaerobic digestion on digestate nutrient availability and crop growth: A review. *Engineering in Life Sciences*. https://doi.org/10.1002/elsc.201100085

Norton, J., & Ouyang, Y. (2019). Controls and adaptive management of nitrification in agricultural soils. *Frontiers in Microbiology*. Frontiers Media S.A. https://doi.org/10.3389/fmicb.2019.01931

Msayleb, N., Kanwar, R., Wu, H., & van Leeuwen, J. (2021). Effects of Ozonation on the Viability of *Fusarium Oxysporum* Conidia in Hydroponic Nutrient Solutions. *Ozone: Science & Engineering*, https://doi.org/10.1080/01919512.2021.1928476

Miles, A., Burris, R., Evans, H., Stacey, G. (1992). Biological nitrogen fixation, Chapman & Hall, New York.

Miyama, Y., Sunada, K., Fujiwara, S., & Hashimoto, K. (2009). Photocatalytic treatment of waste nutrient solution from soil-less cultivation of tomatoes planted in rice hull substrate. *Plant and Soil*, *318*(1–2), 275–283. https://doi.org/10.1007/s11104-008-9837-4

Miyama, Y., Hara, Y., Hashimoto, K., & Sunada, K. (2012). Closed Soilless Cultivation System of Roses Planted in Rice Hull Substrate with TiO2 Photocatalytic Treatment of Waste Nutrient solution. *Shokubutsu Kankyo Kogaku*, *24*(1), 31–37. https://doi.org/10.2525/shita.24.31

Miyama, Y., Kawashima, Y., Ogawa, J., Uekusa, H., Okamoto, T., Kita, N., … Hashimoto, K. (2013). Inactivation of bacterial wilt in closed soilless Cultivation by Photocatalytic treatment and silver. *Environmental Control in Biology*, *51*(4), 173–178. https://doi.org/10.2525/ecb.51.173

Neal, J., & Wilkie, A. C. (2014). Anaerobic Digester Effluent as Fertilizer for Hydroponically Grown Tomatoes. *Journal of Undergrad Research*, *15*(3), 1–5.

Park, J. B. K., Craggs, R. J., & Sukias, J. P. S. (2008). Treatment of hydroponic wastewater by denitrification filters using plant prunings as the organic carbon source. *Bioresource Technology*, *99*(8), 2711–2716. https://doi.org/10.1016/j.biortech.2007.07.009

Pelayo Lind, O., Hultberg, M., Bergstrand, K. J., Larsson-Jönsson, H., Caspersen, S., & Asp, H. (2021). Biogas Digestate in Vegetable Hydroponic Production: pH Dynamics and pH Management by Controlled Nitrification. *Waste and Biomass Valorization*, *12*(1), 123–133. https://doi.org/10.1007/s12649-020-00965-y

Pitts, M., & Stutte, G. (1999). Computer model of hydroponics nutrient solution pH control using ammonium. *Life support & biosphere science : international journal of earth space*, *6*(2), 73–85. PMID:11542244

Pramanik, M., Nagai, M., Asao, T., Matsui, Y. (2000). Effects of temperature and photoperiod on phytotoxic root exudates of cucumber (Cucumis sativus) in hydroponic culture. *Journal of Chemical Ecology 26(8)*, 1953–1967. https://doi.org/10.1023/A:1005509110317

Prystay, W., & Lo, K. V. (2001). Treatment of greenhouse wastewater using constructed wetlands. *Journal of Environmental Science and Health - Part B Pesticides, Food Contaminants, and Agricultural Wastes*, *36*(3), 341–353. https://doi.org/10.1081/PFC-100103574

Qiu, Z., Yang, Q., & Liu, W. (2013). Photocatalytic degradation of phytotoxic substances in waste nutrient solution by various immobilized levels of Nano-TiO2. *Water, Air, and Soil Pollution*, *224*(3). https://doi.org/10.1007/s11270-013-1461-0

Quinlan, A. V. (1984). Prediction of the optimum pH for ammonia-N oxidation by nitrosomonas Europaea in well-aerated natural and domestic-waste waters. *Water Research*, *18*(5), 561–566. https://doi.org/10.1016/0043-1354(84)90204-5

Raistrick, N. (1999). An automated relative-addition rate nutrient-dosing system for use in flowing solution culture. *Journal of Experimental Botany*, *50*(331), 263–267. https://doi.org/10.1093/JXB/50.331.263

Raven, A. (1985). Regulation of pH and generation of osmolarity in vascular plants: a cost-benefit analysis in relation to efficiency of use of energy, nitrogen and water. *New Phytologist*, *101*(1), 25–77. https://doi.org/10.1111/j.1469-8137.1985.tb02816.x

Richa, A., Touil, S., Fizir, M., & Martinez, V. (2020, December 1). Recent advances and perspectives in the treatment of hydroponic wastewater: a review. *Reviews in Environmental Science and Biotechnology*. Springer Science and Business Media B.V. https://doi.org/10.1007/s11157-020-09555-9

Rufí-Salís, M., Calvo, M. J., Petit-Boix, A., Villalba, G., & Gabarrell, X. (2020). Exploring nutrient recovery from hydroponics in urban agriculture: An environmental assessment. *Resources, Conservation and Recycling*, *155*. https://doi.org/10.1016/j.resconrec.2020.104683

Russel, D. A., & Williams, G. G. (1977). History of Chemical Fertilizer Development. *Soil Science Society of America Journal*, *41*(2), 260–265. https://doi.org/10.2136/sssaj1977.03615995004100020020x

Salazar, J., Valev, D., Näkkilä, J., Tyystjärvi, E., Sirin, S., & Allahverdiyeva, Y. (2021). Nutrient removal from hydroponic effluent by Nordic microalgae: From screening to a greenhouse photobioreactor operation. *Algal Research*, *55*, 102247. https://doi.org/10.1016/j.algal.2021.102247

Saxena, P., & Bassi, A. (2013). Removal of nutrients from hydroponic greenhouse effluent by alkali precipitation and algae cultivation method. *Journal of Chemical Technology and Biotechnology*, *88*(5), 858–863. https://doi.org/10.1002/jctb.3912

Schindler, D. W., & Vallentyne, J. R. (2008). The Algal Bowl: Overfertilization of the World's Freshwaters and Estuaries, University of Alberta Press, ISBN 0-88864-484-1.

Seo, D. C., Hwang, S. H., Kim, H. J., Cho, J. S., Lee, H. J., DeLaune, R. D., … Heo, J. S. (2008). Evaluation of 2- and 3-stage combinations of vertical and horizontal flow constructed wetlands for treating greenhouse wastewater. *Ecological Engineering*, *32*(2), 121–132. https://doi.org/10.1016/j.ecoleng.2007.10.007

Silberbush, M., & Ben-Asher, J. (2001). Simulation study of nutrient uptake by plants from soilless cultures as affected by salinity buildup and transpiration. *Plant and Soil*, *233*(1), 59–69. https://doi.org/10.1023/A:1010382321883

Smith, F. A., & Raven, J. A. (1979). Intracellular pH and its regulation. *Annual Review of Plant Physiology*, *30*, 289–311. https://doi.org/10.1146/annurev.pp.30.060179.001445

Sonneveld, C., & Voogt, W. (2009). Plant Nutrition of Greenhouse Crops, Springer, ISBN 9048125316, New York, U.S.A.

Steiner, A. A. (1961). A universal method for preparing nutrient solutions of a certain desired composition. *Plant and Soil*, *15*(2), 134–154. https://doi.org/10.1007/BF01347224

Steiner, A. A., 1984. The universal nutrient solution. Proceedings of the 6th International Congress on Soilless Culture, Wageningen, The Netherlands, 29 Apr - 5 May, 1984, pp 633–650

Stiles, W. A. V., Styles, D., Chapman, S. P., Esteves, S., Bywater, A., Melville, L., … Llewellyn, C. A. (2018, November 1). Using microalgae in the circular economy to valorise anaerobic digestate: challenges and opportunities. *Bioresource Technology*. Elsevier Ltd. https://doi.org/10.1016/j.biortech.2018.07.100

Stoknes, K., Scholwin, F., Krzesiński, W., Wojciechowska, E., & Jasińska, A. (2016). Efficiency of a novel “Food to waste to food” system including anaerobic digestion of food waste and cultivation of vegetables on digestate in a bubble-insulated greenhouse. *Waste Management*, *56*, 466–476. https://doi.org/10.1016/j.wasman.2016.06.027

Sublett, W. L., Barickman, T. C., & Sams, C. E. (2018). The effect of environment and nutrients on Hydroponic Lettuce yield, quality, and Phytonutrients. *Horticulturae*, *4*(4). https://doi.org/10.3390/horticulturae4040048

Sunada, K., Ding, X. G., Utami, M. S., Kawashima, Y., Miyama, Y., & Hashimoto, K. (2008). Detoxification of phytotoxic compounds by TiO2 photocatalysis in a recycling hydroponic cultivation system of asparagus. *Journal of Agricultural and Food Chemistry*, *56*(12), 4819–4824. https://doi.org/10.1021/jf8001075

Svehla, P., Radechovska, H., Pacek, L., Michal, P., Hanc, A., & Tlustos, P. (2017). Nitrification in a completely stirred tank reactor treating the liquid phase of digestate: The way towards rational use of nitrogen. *Waste Management*, *64*, 96–106. https://doi.org/10.1016/j.wasman.2017.03.041

Tabatabaei, S., Fatemi, L., & Fallahi, E. (2006). Effect of ammonium: Nitrate ratio on yield, calcium concentration, and photosynthesis rate in strawberry. *Journal of Plant Nutrition*, *29*(7), 1273–1285. https://doi.org/10.1080/01904160600767575

Trejo-Téllez, L., & Gómez-Merino, F. (2012). Nutrient solutions for hydroponic systems. Colegio de Postgraduados, Montecillo, Texcoco, State of Mexico, Mexico

Tyson, R. V., Simonne, E. H., Davis, M., Lamb, E. M., White, J. M., & Treadwell, D. D. (2007). Effect of nutrient solution, nitrate-nitrogen concentration, and pH on nitrification rate in perlite medium. *Journal of Plant Nutrition*, *30*(6), 901–913. https://doi.org/10.1080/15226510701375101

van't Hoff, J. H. (1887) The Role of Osmotic Pressure in the Analogy Between Solutions and Gases, *Zeitschrift für physikalische Chemie 1*, 481–508

Wang, B., & Shen, Q. (2012). Effects of ammonium on the root architecture and nitrate uptake kinetics of two typical lettuce genotypes grown in hydroponic systems. *Journal of Plant Nutrition*, *35*(10), 1497–1508. https://doi.org/10.1080/01904167.2012.689910

Wang, Q., Liu, J., & Zhu, H. (2018, March 9). Genetic and molecular mechanisms underlying symbiotic specificity in legume-rhizobium interactions. *Frontiers in Plant Science*. Frontiers Media S.A. https://doi.org/10.3389/fpls.2018.00313

Weiland, P. (2010). Biogas production: Current state and perspectives. *Applied Microbiology and Biotechnology*. Springer Verlag. https://doi.org/10.1007/s00253-009-2246-7

Xiao, D., Yuan, H. Y., Li, J., & Yu, R. Q. (1995). Surface-Modified Cobalt-Based Sensor as a Phosphate-Sensitive Electrode. *Analytical Chemistry*, *67*(2), 288–291. https://doi.org/10.1021/ac00098a009

Yamamoto-Ikemoto, R., Komori, T., Nomura, M., Ide, Y., & Matsukami, T. (2000). Nitrogen removal from hydroponic culture wastewater by autotrophic denitrification using thiosulfate. In *Water Science and Technology* (Vol. 42, pp. 369–376). Int Water Assoc. https://doi.org/10.2166/wst.2000.0405

Yu, J. Q., & Matsui, Y. (1994). Phytotoxic substances in root exudates of cucumber (Cucumis sativus L.). *Journal of Chemical Ecology*, *20*(1), 21–31. https://doi.org/10.1007/BF02065988

Zhang, W. & Tu, J. (2000) Effect of Ultraviolet Disinfection of Hydroponic Solutions on Pythium Root Rot and Non-target Bacteria. *European Journal of Plant Pathology 106***,** 415–421. https://doi.org/10.1023/A:1008798710325

Zhang, X., Davidson, E. A., Mauzerall, D. L., Searchinger, T. D., Dumas, P., & Shen, Y. (2015, December 3). Managing nitrogen for sustainable development. *Nature*. Nature Publishing Group. https://doi.org/10.1038/nature15743